The Pennsylvania State University

The Graduate School

John and Willie Leone Family Department of Energy and Mineral Engineering

FORECASTING THE PRODUCTION PERFORMANCE OF WELLS LOCATED IN TIGHT OIL PLAYS USING ARTIFICIAL EXPERT SYSTEMS

A Dissertation in

Petroleum and Mineral Engineering

by

Yogesh Bansal

Submitted in Partial Fulfillment
of the Requirements
for the Degree of

Doctor of Philosophy

December 2011

The dissertation of Yogesh Bansal was reviewed and approved* by the following:

Turgay Ertekin
Professor of Petroleum and Natural Gas Engineering
George E. Trimble Chair in Earth and Mineral Sciences
Dissertation Co-Advisor and Co-Chair of Committee

Zuleima T. Karpyn
Associate Professor of Petroleum and Natural Gas Engineering
Quentin E. and Louise L. Wood Faculty Fellow in PNGE
Dissertation Co-Advisor and Co-Chair of Committee

Luis F. Ayala
Associate Professor of Petroleum and Natural Gas Engineering

Li Li
Assistant Professor of Petroleum and Natural Gas Engineering

Kultegin Aydin
Professor of Electrical Engineering

R. Larry Grayson
Professor of Energy and Mineral Engineering
George H., Jr., and Anne B. Deike Chair in Mining Engineering
Graduate Program Officer of Energy and Mineral Engineering

*Signatures are on file in the Graduate School.

Abstract

The potential of unconventional oil and gas reservoirs is promising to account for the declining conventional supplies in the future. However, because of their complex nature, it is uneconomical to produce from of these resources with the current state of technology. In addition, these resources are relatively new (from the development point of view), thus, it is difficult to completely characterize these resources in the absence of their respective analogs. This study focuses on tight oil reservoirs. Characterization of these resources is a complex problem as tight oil systems are discontinuous hydrocarbon sources. Developing these resources by identifying the location to drill, estimating well performance and suggesting a completion strategy will be a challenge in the absence of a representative reservoir model.

An inexpensive and field-deployable expert systems-based tool has been proposed in this study to characterize such unconventional reservoirs. A group of inter-assisting expert systems are developed, where the individual capabilities lie in suggesting completion parameters and predicting quarterly cumulative production of oil, water and gas for a two-year period. These expert systems are grouped together to suggest the best infill drilling location in the field with a forecast of their respective cumulative

productions by the end of two years. The predictions from the expert systems-based tool are found to be in good agreement with field performance. Production surfaces generated by these expert systems are found to reflect the actual productions obtained in the field. In addition, a hybrid optimization method is also developed in this work. The method is used to optimize the well completion parameters in a tight oil reservoir.

The tools developed in this work will help in a quick evaluation of tight oil reservoirs. The results discussed in the dissertation show the accuracy of predictions made by the expert systems. The production characteristics and optimized completion design parameters of a well predicted by the expert systems will help in developing a tight oil reservoir more efficiently and economically.

Table of Contents

List of Figures

List of Tables

Acknowledgements

My studies at Penn State have been extremely rewarding and have contributed towards my overall growth. I would like to take the opportunity to thank the people who have contributed in my professional and personal life to help me achieve this milestone.

Firstly, I would like to thank Dr. Turgay Ertekin for his immense help and guidance during my PhD. His consistent advices helped me in keeping the pace and track of my research. His advices helped me to look ahead in the future and work hard for the opportunities that came for me during my stay at Penn State. I have learned a lot by interacting with him, taking classes under him and through our research meetings. I am grateful to him for making my experiences and learnings, both enjoyable and rewarding.

I would like to express my sincere gratitude towards my co-advisor, Dr. Zuleima Karpyn, for her constant support and guidance during my studies. She provided critical suggestions, encouragement and ideas that contributed towards this research work.

I am grateful to Dr. Luis Ayala, my committee member, for closely looking at my work and helping me to improve consistently throughout this research work. He, along with my advisors, helped me in learning the importance of *"Why? What? and How?"* during my research.

I would like to extend my appreciation to my committee members, Dr. Li Li and Dr. Kultegin Aydin for their interest in serving in my committee. In addition, I would like to extend my appreciation to Dr. Sridhar Anandakrishnan for over viewing my work during my comprehensive examination.

I gratefully acknowledge the research grant from Chevron. I would like to thank Mr. Tim Magner, Mr. Robert Lestz, Mr. David Liebmann, Mr. John Best, Mr. Balogun Oluwafemi, Mr. Suleen Bhagat and Dr. Qiang Sun for providing the data and support in the research.

I would like to thank my friends who have been helpful and supportive at the time of needs. I have been a part of different groups at Penn state that made my stay enjoyable. At Penn State, I mostly interacted and share memories with Clayton, Jeff, Alisha, Amir, Burak, Ghazal, Bahareh, Dennis, Harisha, Hemant, Emre Artun, Prob, Aseem, Adarsh, Mohata, Priyanka, Sandeep, Kshitij and Jaswanth.

I am very much indebted to my mother, Kanta Bansal, whose fond memories will always cherish in my heart. She had always been very supportive and attached to me. I wish you were still around to continue to love and support me, and see me achieve this academic honor. My father, Satyapal Bansal, has played an important role in my life. His loving and caring nature have been the source of inspiration for me. I would like to thank

To my father, Satyapal
my mother, Kanta
my brother, vijay
and my sister, Savita

Chapter 1 Introduction

Meeting the continuously increasing energy demands with depleting conventional hydrocarbon resources has proven to be unsustainable. Investigations in developing unconventional resources will help in complementing the conventional resources for a more stable supply. The unconventional resources are evaluated to be three times the proven reserves of conventional resources [Richard, 2010]. However, production from these resources is not economical with the current state of technology. Geology of unconventional reservoirs is quite complex; making their characterization a challenging task. The conventional methodology of characterizing these reservoirs are not effective, therefore; alternative methods should be adopted to find probable solution in the near future that can efficiently understand the complexities of these reservoirs.

This research focuses on evaluation of tight oil reservoirs with expert system applications. This research proposes a methodology that can be applied in tight oil reservoir systems to evaluate the reservoir potential. The capabilities of the expert systems developed include predicting cumulative oil, water and gas productions, and completion trends by establishing a neural relationship between the geo-physical data, completion and production characteristics. Different sets of integrated expert systems are

developed and applied in this research program. This dissertation is divided into different chapters to describe the development of expert systems. An outline of the different chapters is given here as follows:

- Chapter 2: In this chapter, a background of unconventional resources, their characterization, tools utilized and optimization algorithm are discussed.

- Chapter 3: This chapter states the problem solved in this research

- Chapter 4: The methodology developed in this research to characterize tight oil reservoirs is discussed.

- Chapter 5: A field application of the methodology developed in Chapter 4 is demonstrated.

- Chapter 6: In this chapter, results obtained and relevant discussions are provided.

- Chapter 7: This chapter summarizes the work carried and discusses some potential future work as a continuation project.

The results discussed in this dissertation show the ability of artificial expert systems in providing probable locations to drill a new well in a discrete tight oil reservoir. This work aids in establishing a relationship between geophysical properties and production characteristics of a tight oil reservoir. The developed methodology can be used in developing tight oil reservoirs efficiently.

Chapter 2 Literature Review

Unconventional reservoirs are sought to play a major role in the near future in meeting constantly increasing global energy needs. It is considered that unconventional resources could prove to be complimentary to conventional resources [Vassilellis, 2009]. Existence of these resources is known for decades but these accumulations were overlooked from economical point of view by various corporations. In general, these reservoirs, in a number of ways, have inferior characteristics as compared to conventional reservoirs; but have huge hydrocarbon storage capacities [Vassilellis, 2009]. Unconventional hydrocarbon resources have attracted different oil and gas operators recently due to their location and extent. It is believed that these resources will offer long life production [Stark, et al., 2007]. However, characterization and development of these resources efficiently possesses technological challenges. This chapter discusses about different unconventional resources, challenges posed in developing these formations and methods to evaluate them.

2.1 Unconventional Reservoirs

Definition of unconventional resources has changed over time. Earlier the definition was based on economics of the production; the reservoirs producing at un-

economical flow rates were referred as unconventional reservoirs [Lakatos, et al., 2009]. This definition will change with time, since; the reservoirs that have not been producing at economical rates can be produced economically with the advancement in technology. Therefore, more prudent definition of unconventional reservoir is based on the geological properties of the reservoirs and physical properties of the fluids [Lakatos, et al., 2009]. Based on the current definition, unconventional oil and gas reservoirs are grouped as follows:

- Unconventional oil: oil shale, tight oil reservoirs, heavy oilreservoirs, oil/tar sand and pyrobitumen deposits.

- Unconventional gas: gas shale, gas sand, tight sand gas, basin concentrated gas accumulation, associated gas, coalbed methane and methane hydrates.

Conventional and unconventional resources can be compared together using a resource triangle, where different resources for hydrocarbons are arranged on the basis of the complexity involved in producing from these resources as shown in **Figure 2.1** [Holditch, et al., 2007]. The resource triangle is applicable to all the natural resources and suggests that theses resources are distributed log-normally in nature. The conventional hydrocarbon resources are placed at the top of the triangle, representing the ease with which these resources can be produced. In addition, the volumes of these resources are

small as compared with unconventional resources, which cover most of the area on the resource triangle. As we move towards the base of the triangle, the reservoirs are lower grade; which usually means the reservoir permeability is decreasing. An improved technology will be required in order to efficiently produce from these resources. Each unconventional reservoir has a unique petrophysical property; increasing the complexity in analyzing their optimal development plans [Cramer, 2008]. Not only do the resources differ from each other, the reservoirs may behave quite differently within their own group. Therefore, a unique strategy will be required to develop these reservoirs [Slatt, et al., November 2008] [Russum, 2010]. Technical innovations in characterizing and optimally developing these resources will be required to make them economical in future [Yuko, et al., April, 2001].
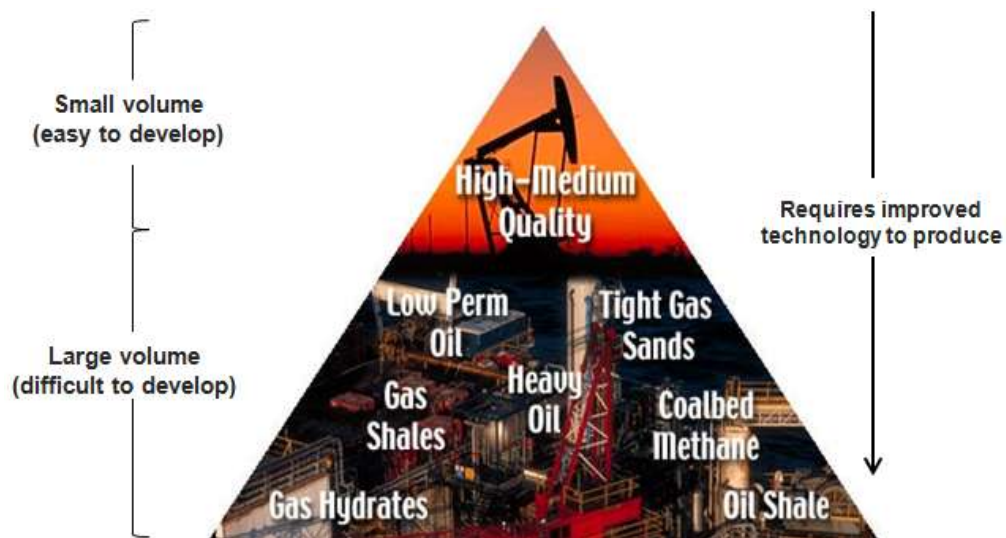
Fig. 2.1: Resource triangle (Holditch, et al., 2007)

2.1.1 Shale Oil and Gas Reservoirs

The origin of shale oil is not well known but it primarily is considered to be the remains of algae, spores, pollen, plant cuticle and corky fragments of herbaceous and woody plants, and other cellular remains of lacustrine, marine, and land plants [Dyni, 2006]. Shale oil is a kerogen bearing rock which is considered to be a pre-phase of petroleum bearing rock [Erturk, 2011]. Shale reservoirs are one of the largest known hydrocarbon resources in the world [Biglarbigi, et al., 2008]. Shale oil bears huge resources with an estimation of ~3 trillion barrels of recoverable oil worldwide [Klienberg, et al., July 2007]. Global shale oil reserves are listed in **Table 2.1** (adapted from Dyni 2006). A significant part of global energy supply is expected to come from shale oil in the wake of conventional oil peaking [Moritis, 2008]. Development of these resources will be crucial to world's economics. Therefore, good investment strategies should be in place to maintain the supplies from these reservoirs [Johnson, et al., 2004]. Johnson et al. (2004) suggested that nearly 750 billion barrels of oil can be recovered from shale in US with 2004's technological standards. Thus, these resources will provide oil security for 100 years or more. Potential of these resources is huge, making shale oil strategically important for energy security in United States. Green river formation alone has ~1.2 trillion barrels of oil [Klienberg, et al., July 2007]. Shale oil and gas reservoirs are abundant and scattered in the North America as shown in **Figure 2.2**.

Table 2.1: World shale oil reserves

Country	Reserves (Billion bbl)	Date of estimation
Australia and NewZealand	31.73	1987
Belarus	7	
Brazil	82	1969
Canada	15.25	1981
China	18.3	1985
Republic of Congo	100	1958
Egypt	5.7	1984
Estonia	16.2	1998
France	7	1978
Germany	2	1965
Israel	4	1982
Italy	73	1978
Jordan	34.2	1997
Kazakhstan	2.8	1996
Morocco	53.3	1984
Myanmar	2	1924
Russia	247.9	
Sweden	6.1	1985
Thailand	6.4	1988
Turkmenistan & Uzbekistan	7.7	
Turkey	2.24	1993
Ukraine	4.2	1998
UK	3.5	1975
USA	2085	1980
Uzbekistan	8.4	

Fig. 2.2: North American shale plays [EIA, 2011]

The history of first shale project in U.S. dates back to 1910 and was incorporated in naval petroleum reserves [Klienberg, et al., July 2007]. The first shale oil production is reported in 1880 by Scotland [Dyni, 2006]. In the past, shale oil has been recovered by mining, and currently Shell [Shell oil, 2006] and Chevron [Chevron USA, 2006] are testing the feasibility of in-situ conversion processes. It is estimated that shale oil could be commercial with $30/bbl oil and production of 500,000 bbl/day could be achieved by drilling 150 acres/well [Stark, et al., Dec, 2007].

Gas production from shale plays will contribute towards ~46% of the total gas production in U.S. by the year 2035 as shown in **Figure 2.3**. Unconventional gas resources in US accounts for 43% of the total production. The reported production is coming from 30% of the proven reservoirs in the country [Khlaifat, et al., 2010] [Khalifat, et al., 2011]. The development of the aforementioned resources is primarily carried by mid to small sized companies rather than the majors [Klienberg, et al., July 2007]. Production of shale gas started with Barnett Shale located in the Bend Arch-Fort Worth basins of Texas. The Barnett group is estimated to have over 30 trillion cubic feet (Tcf) of resource [Holditch, et al., 2007]. Unconventional hydrocarbon potential in North Africa is estimated to be approximately 134 billion barrels of oil equivalent [Chelini, et al., 2010]. Tight oil play in North and South Dakota, Montana alone has 3-4.3 billion barrels of technically recoverable oil equivalents. This estimate is 25 times the initial estimate reported in 1995. Although, it is proven that unconventional resources are huge but information about their potential is inconsistent and requires a correct and consistent evaluation [Russum, 2010] [Lakatos, et al., 2009].
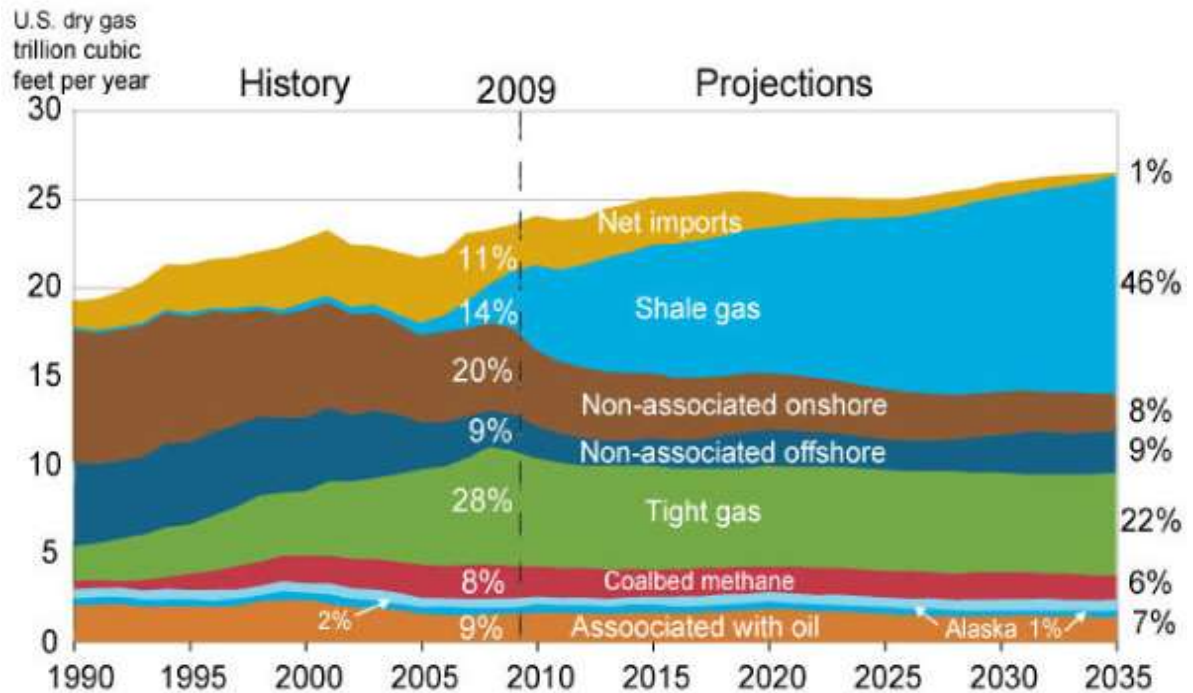
Fig. 2.3: U.S. natural gas supplies [EIA, 2011]

2.1.2 Tar Sands

Sands that contain highly viscous hydrocarbons cannot be produced using conventional methods of oil industry are identified as tar sands [Nilsen, et al., 2008]. Typically composition of oil sand is 75% inorganic matter, 10% bitumen, 10% silt and clay, and 5% water [Humphries, 2008]. The API gravity of the crude oil is less than 10 [Erturk, 2011]. The first tar sand formation in North America was discovered near Athabasca River in 1875 [Sheppard, 2005]; and presently, tar sands account for 46% of total oil production in Canada. Tar sands contribute in high hydrocarbon reserves in

Canada, making the country second largest with crude reserves after Saudi Arabia [Humphries, 2008]. Potential of tar sands is huge around the world as shown in the **Table 2.2** [Meyer, et al., 2003]. However, producing tar sand is a challenging task given the extreme properties of the fluid. Presently, based on the depth of the resource, two methods are employed to produce from them. If the reservoir is shallow then open pit mining is carried and for deeper formations, where mining cannot be carried, in-situ methods are used. In-situ methods, in general, include steam assisted gravity drainage (SAGD) and cyclic steam stimulation (CSS).

Table 2.2: Regional distribution of heavy oil and natural bitumen

Region	Heavy Oil		Natural bitumen	
	Recovery factor	Technically recoverable BBO	Recovery factor	Technically recoverable BBO
North America	0.19	35.3	0.32	530.9
South America	0.13	265.7	0.09	0.1
W. Hemisphere	**0.13**	**301**	**0.32**	**531.0**
Africa	0.18	7.2	0.10	43.0
Europe	0.15	4.9	0.14	0.2
Middle East	0.12	78.2	0.10	0.0
Asia	0.14	29.6	0.16	42.8
Russia	0.13	13.4	0.13	246.1
E. Hemisphere	**0.13**	**133.3**	**0.13**	**332.1**
World		**434.3**		**863.1**

2.1.3 Tight Oil and Gas Reservoirs

Reservoirs with very low porosity and permeability are considered to be tight reservoirs [Tang, 2009]. Typically, the permeability of these reservoirs is lower than 0.1 md [Wattenbarger, 2002] and may range to micro Darcy level. These reservoirs are usually very thick, the net pay of these reservoirs can be several hundred feet. These resources are vast and widely dispersed. Production from individual wells in these reservoirs is not considered to be significant as compared to conventional oil and gas reservoirs but have much longer producing lives [Khalifat, et al., 2011]. In general, these reservoirs have natural fractures; which helps for the wells to flow for long terms [Arevalo-Villagram, et al., 2005]. Properties of these reservoirs provide challenging conditions for improved oil recovery by water or gas injection; however the depletion drive is proven to be more efficient than conventional reservoirs [Legrand, et al., 2010]. Improved technology is foreseen in order to increase production from these resources. Recent advances in hydraulic fracturing improved the production in Bakken play. Increased production and reassessment of the play led the belief that this area has the potential to become "the next Saudi Arabia" [Miller, et al., 2008].

Bakken formation is a tight formation with characteristics of low permeability and porosity shale. The depth of the formation ranges from 8000 to 12000 ft. This formation is considered to be the most significant tight oil reservoir in the United States in the last

decade. USGS re-estimated the potential of the Bakken play in 2008 where the technically recoverable oil was identified to be 4-4.3 billion barrels. This estimate was 25 times higher than the 1995 estimate of 151 million barrels [USGS, 2008]. Advancements in technology, mainly, geological modeling, exploration techniques, drilling and completion technologies have helped in making Bakken as the largest oil play in the Continental U.S. This estimate is expected to increase with improvement in the current practices and technology for production from these resources. These resources have been identified to be important for U.S. energy needs; therefore, analyzing production has gained considerable interest over the past few years [Kabir, et al., 2010]. However, production analysis and forecasting is a daunting task due to the complex geology, completion and fracture complexities, and absence of representative hard computing methodologies.

2.1.4 Coal Bed Methane

Methane stored in coal seams is referred as coal-bed methane. Coal bed is a sedimentary rock that contains more than 50% of organic matter [Jenkins, et al., 2008]. Methane in the formation is generated by bacterial and/or geochemical action on the organic matter. Production of methane gas from coal mines has changed the fate of energy industry and coal mining industry. Methane was considered as a hazard in the coal

mines from early 1800's to mid 1950's [Flores, 1998]. Initial investigations in coalbed methane in U.S. started by Bureau of Mines and DOE in 1970 [Clarkson, et al., 2010]. According to USGS survey carried in 2000, U.S. has ~700 TCF in coal bed methane and ~100 TCF is economically recoverable with existing technology [USGS, 2000].

With the advancement in technology and increased number of wells, coalbed contributes ~8% of the total gas production in U.S. Production from individual basins in U.S. have increased significantly over the last 3 decades as shown in **Figure 2.4** [Chakhmakhchev, et al., 2008]. CBM is being produced from shallower coal seams making the CBM wells cheaper [Palmer, 2010] (costs ~$300K-$1,200K/well) as a result nearly 40,000 CBM wells are employed to produce methane from coal beds. Currently, coal bed methane is produced majorly in U.S., Canada, Australia, China and India as shown in **Figure 2.5** [Chakhmakhchev, et al., 2008]. The detailed reserves of CBM in the world are shown in **Table 2.3** [Clarkson, et al., 2010]. It can be seen in the table that the potential of CBM is huge but the recovery with the current state of technology is low. CBM reservoirs are considered as potential storage sites for sequestering CO_2 and to enhance the CBM production [Mazzotti, et al., 2009].
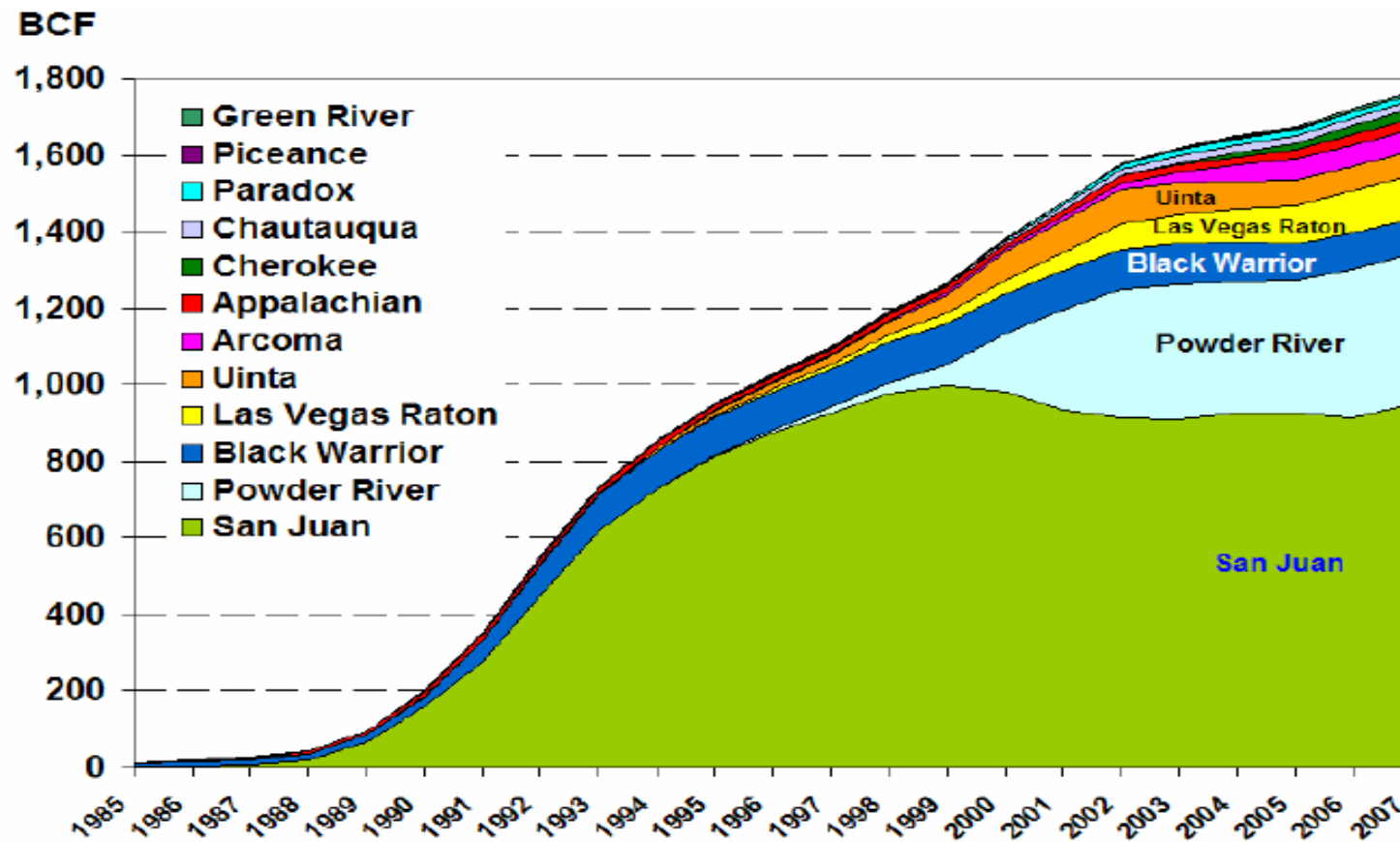
Fig. 2.4: Production history of major coalbed reservoirs in U.S. [Chakhmakhchev, et al., 2008]
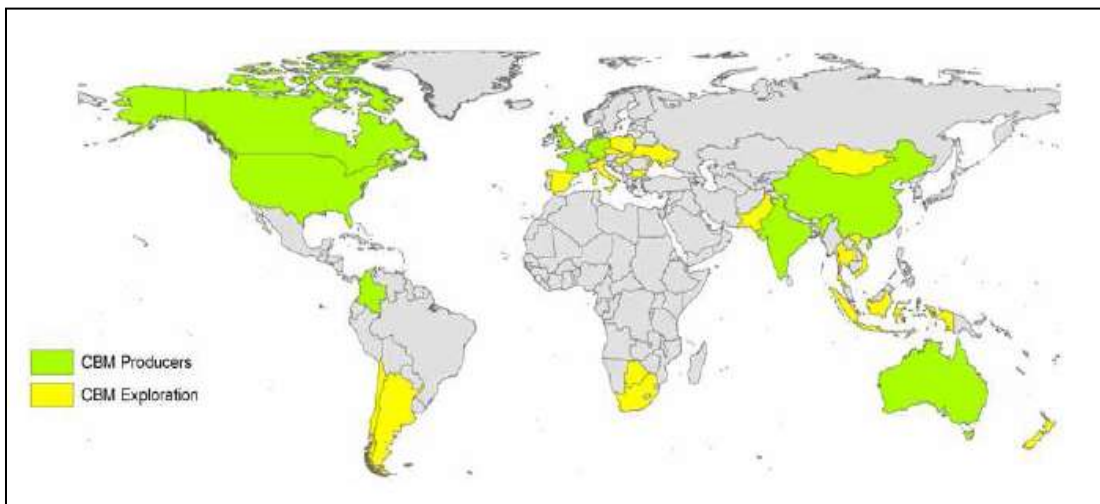
Fig. 2.5: CBM producing countries [Chakhmakhchev, et al., 2008]

Table 2.3: World CBM resources

Country/ Region	CBM Resource in place (TCF)	CBM Recoverable Resource (TCF)
Russia	450-2000+	200
China	700-1270	100
United States	500-1000	140
Canada	360-460	120
Indonesia	340-450	90
Southern Africa	90-220	50
Western Europe	200	30
Ukraine	170	20
Turkey	50-110	10
India	70-90	20
Kazakhstan	40-60	10
South America + Mexico	50+	10
Poland	20-50	5

2.1.5 Gas Hydrates

At low temperature and high pressure, light natural gas combines with water to form gas hydrates. Methane is a dominant component, besides other natural gases. The hydrates are stored underground in deepwater and permafrost regions [Saeki, et al., 2008]. Methane hydrates are abundant on the Earth and have potential to solve world's energy needs for centuries [Demirbas, 2010]. Current estimates of the amount of gas in the world's marine and permafrost gas hydrate accumulations are in rough accord at about 20,000 trillion m^3 (706,300 trillion ft^3) [Collett, 2002]. The known sources of methane hydrates are scattered around the globe as shown in **Figure 2.6** [Collett, 2002].

Unlocking the potential of methane hydrates will require massive research in the future. The stability of gas hydrates depends on pressure, temperature and composition of the gas in the hydrates [Majorowicz, et al., 2001]. Studies targeting changes in existing pressure, temperature and composition conditions to dissociate the hydrates from its natural form have been conducted [Majorowicz, et al., 2001]. Dissociating methane from hydrates is an endothermic reaction. Use of fossil fuels to heat and break these hydrates will not be an economical process [Ikegawa, et al., 2010]. Recent research suggests use of CO_2 for breaking the hydrates and releasing methane gas. The process will form CO_2 hydrates (an exothermic process) and the chemical reaction will release the heat, that will be used in-situ by methane hydrates [Ikegawa, et al., 2010].
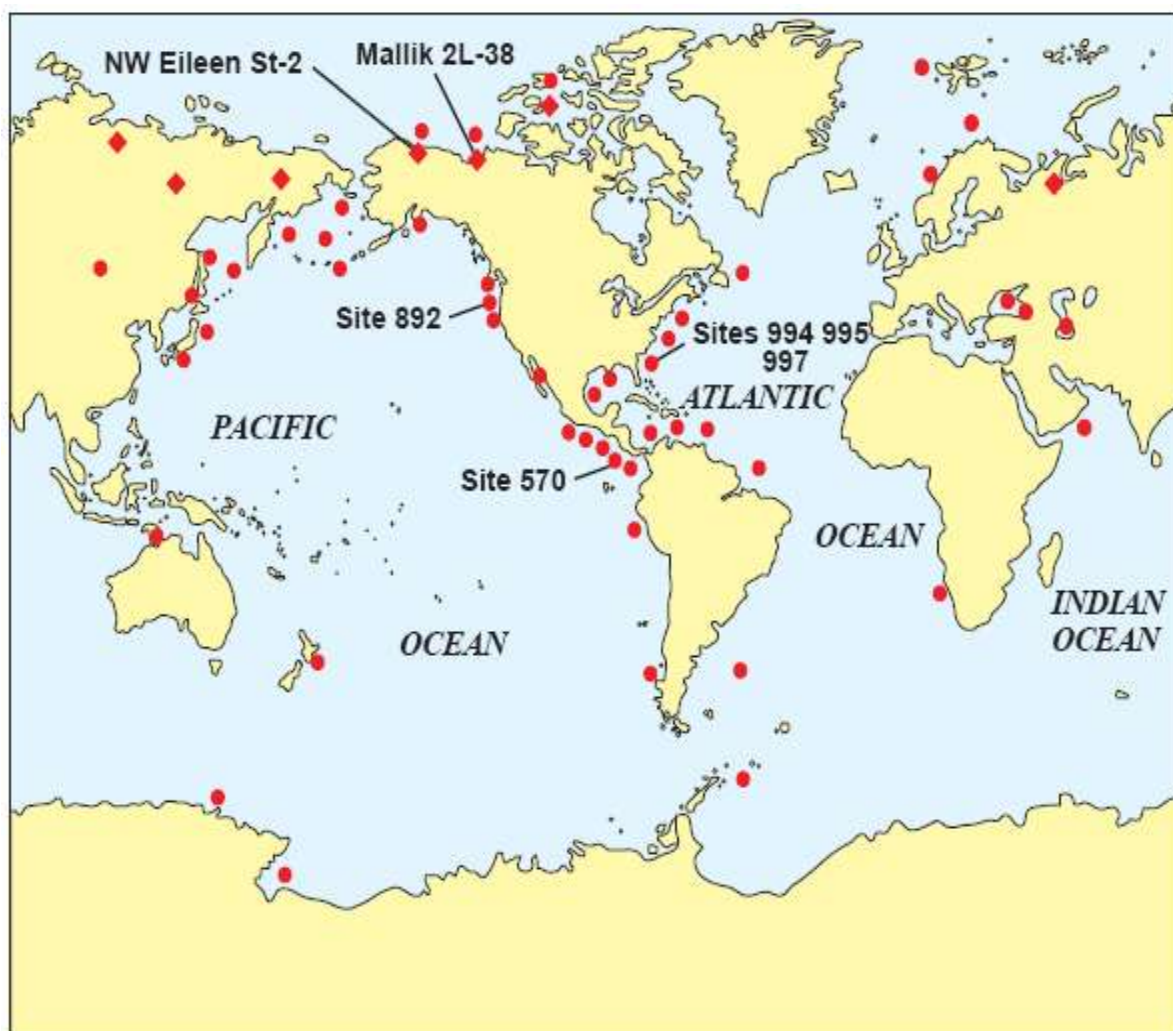
Fig. 2.6: Locations of known gas hydrates [Collett, 2002]

2.2 Unconventional Reservoir Characterization

The process of assigning reservoir properties quantitatively is known as reservoir characterization [Mohaghegh, et al., 1996]. Gaining elaborative information about a reservoir is important for maximizing benefits from the reservoir in the development stages of the reservoir. The first stage of reservoir characterization is to gather seismic information of the reservoir and evaluate the quality of the data [Decker, 2004]. The seismic data is humongous and is extracted in the form of seismic attributes. In the second stage, an exploratory well is drilled with reference to the seismic data to gather information about the reservoir quality and fluid properties. Typical information gathered includes core data, formation pressure data, micro-seismic data, well logging data, well images, fluid samples etc [Samuel, et al., 2000] [Vefring, et al., 2002] [Artun, et al., 2005]. The information gathered is collectively used to characterize the properties of the reservoir to optimally develop the field; thus maximizing the production from the reservoir. Traditionally, empirical relationships and hard computing methods are used to characterize and optimize production from the reservoirs. However, for unconventional reservoirs the standard methods for evaluation are not suitable because of the complex geology [Lee, et al., 1994].

Different techniques have been developed in the past to characterize the reservoirs. Vefring et al. (2002) developed a method to estimate permeability and

pressure of the reservoir along the well by evaluating the data collected during underbalanced drilling. Artificial expert systems have been used to predict the permeability of a reservoir using well log data [Aminian, et al., 2005] [Molnar, et al., 1994] [Babadagli, et al., 2002]. Artun et al. (2005) developed a method to predict gamma ray logs using seismic data. Production has been tied with seismic and completion data, and the method was later used to identify top gas producer in a tight gas reservoir [Thararoop, et al., 2008].

2.3 Artificial Neural Networks

Artificial neural networks (ANN) are information processing mathematical models that attempt to simulate biological central nervous systems for processing information [Graupe, 2007]. Artificial neural networks were first introduced in the late 1950s first by McCulloch and Pitts (1943) [Mcculloch, et al., 1943] and later with the invention of perceptrons by Rosenblatt (1962) [Rosenblatt, 1962]. However, for more than twenty years, interest in artificial neural networks diminished before works by scholars such as Hopfield [Hopfield, 1982], Kohonen [Kohonen, 1982] and Hecht-Nielsen [Hecht-Nielsen, 1987] reinvigorated the use of artificial neural networks.

The information in a biological nervous system is processed and transferred through smaller units. **Figure 2.7** shows a typical example of the process. A biological neuron has three major parts: a body (or soma), axon and dendrites [Yegnanarayana, 1999]. The cell contains the nucleus. The action of the cell is to gather all the information from dendrites and once enough information is received, an output signal is fired through axon [Fausett, 1994]. Axon is a cylindrical structure that generates a cell action potential. axon transfers the information from its neuron to next higher neuron. Dendrites are the tree like structure of the neuron. Dendrites act as input receivers for the neuron via a synaptic connection with the axon of the previous neuron [Schalkoff, Robert J., 2009]. In a biological environment, a synapse converts a presynaptic electrical signal into a chemical signal and back into a postsynaptic electrical signal [Shepherd, 2004]. This chemical reaction modifies the input signal into the final form that will add information to the output neurons in the brain [Fausett, 1994]. Gathering, processing and transmitting the signals takes ~1 millisecond in a bio-logical neuron. On the other hand, a silicon logic gate takes 1 nanosecond for processing similar information [Haykin, 1994]. However, brain makes up for the difference in the speed by making massive interconnections via the nearly 10 billion neurons and 60 trillion synapses or connections.
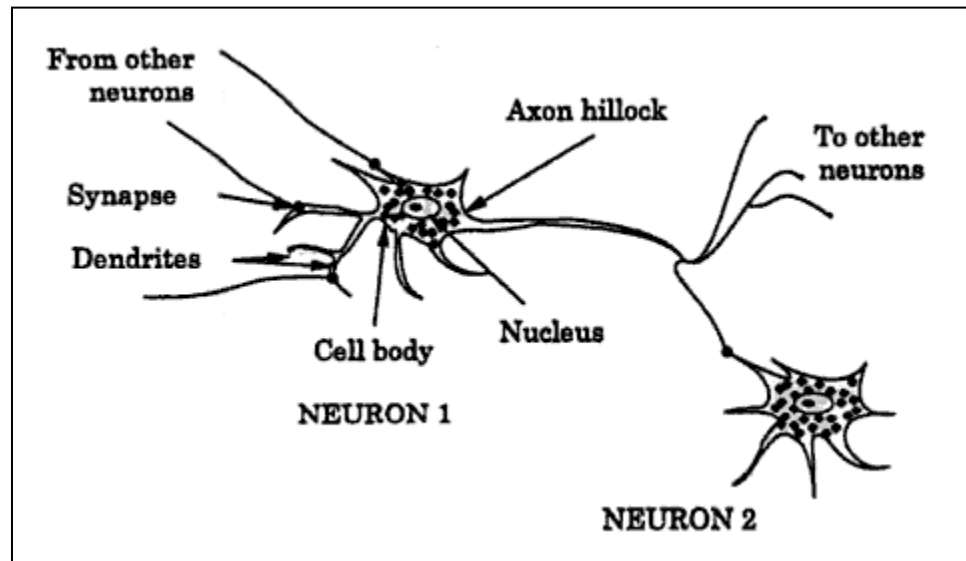
Fig. 2.7: A biological neuron's input and output structure [Yegnanarayana, 1999]

In an ANN, the simplest processing unit is called neuron and the structure of the unit is shown in **Figure 2.8** (adapted from [Priddy, et al., 2005]). The neuron used in ANN is analogous to the biological neuron. As shown in Figure 2.8, functioning of input streams is similar to the dendrites, neuron is similar to body or soma (nucleus) and output stream is similar to axon. Signals are attenuated by weights as opposed to chemical filtering the nervous system. The assumptions made in developing ANNs are:

1) Information is passed between neurons over connections links.

2) Each link has some associated weight which is multiplied by the signal transmitted.

3) The capabilities and robustness of the neural network depend upon the learning

   abilities and can be applied to pattern recognition problems and optimization

   techniques.
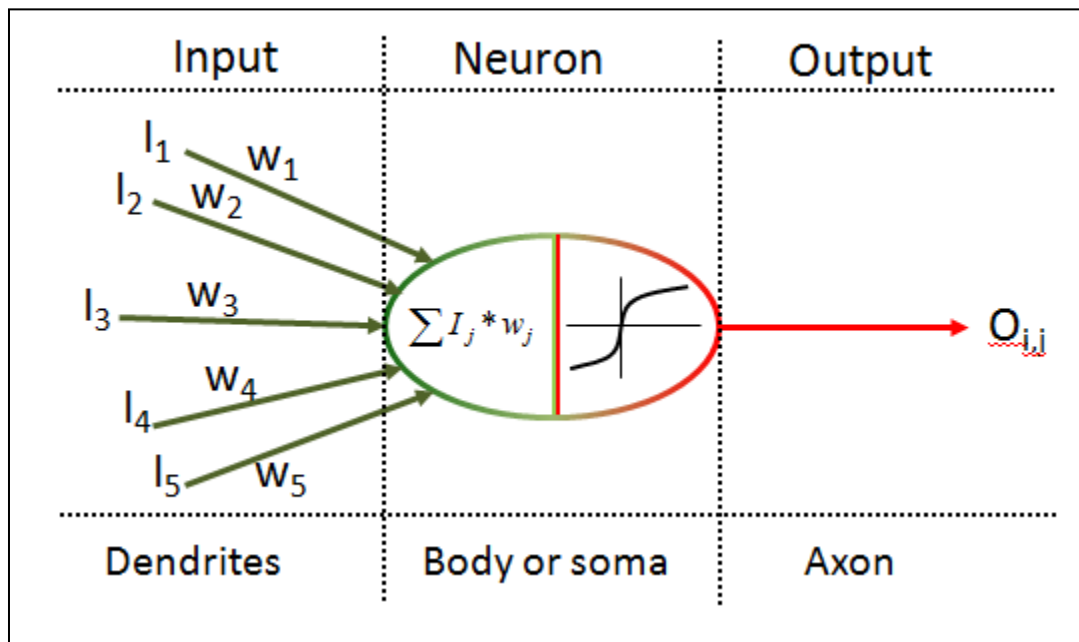
Fig. 2.8: Comparison of biological and mathematical neuron

As shown in Figure 2.8, all the inputs are gathered by the neurons along with their respective weights are processed using an activation function before emitting an output signal. The output of the activation function acts as the input for the next hidden layer neurons and subsequently for the output layer. In general, the activation is same for all

the neurons in a particular hidden layer [Fausett, 1994]. The most common functions

used to transfer the data are:

- ***Linear function***: This function converts the net input to an output value linearly

  between -1 and 1 as shown in **Figure 2.9(a)**.

- ***Tansig function***: This function is also known as bipolar sigmoid function as

  shown in **Figure 2.9(b)**. In this function the net input is converted between -1 and

  1 by the equation

$$f(x) = \frac{2}{1 - e^{-2x}} - 1 = \frac{e^x - e^{-x}}{e^x + e^{-x}}$$
(2.1)

- ***Logsig function***: This function is also known as binary sigmoid function as

  shown in **Figure 2.9(c)**. In this function the net input is converted between 0 and

  1 by the equation

$$f(x) = \frac{1}{1 + e^{-x}}$$
(2.2)

(a) Pure   (b)

(c)
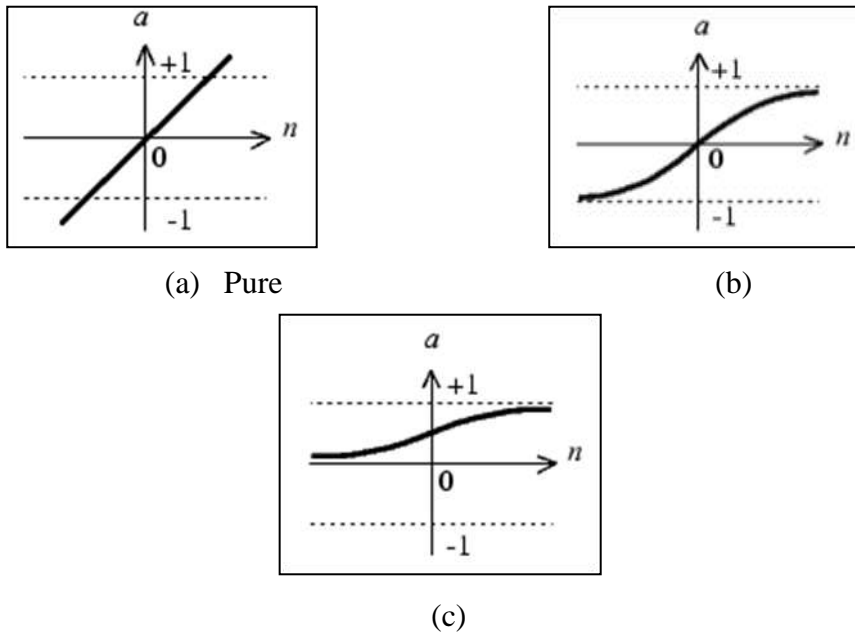
Fig. 2.9: Most common activation functions [MATLAB, 2011]

2.3.1 General Architecture of an ANN

A typical architecture of ANN has three components: an input layer, an output layer and one or more hidden layers and each layer contains different number of neurons that varies from problem to problem. The information of the system is entered through the input layer and simplified by the hidden layers. The outermost layer that provides the output of the neural network is called as the output layer. Each neuron is connected to other neurons by means of a communication link which has an associated weight with it.

Each neuron sends one signal at a time although the signal is broadcasted to several other neurons in the next layer.

A network has to be optimized for the number of the hidden layers and the number of neurons in each of the layers. The optimization process is based on the error observed during the training of the network; and then updating the weights of the neurons. The number of hidden layer neurons, number of layers, transfer functions, learning and training algorithm are independent variables used to optimize the network. Once any of the parameter is changed, the weights of each of the neurons are again optimized by minimizing the error. However, there is no fixed rule to define the entire structure of a neural network. To start the training procedure by selecting total number of neurons, different rule-of-thumbs can be used [Wardsystems, 1998] [Xu, et al., 2008]. The most popular rule to start network training is as follows [Wardsystems, 1998]:

$$N_{HN} = \frac{N_I + N_O}{2} + \sqrt{N_{TP}} \qquad (2.3)$$

where, N_I is the total number of input neurons, N_O is the total number of output neurons, N_{TP} is the total number of training patterns and N_{HN} is the total number of hidden neurons. Changing the number of neurons, hidden layers etc. is a heuristic method which starts with one hidden layer and neurons equal to the number of output neurons (alternately, N_{HN} in equation 2.1). Then, we gradually increase or decrease the number of

neurons in the hidden layers. The structure that gives the least error on the testing sets is chosen as the final architecture of the neural network. A typical fully connected neural network looks like the one shown in **Figure 2.3**.
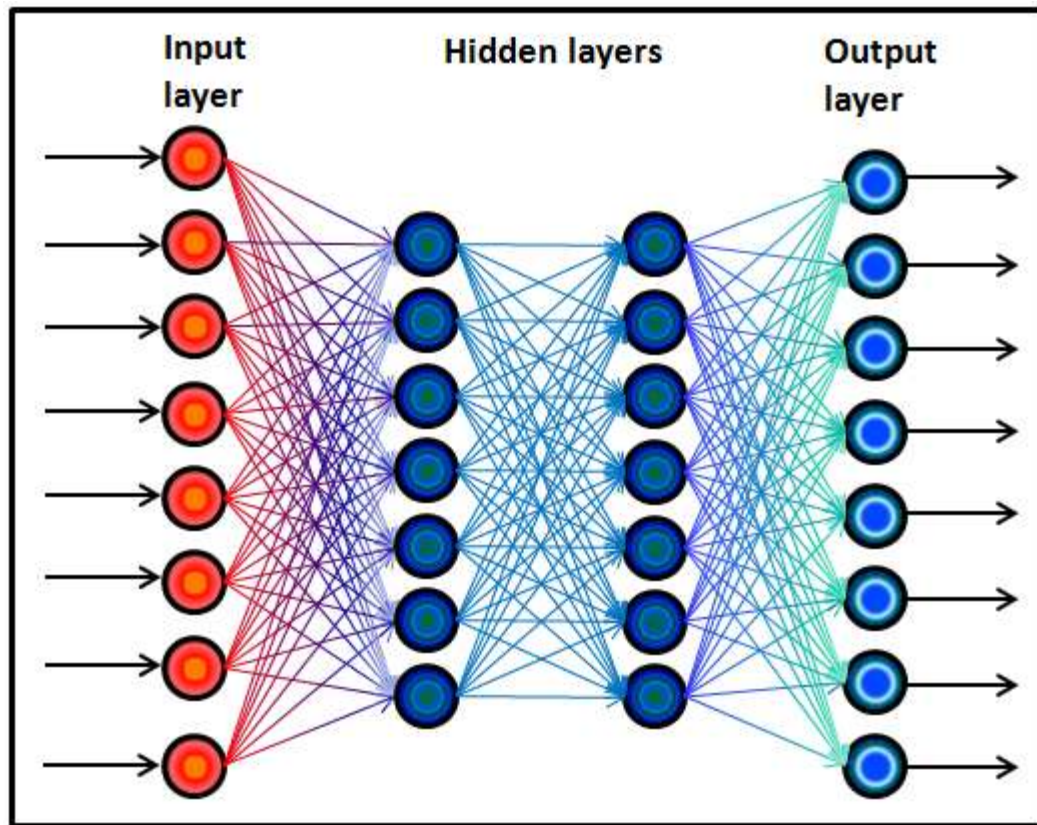
Fig. 2.10: Typical topology of ANN

2.3.2 Feedforward Networks

The earliest and simplest neural network type is the feedforward network. The input data is processed in a layer-by-layer manner [Yegnanarayana, 1999]. Each layer in

this network receives information from the previous layer and transfers the information to the next layer in the network. There are no backward links created in the network. Feedforward networks can consist of a single input and output layer (known as a perceptron) or as many subsequent layers or perceptrons as needed. The network shown in Figure 2.9 is an example of simple feedforward network, where the information is flowing from input layer to the output layer.

2.3.3 Feedforward Back Propagation Networks

Backpropagation is a gradient decent algorithm in which weights and biases of the network are updated in the direction of the decreasing performance function or the negative of the gradient. Backpropagation network is also known as the generalized delta rule. This algorithm is based on other optimization techniques like conjugate gradient method and the Newton methods. One of the iteration of the algorithm can be written as:

$$X_{K+1} = X_K - \alpha_K g_K \qquad (2.4)$$

In **Equation 2.4**, X_K is a vector of current weights and biases, g_K is the current gradient and α_K is the current learning rate. The process in feedforward backpropagation network can be divided into three stages [Schalkoff, 1997]:

- Transfer information from input to the output layer using the feedforward network approach. Flow of information is from input layer to hidden layer 1; hidden layer 1 to hidden layer 2 and finally to the output layer.

- Estimate the error in the calculated output and known output during training phase of the network.

- Use the errors to update the weights of the network from last layer to the first layer (backward propagation of error)

The objective of the process mentioned above is to minimize the error by adjusting the weights of the output neurons, hidden layer neurons and input layer neurons in the same hierarchy as discussed earlier.

2.3.4 Cascade Feed forward Networks

Cascade feed forward networks are feedforward networks employing supervised learning algorithm for artificial neural networks. The output of the network has input from all the neurons in the network. Information is cascaded from input layer to all the subsequent layers in the network [Schalkoff, 1997]. **Figure 2.10** shows a typical architecture of a cascade feedforward network. In this example, there are two hidden layers with 3 and 4 neurons, respectively. The input and output layers have two neurons each. As shown in the figure, information from input layer is transmitted to hidden layer

1, hidden layer 2 and the output layer. Information from hidden layer 1 is transmitted to hidden layer 2 and the output layer, and so on. Thus, the output layer gathers information from all the preceding layers.
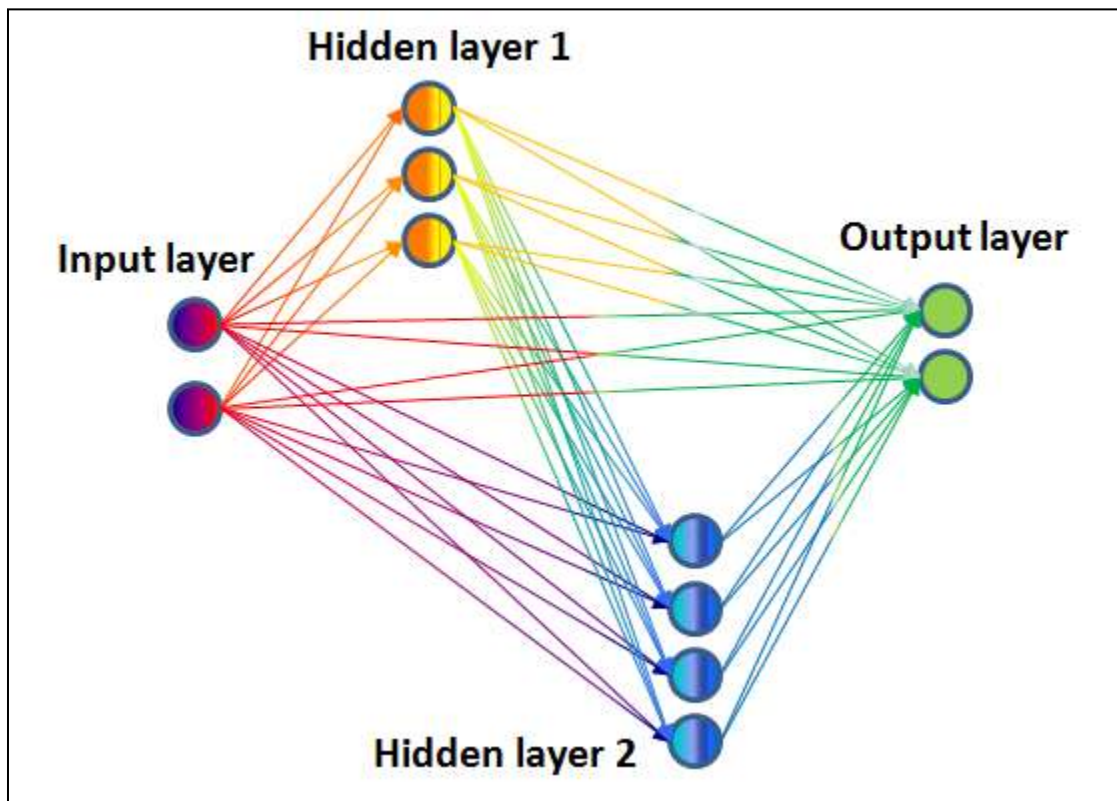
Fig. 2.11: Typical architecture of cascade feedforward network

2.3.5 Examples of Neural Network Applications

Neural networks have been successfully applied in the various fields. The most common applications have been in stock market trading [Vanstone, et al., 2009], food

processing industry [Torrecilla, et al., 2007], material research for defense applications [Ramaiaha, et al., 2010], traffic control [Kalyoncuoglu, et al., 2004], and in the oil industry.

Use of artificial neural networks, fuzzy logic systems, and expert systems started in mid 1980's in the oil and gas industry [Gharbi, et al., 2005]. Applications developed using the three artificial intelligence methods have a major impact in the petroleum industry. ANNs are suitable for identifying pre-existing complex relationships. The successful applications in oil industry include forecasting gas production [Al-Fattah, et al., 2001], evaluating inter-well connectivity [Lim, et al., 1999], infill drilling strategies [Thararoop, et al., 2008], optimal well drilling [Morooka, et al., 2001], formation analysis and evaluation [Ertekin, et al., 2005], enhance oil recovery applications [Artun E. F., 2008], [Karambeigi, et al., 2011] [Elkamel, 1998] etc.

2.4 Ensemble Based Optimization (EnOpt)

The EnOpt is based on Kalman Filter, and the formulation of the methodology started in 1994 [Evensen, G., 1994]. The method is used in the industry for history matching problems [Jafroodia, et al., 2011], production optimization and field development [Chaudhri, et al., An improved approach for ensemble-based production

optimization, 2009], [Chaudhri, et al., 2009]. EnOpt is an iterative procedure to optimize an objective function [Chen, et al., 2008]. This method has two distinct features

- In order to search for an optimum objective function, search direction is approximated by an ensemble. In addition, the magnitude of improvement in the input parameter is based on individual sensitivity of the parameters; also calculated from the ensemble.

- Uncertainty of the parameters affecting the objective function can also be modeled in the algorithm.

The methodology starts with identifying the objective function and the key parameters that are essential for the objective functions. Input vector can be referred to as control variables and can be defined as

$$X = \left[x_1, x_2, x_3, x_4, \dots x_{Nx} \right]$$ (2.5)

where, N_x represents the number of control variables in the system. The optimization procedure starts with setting the upper and lower limits to individual variables and defining a starting vector of these variables (X_0). Normally, an average value of the minimum and maximum value of a variable can be selected. Objective function (F_0) is evaluated using the control variable (X_0). Sensitivity of the control variable with the objective function is approximated by the equation

$$C_{x-F} = \frac{1}{N_e - 1} \sum_{j=1}^{N_e} \left(x_{l,j} - \langle x_l \rangle \right) \left(F\left(x_{l,j}\right) - \langle F(x_l) \rangle \right) \qquad (2.6)$$

where, N_e is the size of the ensemble and $F(x_{l,j})$ is the objective function for the jth control

vector in the ensemble, $\langle x_l \rangle$ is the expected value of the control parameters for iteration

index l and $\langle F(x_l) \rangle$ is the expected value of objective function for iteration index l and

are calculated as

$$\langle x_l \rangle = \frac{1}{N_e} \sum_{j=1}^{N_e} x_{l,j} \qquad (2.7)$$

$$\langle F(x_l) \rangle = \frac{1}{N_e} \sum_{j=1}^{N_e} F\left(x_{l,j}\right) \qquad (2.8)$$

This method is adapted from Chen et al. (2008) and Chaudhri et al. (2009). In the original

method the control variables are permitted to change over time. To counter the problem

of uncertainty in the variables (such as operational conditions changing with time), a

smoothening parameter is used. A smoothening parameter in updating controls will not

be required for a system with fixed control parameters that do not change with time

during the time of study. The updating technique is based on the steepest ascent method

formulated as

$$x_{l+1} = x_l + \frac{C_{x-F}}{\alpha} \qquad\qquad (2.9)$$

where x_{l+1} is the updated control parameters at iteration index of $l+1$, α is the standard deviation of the objective function F calculated for the ensemble of size N_e.

2.5 Hybrid ANN-Optimization Algorithm Approach

Researchers in the past have tied neural network applications with an optimization protocol for making the process time efficient. Algorithms like EnKF, EnOpt and Genetic algorithm (GA) have been used with hard-computing software to optimize a given problem. The coupling of optimizations algorithms with hard computing tools have been successfully used in history matching problems [Evensen, et al., 2007], closed loop production optimization with EnOpt [Chen, et al., 2008], production optimization with CGEnOpt [Chaudhri, et al., 2009] [Chaudhri, et al., An improved approach for ensemble-based production optimization, 2009] production scheduling with GA [Harding, et al., 1998] and pipeline optimization using GA [Goldberg, et al., 1985]. Applications of soft computing tools coupled with GA for optimizing reservoir engineering problems have been studied in the past [Artun E. F., 2008].

Chapter 3 Problem Statement

As the global demand for energy continues to grow, it is known that the energy needs cannot be fulfilled solely by conventional resources for oil and gas. It is expected that the demand for energy will quadruple in the 21st century (Lakatos et al, 2009). Specifically, it is projected that the energy demand will soar by 50% within the first quarter of the century and most of this demand will come from Eastern countries viz. India, China and Indonesia (Stark, et al., December 2008). It is also expected that the current production of hydrocarbons from conventional resources will decline at a rate of 4.5% annually against an expected 1.4% steady increase in demand (Stark, et al., December 2008). Peak production from the conventional oil reservoirs will be observed in 2025 [Mohr, et al., 2009]. Whereas, some researchers have projected an increase in total liquid production from conventional reservoirs by incorporating ramped-up production and new estimated reservoir discoveries around the world as shown in **Figure 3.1** [Richard, 2010]. At the present time, global hydrocarbon (HC) potential of unconventional resources are evaluated to be nearly three times that of conventional resources, though with existing technology these resources are projected to contribute no more than 12% of the HC liquid production by the year 2035 as shown in Figure 1 [Richard, 2010]. It is also believed that because of large resources unconventional

reservoirs can fill the energy gap between the demand and supply represented in **Figure 3.2**.
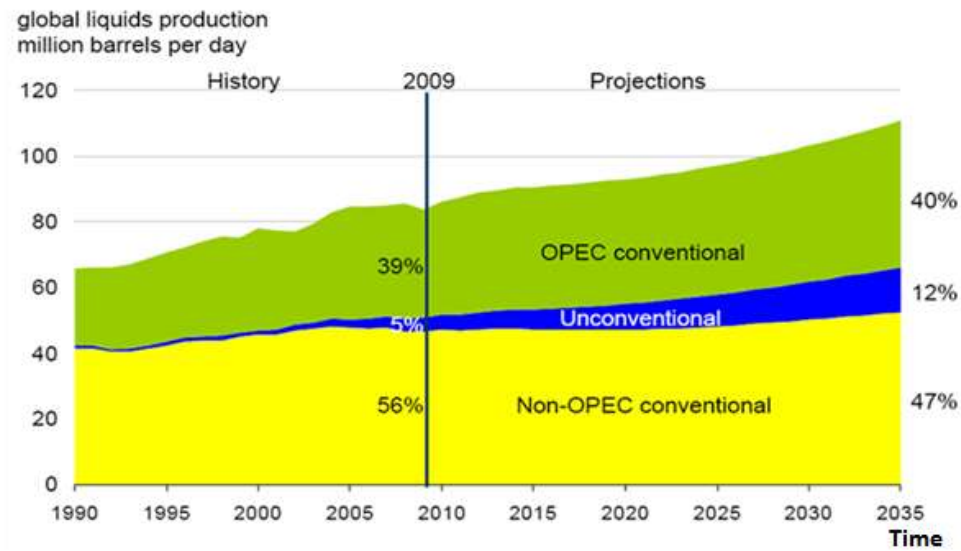
Fig. 3.1: Production potential of unconventional and conventional reservoirs [Richard, 2010]

Fig. 3.2: World oil production and demand

The potential of unconventional hydrocarbon resources is estimated to be nearly seven times that of proven and unproven conventional hydrocarbon resources (Stark and Fryklund 2007). Despite of high potential of unconventional resources, production from these reservoirs is not economical with the current state of technology (Khalifat, et al., November 2010). For unconventional oil, nearly 20% of the oil in place is technologically recoverable and only 2% is economically recoverable (Kawata, et al., 2001). These resources possess huge future potential provided they are exploited effectively, which will require a representative characterization of a complex reservoir. Given the nature of these resources, it will be a challenging task (if not impossible) to characterize these reservoirs with the conventional methods for e.g., distribution of reservoir properties using core data gathered at selected locations or by using pressure transient analysis based on volumetrically averaged permeability (Mohaghegh, et al., 1996). Traditionally, empirical relationships are used to relate geo-physical data with reservoir properties like porosity, permeability, saturation etc. However, these relationships are mainly developed for conventional reservoirs where grain size, porosity, permeability values do not change drastically, thus often characterize the conventional reservoirs well and contrary pose challenges in characterizing unconventional reservoirs (Aminian, et al., May 2005).

In order to characterize unconventional resources, special evaluation methods will need to be developed and applied. These reservoirs can be studied with

simple mathematical models, complex models or pattern-recognition techniques (Nikravesh, et al., 2001). Simple models may become inaccurate because of the assumptions made in simplifying the problem especially for unconventional resources. Inaccuracies in complex models arise due to uncertainties associated with additional layer of data required by the model (Nikravesh, et al., 2001). The third category involves artificial intelligence methodologies like fuzzy logic, genetic algorithm, neural networks, their combinations etc. The third category methods started gaining popularity in oil and gas industry in mid-nineties. Neural networks have been widely tested to study and mimic experimental data in laboratories. Some extensive work has been carried in relating seismic data and rock properties of sandstone (Nikravesh, 1998), predicting density logs using vertical seismic data (Artun, et al., 2005), predicting relative permeability characteristics for three-phase systems (Silpngarmlers, et al., 2002), enhanced oil recovery (Surguchev, 2000), assisted history matching techniques (Ramgulam, et al., 2007;), well test analysis (Dakshindas, et al., 1999) etc.

As mentioned earlier, an inexpensive and field deployable expert system based tool to characterize tight oil reservoir is developed in this study. In order to characterize the unconventional reservoirs the following questions will need to be answered from development point of view:

- Is the new well going to be economical?

- What will be the production for a new well location?

- Can the decline of production be predicted?

- What should the completion pattern be at a new location?

- What are the optimum completion parameters for a new well?

Artificial expert systems (AES) are developed in this research to provide a methodology useful in answering the aforementioned questions. These AES are validated in the ATM region of the Wolfcamp play in West Texas. These expert systems are divided into three different groups listed as follows:

- Completion parameters expert system: Completion network predicts suggestive completion parameters based on an overall trend and practices of the completion parameters observed in the ATM region. As a next step, optimization of completion parameters is proposed where completion strategy will be suggested so as to maximize the production from a proposed well.

- Performance prediction expert system: Two-year cumulative production values for oil, water and gas volumes are predicted using these networks. These expert systems are seen as an aid to identify the potential infill drilling locations based on the performance predicted by these networks.

- Hybrid ANN-EnOpt approach: A methodology is developed along the idea of neuro-genetic approach [Artun E. F., 2008]. This methodology is used to optimize the completion parameters.

Chapter 4 Methodology

In this chapter, the details of the expert system development is discussed. The methodology is based on developing inter-assisting expert systems suitable for understanding the existing complex relationships between geological data and the production characteristics of a well.

4.1 Data Availability

Data from a reservoir can be broadly classified into well information, geological data, drilling and completion data, and production data as shown in **Figure 4.1**. Well information, like the co-ordinates, can be used to evaluate the production interference effects of other surrounding wells. Geologic data have information related to the production potential of the hydrocarbon bearing rock. Completion data has information about the productivity of the completed well. The three categories of the data mentioned have information about the productivity of a well. On the other hand, production data bears the information of the general properties of the reservoir like permeability, porosity, formation damage, presence of fracture etc. Therefore, the first step in developing an expert system to characterize a reservoir involves the analysis of the available data.

The identified data is divided into three groups; training, testing and validation data. The dataset is randomly selected for each group by a random data generator. The expert is trained with the training data set. The weights and biases set in the activity are used to compare results with validation data set for adjustments in the calculations. Finally, the testing group cases are used to check the performance of the established network.
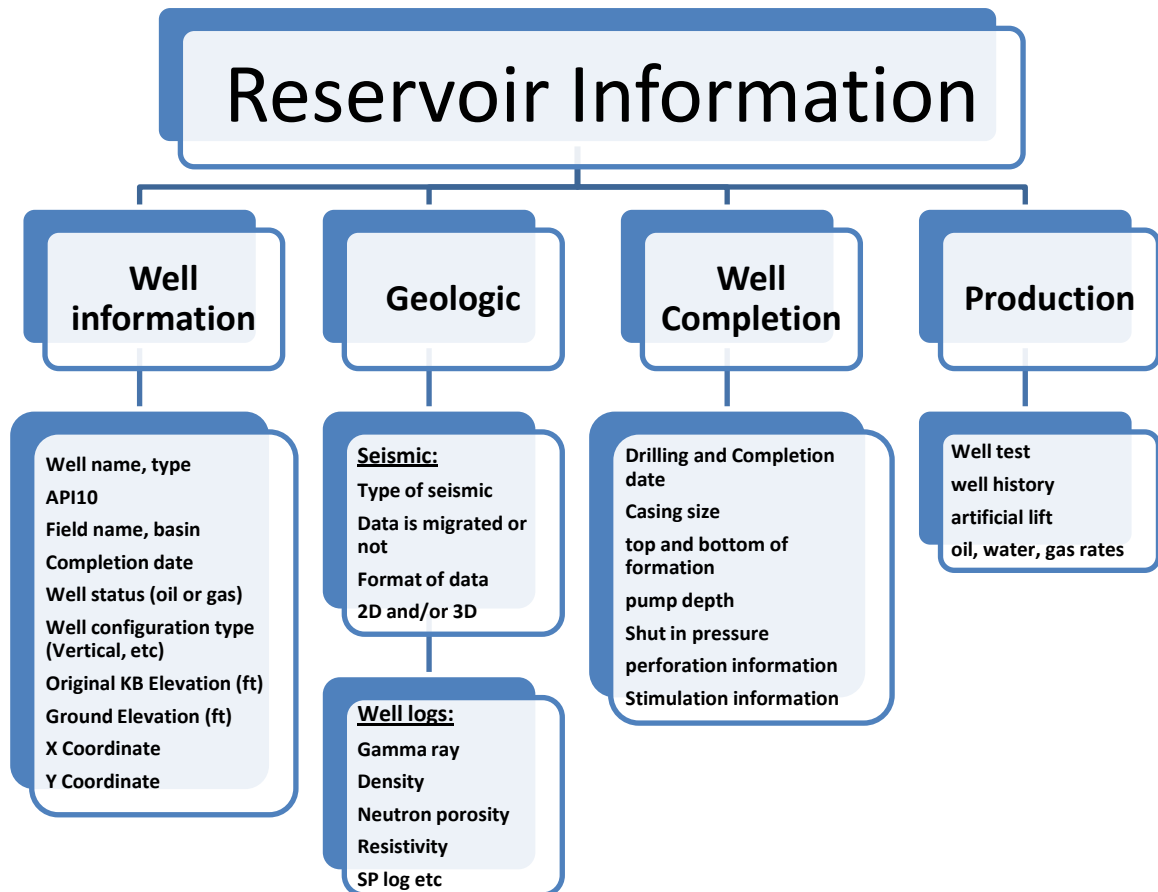
Fig. 4.1: Reservoir information classification

4.2 Scope of Expert Systems

The capabilities of artificial expert systems (AES) have to be pre-defined since they play an important role in identifying the initial topology of the AES. The work focuses on the development of a methodology to predict cumulative production at undeveloped locations. The results generated by the proposed AES are expected to help in identifying the sweet-spots in the reservoir for infill drilling strategies. In addition, a hybrid optimization approach has been developed combining AES and EnOpt. The entire scope of study has been divided into different sub-sections with an overall objective to predict production characteristics with the available information.

4.2.1 Production Prediction Expert System (PPES)

It is believed that the geological data has information about the hydrocarbon productivity of the well. The geological data is broadly classified as seismic data and well log data as shown in Figure 4.1. The other broad factors that affect the production from a well include interference of the nearby wells and completion strategy. Therefore, the initial topology of the expert system will utilize well information, seismic data, well logs, completion data and production characteristics as shown in **Figure 4.2**. The input data of the network is grouped into two different classes. The data readily available at an

undrilled location is assigned into *'Group A'*, whereas; the data unavailable before drilling is assigned into *'Group B'*. The information for *'Group B'* data is generated through individual expert systems as shown in **Figure 4.3**. Well logs are correlated with seismic data and well information [Mohammadnejad, 2011]. The expert systems to predict 5 types of well logs developed by Mohammadnejad (Ongoing work) are incorporated into the workflow shown in Figure 4.3. The completion information at an undrilled location is predicted by the completion networks. The network represented in Figure 4.2 is used to develop separate expert systems for oil (OPES), water (WPES) and gas (GPES) volumes.
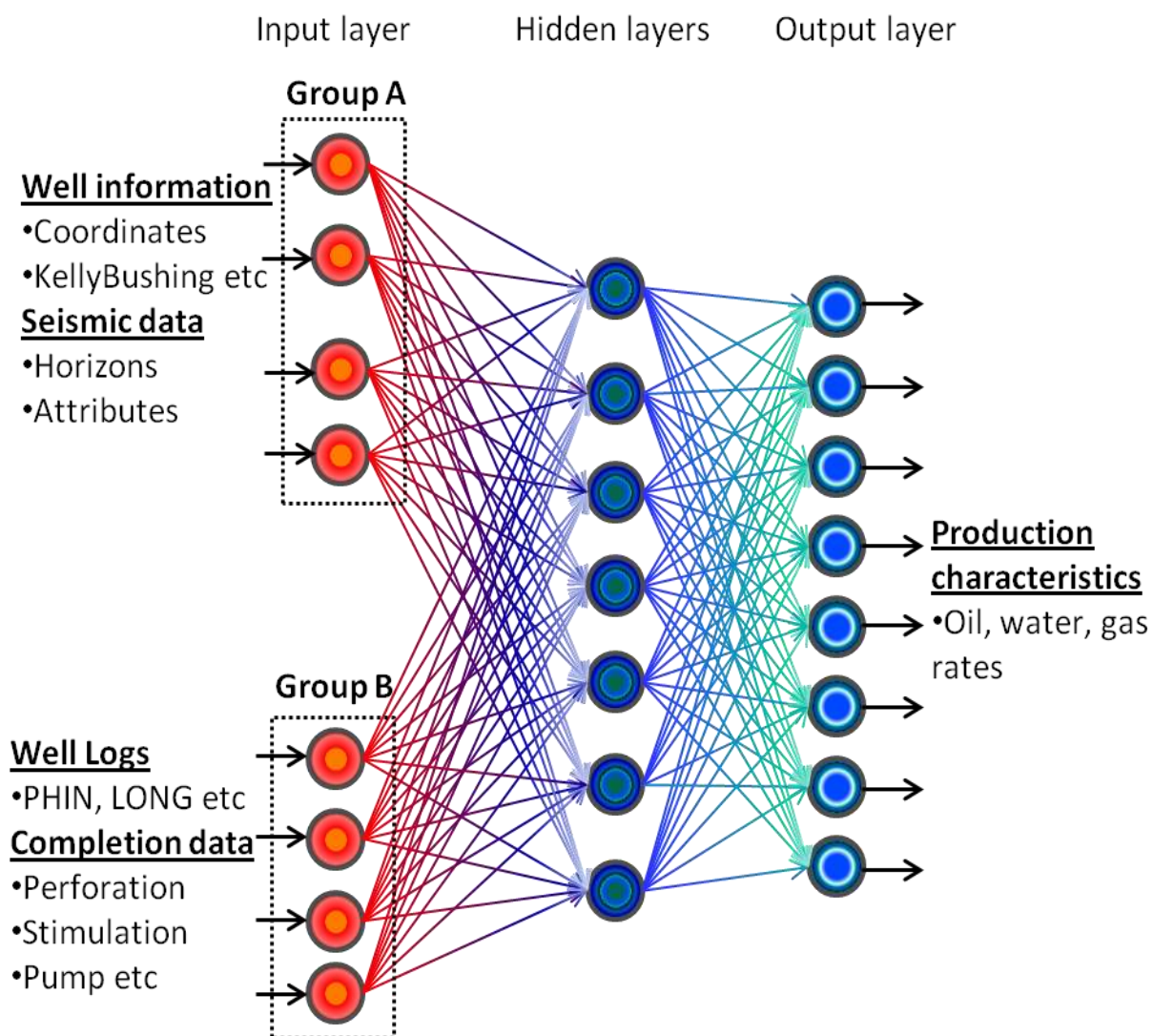
Fig. 4.2: Data structure for well performance networks
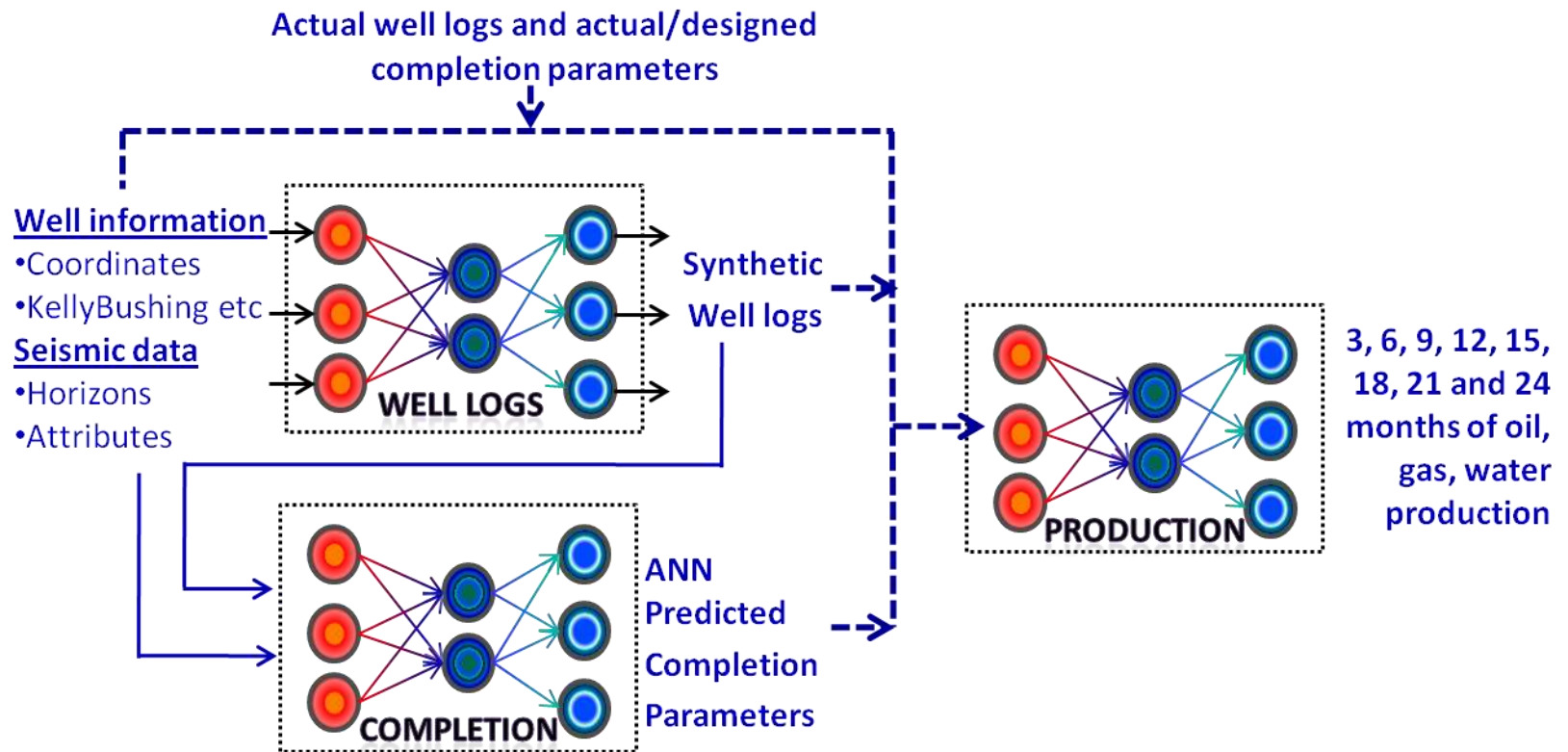
Fig. 4.3: Overall topology of the production expert systems

4.2.2 Completion Prediction Expert System (CPES)

The completion data network is used to predict the best practice completion parameters at any selected undrilled location. Completing a hydrocarbon zone will involve decisions related to geology of the formation. The main factors that are correlated with completion parameters are well information, seismic data and well logs. A generalized approach will involve arranging the information as shown in **Figure 4.4**. The sub-categories of these data ranges will be different for different fields, for example, the seismic data processing by different operators may result in different attributes for different fields. But the overall, methodology is expected to remain same in predicting the generalized trend for completion parameters in a given field. As described before, for an undrilled location well logs are generated using the synthetic well log tool [Mohammadnejad, 2011].
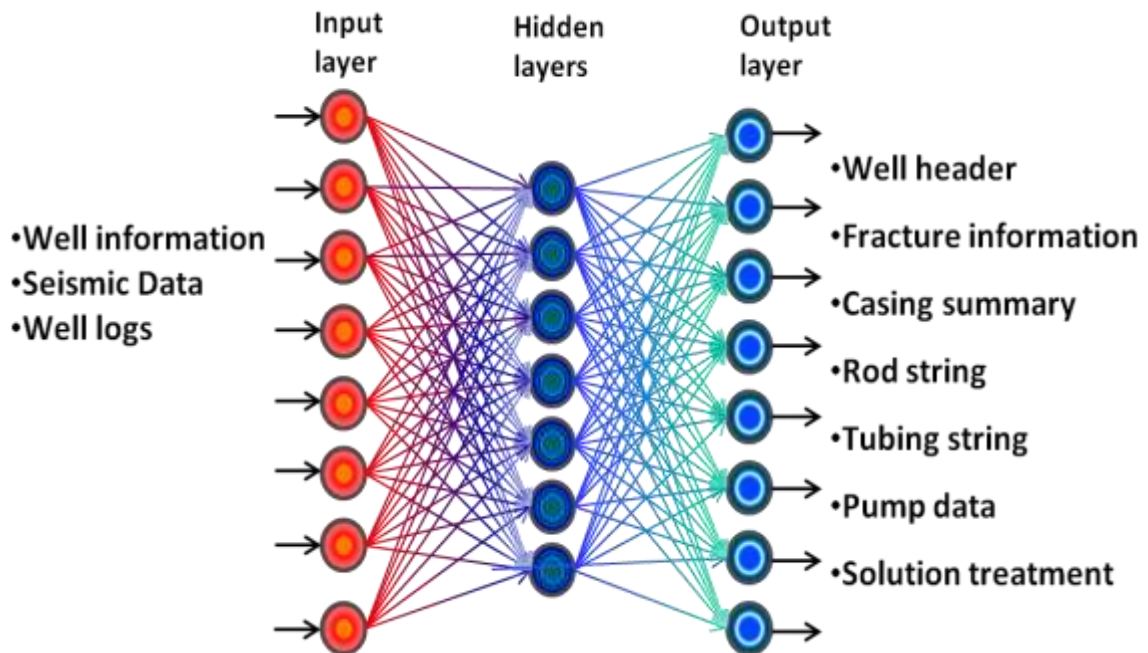
Fig. 4.4: Generalized design for completion prediction network

4.3 Optimizing Completion Parameters

An ANN-EnOpt hybrid approach is used to optimize the completion parameters. A net present value (NPV) function is defined that combines cost of different completion parameters, operating cost, royalty and revenue generated with oil production. The method presented here is general and can be used for other optimization problems. The algorithm is summarized in **Table 4.1**. The protocol starts with a known value of the input parameter in the optimization function. The method described here is modified from the original EnOpt. **Figure 4.5** shows the hybridization of ANN and EnOpt to calculate NPV. Here, oil production expert system is used to predict production with new completion parameters predicted by EnOpt algorithm in steps 1, 3 and 7.
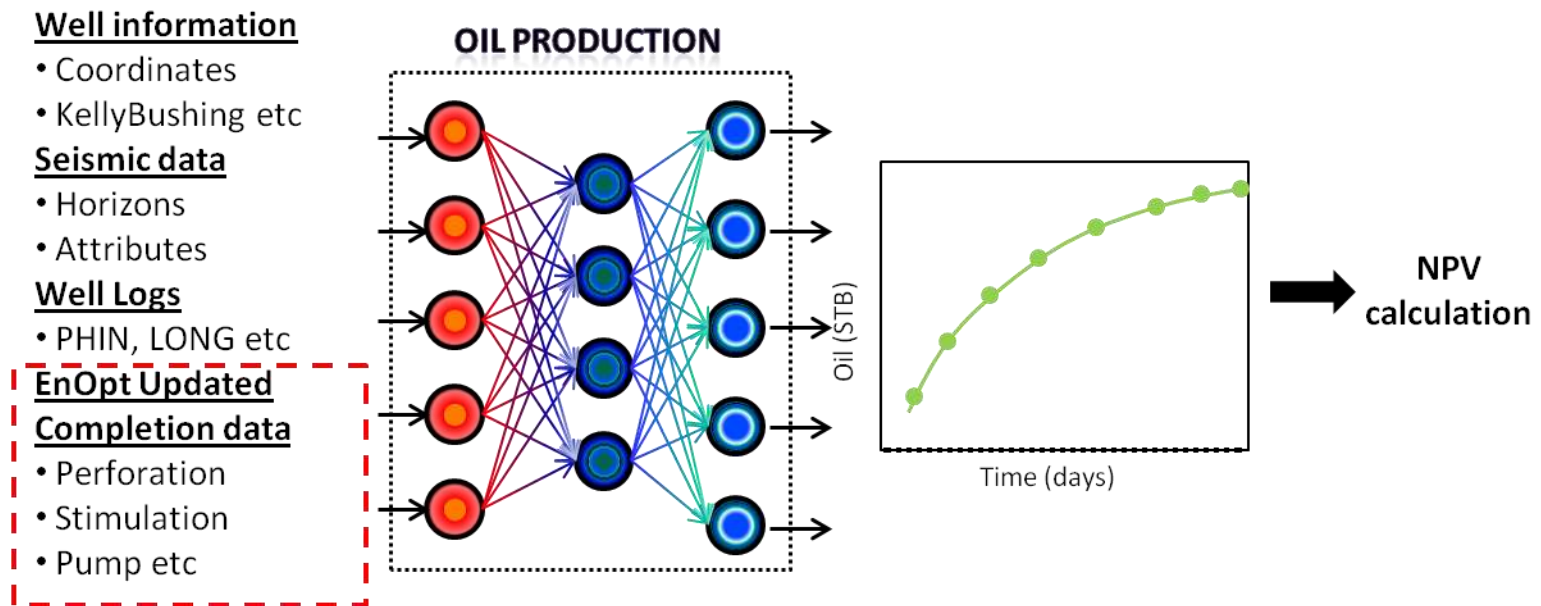
Fig. 4.5: Hybridization of ANN and EnOpt

Table 4.1: Implementation of ANN-EnOpt

1. Define completion parameters needs to be optimized and define mean value x_l for l=0. Initial values of the parameters are observed values in the field. To start the procedure, an average value of the upper and lower bound is used

2. Calculate $NPV_{,l}$ for control variable x_l.

Iterative loop to satisfy convergence criteria

3. Generate an ensemble of control variables $x_{l,Ne}$ with a size of N_e. Here, $x_{l,Ne}$ is generated by adding a uniform distribution with a desired variance around x_l.

4. Calculate $NPV_{,Ne}$ for $x_{l,Ne}$.

5. Find the highest value of the objective function i.e. $NPV_{,Ne}$ and check if it is higher than $NPV_{,l}$. If we are able to find a higher NPV within the ensemble generated then we swap $x_{l,min}$ and $NPV_{,max}$ with x_l and $NPV_{,l}$ and move to step 6. Else, do not swap and move to step 6.

6. Compute cross-variance C_{x-LC} and standard deviation, α of $L_{C-HC,Ne}$.

Ensemble based optimization loop

7. Update the control variable by the following equation

$$x_{l+1} = x_l + \frac{C_{x-LC}}{\alpha}$$

8. Calculate NPV_{l+1}.

9. If $NPV_{,l+1}$ is higher than or equal to $NPV_{,l}$ then exit the ensemble based optimization loop. Else, increase α and go to step 7.

   If convergence criteria (0.01% in our case) is met then x_{l+1} represents the completion parameters that will provide the optimum net present value, otherwise go to step 3 and repeat the process until NPV is maximized.

Chapter 5 Case Study

In this chapter, a field case study is presented and discussed. A brief introduction of the reservoir is discussed in the beginning, followed by data availability and selection. Finally, developments of different expert systems are discussed.

5.1 Introduction - ATM

ATM is a field in the Wolfcamp play. The Wolfcamp play is located in the Delaware and Midland basins as shown in **Figure 5.1** [Mongomery, 1996]. The initial exploration started in 1960s with intermediate success because of the complex nature of the play. The reservoir lithology is a combination of detrital carbonates, siltstones and black shales. The reservoir is reported as a discontinuous formation with unconnected oil pockets, making the characterization of the reservoir a challenging task. As a result, a representative simulation model for the reservoir is not available. The gross thickness is observed to be ~600-1500 feet. The black shales are likely the source rock and provide the seal for the complex reservoir. It is reported that pay determination is difficult and at present the best estimate seems to be "clean carbonate" denoted by lower than 75 API units of gamma ray signature. The reservoir is rich in data, where 3D seismic, well logs, micro-seismic (at couple of locations), extensive completion and production data. An

average value of air permeability is suggested to be ~0.013 millidarcy as obtained from 43 core samples. The expected value of the play is reported to be 250 MMBOE.

This resource is a good prospect for the study because of the limited data availability. Conventional techniques of evaluating and further developing this field are reported to be inefficient. There are ~600 wells drilled in this reservoir with partial success. Currently, patterns are used in order to identify a new location (see **Figure 5.2**) and this field lacks a formulated methodology for further development.
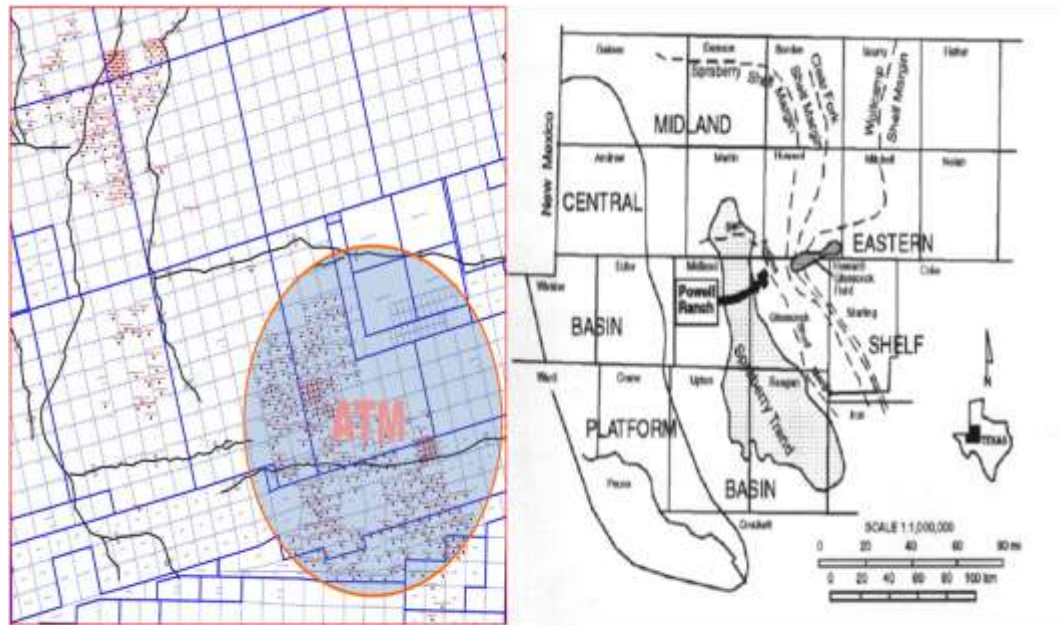
Source: Montgomery, AAPG, Sep(1996)

Fig. 5.1: Wolfcamp and ATM location
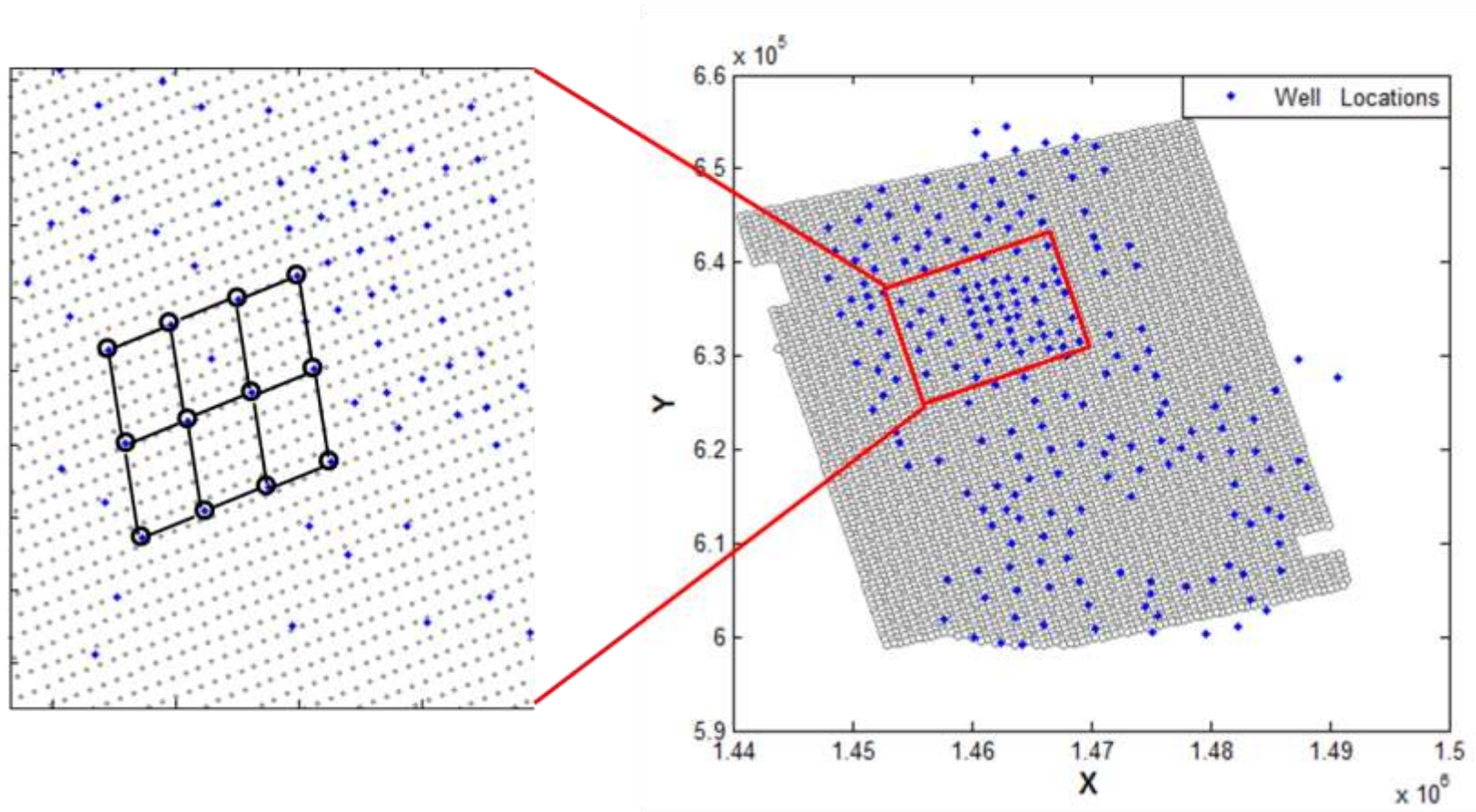
Fig. 5.2: Well patterns in the ATM field

5.2 Data Availability

There are over 600 wells in the entire Wolfcamp play, whereas seismic data is available only for the ATM region shown in **Figure 5.3**. There are 144 wells in this region with production history of more than 1 year and have completion parameters and 87 wells with production history of 2 years or more with consistent completion information and 5 different types of well logs (PHIN, LONG, SHORT, GR and GKUT). The seismic data is collected over a thickness range of ~6000 ft which is divided into 7 horizons shown in **Figure 5.4**. Each seismic horizon has 30 attributes. In addition, 46 completion parameters and production data (oil, water and gas) are also available.
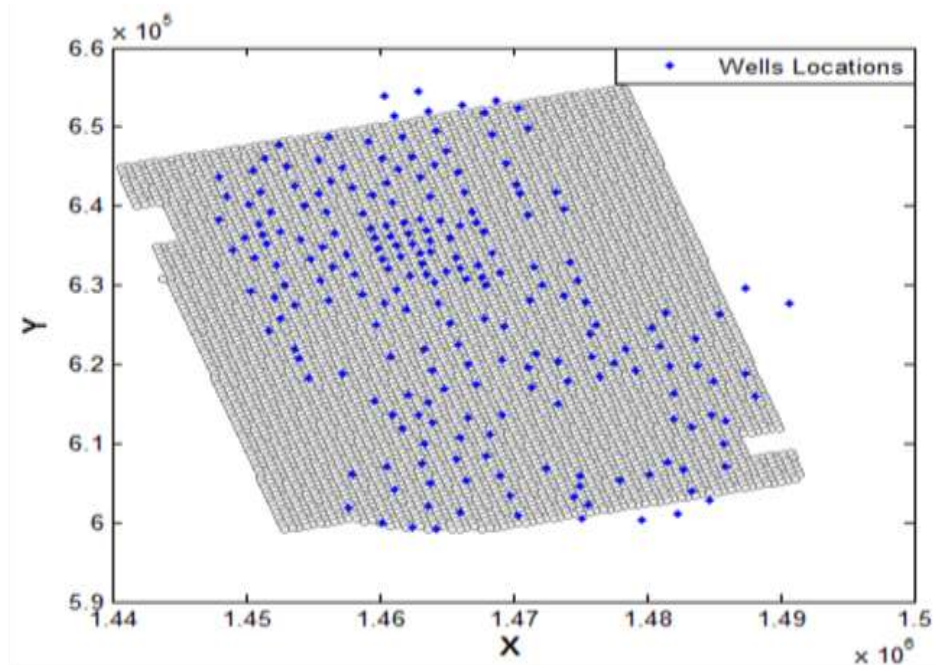
Fig. 5.3: ATM seismic region and wells

Fig. 5.4: Seismic horizon used in ATM region

5.2.1 Seismic Data

Any quantity calculated from seismic data is called a seismic attribute [Barnes, 2001]. These attributes are subsets of total seismic information which can be decomposed from seismic data in numerous ways. In addition there are no defined rules on what these parameters are or relate to [Barnes, 2001]. In this study, the following 30 attributes are used for each seismic horizon:

Attribute 1- RMS Amplitude (50 ms sliding window): This value is calculated in a specified time window of 50 ms. Amplitude is one of the fundamental parameters of the seismic wavelet information gathered at geophones. This value provides a scaled estimate of the trace envelope. RMS value is calculated as:

$$x_{RMS} = \sqrt{\frac{1}{N}\sum_{i=1}^{N} x_i^2}$$

Attribute 2- Amplitude Acceleration: This value is the second derivative of the logarithmic value or reflection strength. Variation of the value should be read qualitatively and not quantitatively.

Attribute 3- Dominant Frequency (average over 100 ms): Instantaneous dominant frequency 'fd' is defined as the square root of the sum of squares of instantaneous frequency 'f(t)' and bandwidth 'σ' and can be calculated as:

$$\boldsymbol{f_d(t)} = \sqrt{f^2(t) + \sigma^2(t)}$$

Attribute 4- Instantaneous Frequency (average over 100 ms): Instantaneous frequency '*f(t)*' is defined as the rate of change of instantaneous phase as a function of time, in other words, it measures the slope of the phase trace.

Attribute 5- Reflection Strength: It is also known as instantaneous amplitude. It can be calculated as the square root of the total energy of the seismic signal at an instance of time.

Attribute 6- Quadrature Trace: It is identical to the recorded trace but phase-shifted by 90 degrees. This value can be thought of as representing potential energy while recorded trace represents the kinetic energy of particles moving in response to the seismic wave.

Attribute 7- Thin Bed Indicator (window length 100 ms): It is defined as the absolute value of the instantaneous frequency minus weighted average instantaneous frequency. This value indicates overlapped events **Invalid source specified.**.

Attribute 8- Bandwidth (window length 200 ms): Instantaneous bandwidth 'σ' is defined as the time rate of change of natural logarithm of the instantaneous amplitude '$a(t)$' divided by '2π', as shown below. This value can be considered as a measure of half bandwidth.

$$\sigma(t) = \frac{1}{2\pi}\left|\frac{d}{dt}\ln(a(t))\right| = \frac{|a'(t)|}{2\pi\,a(t)}$$

Attribute 9- Response Frequency: It is defined as instantaneous frequency calculated at the peak of the amplitude envelope (reflection strength).

Attribute 10- Instantaneous Q Factor (average over 200 ms): This value indicates local variation of Q factor. It is similar to the relative acoustic impedance computation

from the seismic trace. This value may indicate liquid content by analyzing pressure versus shear wave section Q factors **Invalid source specified.**.

Attribute 11- Amplitude Change (average over 100 ms): It is calculated in a similar way as instantaneous bandwidth. It highlights the places where amplitude changes in the data; the value is positive with an increase in amplitude and it is negative when the amplitude decreases.

Attribute 12- Energy Half-time (average over 100 ms): It is a relative measure of the location where energy is concentrated in the specified time window. The average time 't_a' of the trace power is

$$t_c = \frac{\sum_{i=1}^{N} t_i x_i^2}{\sum_{i=1}^{N} x_i^2}$$

where, 'x' are the window trace samples, this value is referenced from time interval 't_1'. Energy half time 'E_{ht}' at the end of time interval 't_N' can be calculated as

$$E_{ht} = 200\% \frac{t_c - t_1}{t_N - t_1}$$

Attribute 13- Energy Half-time (average over 50 ms): Same as before, time interval is changed to 50 ms.

Attribute 14- Thin Bed Indicator (window length 50 ms): Please refer to Attribute 7, here time interval is changed to 50 ms.

Attribute 15- Differentiation: Trace is differentiated using Fourier transform. It represents a trace value as the difference between the preceding sample and the succeeding sample divided by the difference in time.

Attribute 16- Integration: Trace is integrated using Fourier transform. It represents a trace value as the sum of the original samples.

Attribute 17- RMS Amplitude (25 ms sliding window): Same as attribute 1. This value is calculated in a specified time window of 25 ms.

Attribute 18- Reflection Curvature: This value is based on a simplified formula that employs second derivatives in X and Y directions.

Attribute 19- Absolute Amplitude: It is an absolute value of all the amplitudes.

Attribute 20- Amplitude Change (average over 50 ms): Same as attribute 11. This value is calculated in a specified time window of 50 ms.

Attribute 21- Amplitude Change (average over 200 ms): Same as attribute 11. This value is calculated in a specified time window of 200 ms.

Attribute 22- RMS Amplitude (100 ms sliding window): Same as attribute 1. This value is calculated in a specified time window of 100 ms.

Attribute 23- Cosine of Phase: This value describes a normalized trace and is calculated as a ratio of the recorded trace with the amplitude (reflection strength) of the trace . Before scaling, value of cosine phase ranges between -1 to +1

Attribute 24- Bandwidth (window length 100 ms): Same as attribute 8. This value is calculated in a specified time window of 100 ms.

Attribute 25- Instantaneous Q Factor (average over 100 ms): Same as attribute 10. This value is calculated in a specified time window of 100 ms.

Attribute 26- Dominant Frequency (average over 50 ms): Same as attribute 3. This value is calculated in a specified time window of 50 ms.

Attribute 27- Arc Length (50 ms sliding window): Arc length is sometimes called reflection heterogeneity.

Attribute 28- Arc Length (100 ms sliding window): Same as attribute 27.

Attribute 29- Amplitude Variance (3 traces, 3 lines, 5 samples): Reflection amplitude variance is how much seismic amplitude varies from the average amplitude.

Attribute 30- Amplitude Variance (7 traces, 7 lines, 5 samples): Same as attribute 29.

5.2.2 Well logs

In this study, neutron porosity (PHIN), long spaced neutron (LONG), short spaced neutron (SHORT), gamma ray (GR) and normalized gamma ray (GKUT) are consistently available in the ATM region. These wells logs are used in the training the completion prediction and well performance networks. Whereas, well log prediction networks are used to generate the above mentioned well logs during prediction of completion parameters and well performance at an undrilled location. The entire well log is divided into 50 equal intervals after identifying the top and bottom depths of each well log, an average well log response for each interval is then selected as input for the expert system. These depths were identified by matching the well logs with depth of seismic trace given at that location.

5.2.3 Completion Parameters

Completion data were screened in order to identify the maximum possible information in the development of an effective expert system. According to the data supplied in September, 2009; 149 different completion parameters were identified for 612 wells in the Wolfcamp region. The information for the aforementioned completion parameters was not consistently available for all the wells, therefore; only uniformly available parameters were used in the analysis. In addition, the expert system discussed in the study is focusing on ATM region where only 87 wells out of 612 wells were

identified in ATM region with a production history of more than 2 years. During the quality check of the data for the expert system, some anomalous data were observed for completion parameters as shown in **Figure 5.5**. Therefore, similar data types were removed from further analysis to reduce the noise in the database.
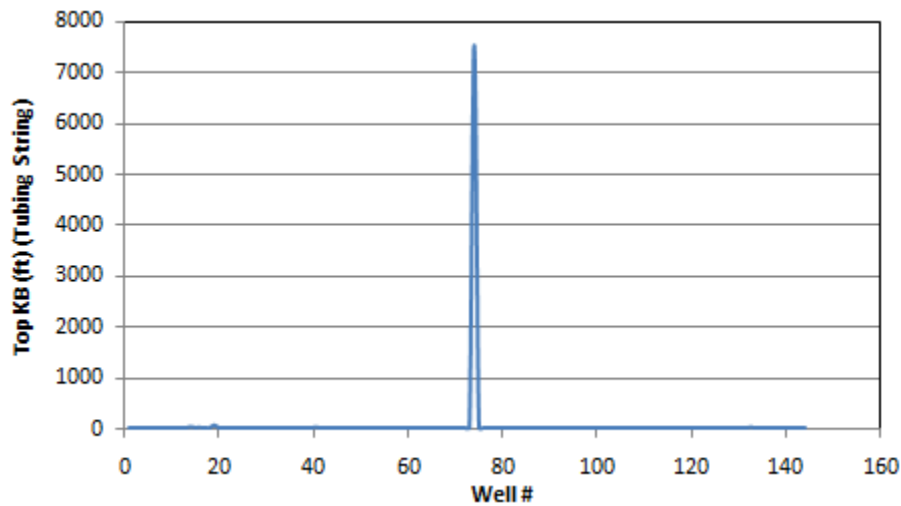
Fig. 5.5: An example of anomalous data observed in completion parameters

In addition, some of completion parameters were constant for the wells under study. Such constant parameters do not add any useful information to the expert system thus they are not incorporated in the model (please note that, any constant parameter is automatically removed by the network during the training stage).

A total of 46 completion parameters are identified after the above mentioned screening criteria. These parameters were consistently available for 87 wells with two

years of production history in ATM region (as per data supplied in Sep, 2009). The parameters are grouped in the following categories:

- Well header data
- Fracture summary data
- Perforations data
- Rod string data
- Tubing string data
- Pump data
- Solution treatment data

A detailed list of individual well completion category is shown in **Table 5.1**. This table also shows the ranges of parameters observed in the ATM region (complete descriptive information for each of the individual parameter was not available). Details of individual important parameters and value selection are given in **Appendix A**.

Table 5.1: List of completion parameters

| Completion category	Completion Parameter	Minimum	Maximum
Well Header	Original KB Elevation	2631	2839
Well Header	Ground Elevation	2613	2822
Fracture Information	Fracture stages	8	18
Fracture Information	Total proppant used (lb)	276701	1734307
Fracture Information	Max Btm Depth (ftKB)	9600	10360
Fracture Information	min Btm Depth (ftKB)	3856	8942
Fracture Information	Q (end) Max (gpm)	2562	3444
Fracture Information	P (tub-st) Min (psi)	46	4800
Fracture Information	Min Top Depth (ftKB)	9690	10340
Fracture Information	Min Top Depth (ftKB)	6944	8932

Fracture Information	Total proppant recovered	1.87E+04	7.76E+04
Casing Summary	Set Depth (ftKB)	9925	10630
Casing Summary	String OD (in)	5.5	13.375
Casing Summary	String Wt (lbs/ft)	17	48
Casing Summary	Len (ft)	8.72E+03	10611
Casing Summary	OD Max (in)	5.5	13.38
Casing Summary	ID Min (in)	4.892	12.715
Casing Summary	String ID (in)	4.892	12.715
Casing Summary	Top (ftKB)	9	20
Rod String	String OD (in)	0.75	1
Rod String	Set Depth (ftKB)	5066	1.04E+04
Rod String	Set Depth (ftKB)	324	1.03E+04
Rod String	OD Max (in)	1.5	2.5
Tubing String	String wt (lbs/ft)	4.7	6.5
Tubing String	Set depth (ftKB)	7.00E+03	1.06E+04
Tubing String	OD MAX (in)	2.375	5.5
Tubing String	Stick up (ftKB)	-63.9	-9
Tubing String	Len (ft)	7.00E+03	1.06E+04
Tubing String	Top (ftKB)	9	63.9
Pump Data	Max. OD (in)	2.375	2.875
Pump Data	Min. OD (in)	2.375	2.875
Pump Data	Max. Top (ftKB)	6.94E+03	1.05E+04
Pump Data	Min. Top (ftKB)	82	1.03E+04
Pump Data	Max. Btm (ftKB)	6.94E+03	1.05E+04
Pump Data	Min. Btm (ftKB)	83	1.03E+04
Pump Data	Cum Len (ft)	1.1	182.5
Pump Data	Cum Vol Disp (bbl)	1	1.1
Solution Treatment	Sum of proppant frm (lb)	276701	1734307
Solution Treatment	Max top Depth (ftKB)	9690	10340
Solution Treatment	Min top Depth (ftKB)	6944	8932
Solution Treatment	Max Btm Depth (ftKB)	9600	10360
Solution Treatment	Min. Btm Depth (ftKB)	3856	8942
Solution Treatment	EOS ISIP (psi)	2530	4750
Solution Treatment	Q (end) Max (gpm)	2562	3444
Solution Treatment	P (tub-st) Min (psi)	46	4800
Solution Treatment	Total vol recovered(bbl)	1.87E+04	7.76E+04

5.3 Completion Prediction Expert System (CPES)

The completion data network is used to predict the best practice completion parameters at any selected undrilled location. The network described in this section is trained on the existing completion practices in the ATM region; thus captures the general trends of the current practices. This network uses the geological coordinates of the location, seismic data for 10 horizons with 30 attributes as described earlier in the report (synthetic well log generation section) and 5 well logs (PHIN, Long, Short, GR and GKUT) to predict the completion parameters. Selection of completion parameters to be predicted by this network was based on the availability of the consistent information for the parameters. The expert system discussed requires an existing database to understand the patterns and identify the existing relationship between inputs and outputs; upon a successful training of the expert system.

A total of 46 completion parameters were identified as discussed in **Section 5.2.3**. As previously discussed, 87 wells were used in this expert system. These available dataset were randomly classified as training (77 wells), testing (5 wells) and validation (5 wells) dataset. Once data screening was completed, the network was designed to train completion parameters using well coordinates, seismic data and available well logs as shown in **Figure 5.6**.
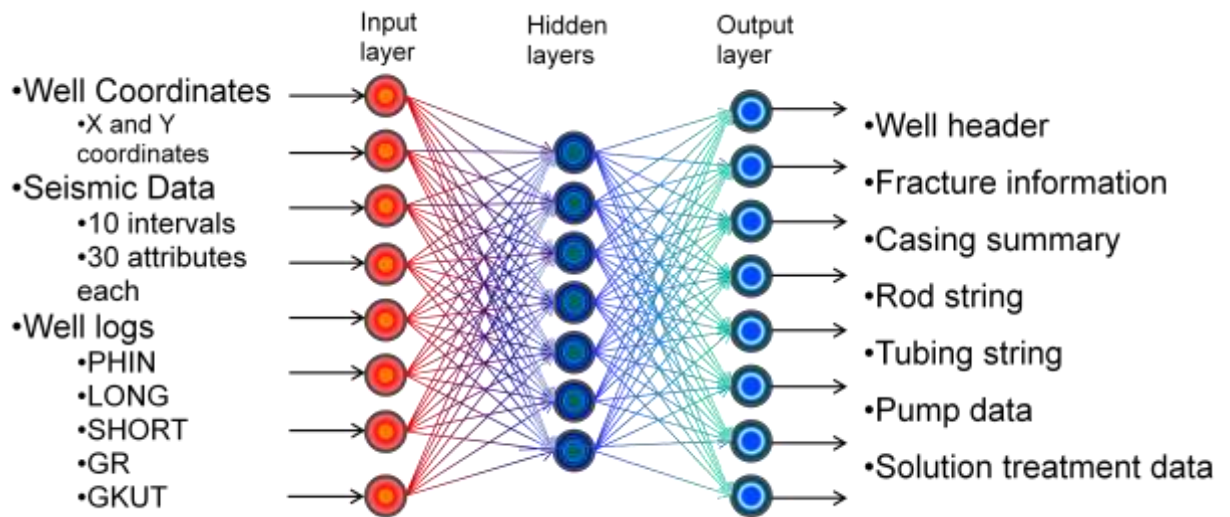
Fig. 5.6: Completion data network design

Once the appropriate data was identified, expert system structure was optimized to identify the weights and biases for each neural link. In the optimization of the structure, weights of each individual inputs and hidden neurons were analyzed to simplify the network architecture. Optimizing the network structure is a heuristic procedure where number of hidden layers, number of neurons in each hidden layer, transfer function, training and learning algorithm and error minimization method are studied to find the most optimum structure for a given complex problem. Different combinations of number of neurons and number of hidden layers were tested. All the architectures were tested on different transfer functions between the layers to optimize the performance of the network. The addition of functional links improved the performance of the network significantly in the training phase. The functional links used in the network are

- Mean of well log record (1 value for each well log; total 5 more inputs)

- Standard deviation of well log record (1 value for each well log; total 5 more inputs)

Figure 5.7 shows the final architecture to predict completion parameters. In this architecture three hidden layers having 49, 38, and 22 neurons in each layer with 'logsig', 'tansig' and 'tansig' as transfer functions for each layer were used, respectively. The training algorithm used in this network is 'trainscg', learning algorithm is 'learngdm' and error minimization function is 'msereg' (Details can be seen in **Appendix A**). The expert system developed in this part of the study was tested with 5 randomly selected wells to predict the completion parameters with an average error of 8%. This network will be useful in predicting completion parameters at an undrilled location based on the trend of completion strategy followed in the ATM region. The outcome of this network will be used in predicting the performance of an infill drilling well as discussed in the next section.
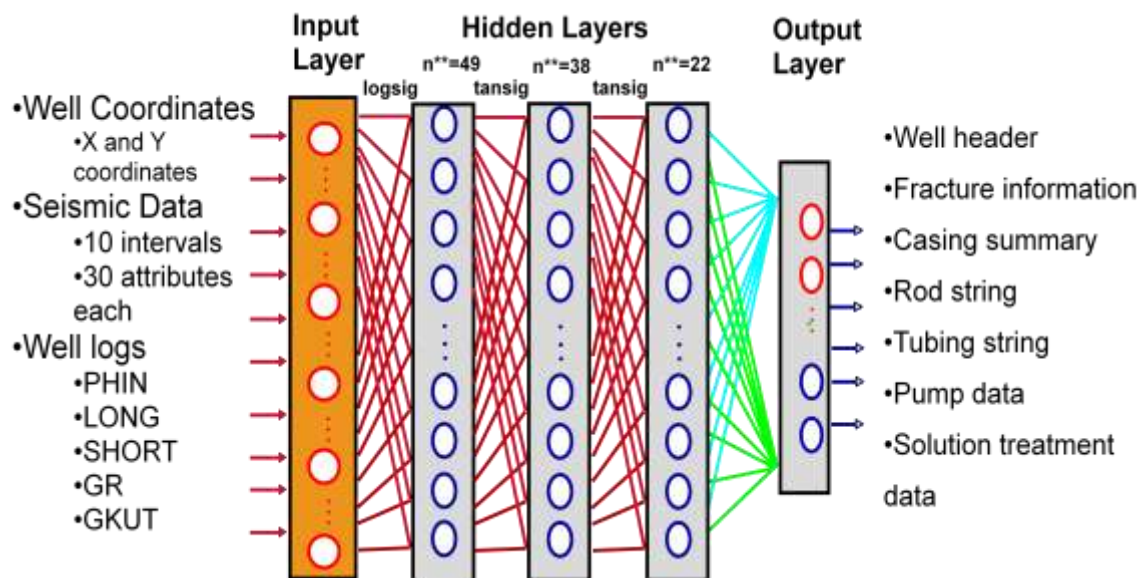

Fig. 5.7: Final architecture of the Completion network

The importance of individual parameters was analyzed in the completion expert system. **Figure 5.8** shows the relative impact of individual groups of input parameters to evaluate the suggested completion parameters at a given location. This figure shows that the importance of all the seismic data is 53.6%, and all the well logs contribute ~46% in making the prediction at a given location. It can also be seen that all the well logs contribute nearly same to predict the outcomes. **Figure 5.9** illustrates the relative importance of seismic attribute when normalized on 53.6%. The highest impact in the seismic data is observed for 'RMS amplitude (50 ms)', 'Energy half time (50 ms) and 'Amplitude change (200 ms)'. The observations ties along with the initial assumptions in relationship with the seismic data.
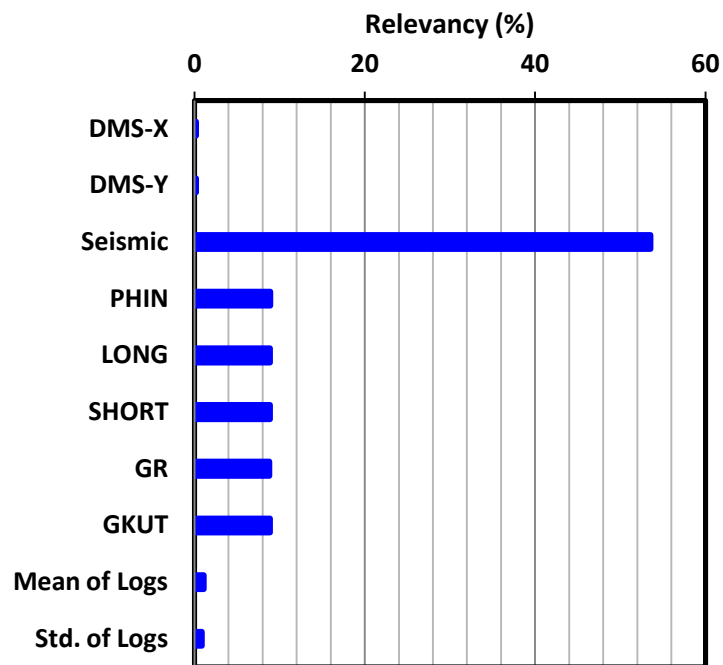
Fig. 5.8: Relevancy chart for completion prediction network

Relative Relevancy of Seismic data (%)
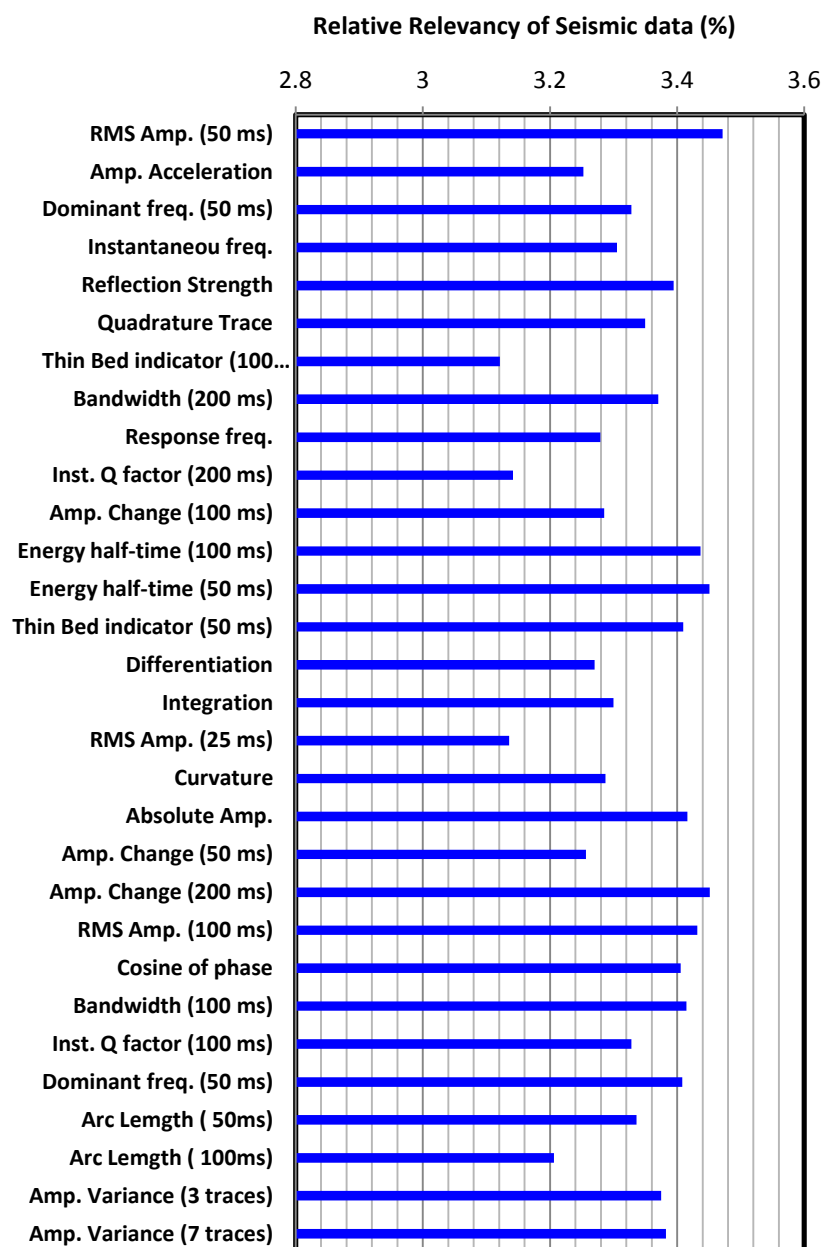
Fig. 5.9: Relative Relevancy of Seismic data for completion network

5.4 Performance Prediction Expert System (PPES)

In this section, an expert system was developed for each of the three volumes (oil, gas and water). The expert systems discussed in this section uses geographical coordinates, seismic data, well logs and completion parameters to predict two year performance of a planned well at intervals of 3 months.

5.4.1 Oil Production Prediction Network (OPPN)

In the oil performance network, well coordinates (X and Y DMS values), seismic data (10 horizons with 30 attributes each), well logs (PHIN (50 intervals), Long (50 intervals), Short (50 intervals), GR (50 intervals) and GKUT (50 intervals)) and completion strategy (46 parameters) are trained against the oil production data for 87 wells as shown in **Figure 5.10**. Different networks were designed before finalizing this structure; some of the expert systems were based on all the producing wells in the ATM region. The expert system are listed below

- Predicting maximum initial production rate
- Predicting average rates for wells
    - Uses 100 wells in training and 43 in testing
    - Well logs not used in training
    - One well selected for testing and rest for training
- Used decline curve parameters for wells

      – 2 year data at intervals of 3 month (8 values)

The first approach, only initial maximum production rate was used as an output, was not proven to be useful as, in general, wells in ATM region decline rapidly within during initial 3 months of production. Therefore, a decision on infill drilling cannot be made solely on the initial maximum production rate at a specified location. Similarly, average production rate approach was discarded where different approaches were used to obtain a good level of accuracy in predicting average flow rates at a given location. In addition, decline curve parameters were also studied to understand the performance of a given well. In this approach decline curve parameters were used as the output of the network without a good level of success. Finally, predicting 2 years of production data were used in the network. However, according to the data supplied in Sep, 2009, only 87 wells were observed to have a production history of 2 years or more. The final design is shown in Figure 5.10.
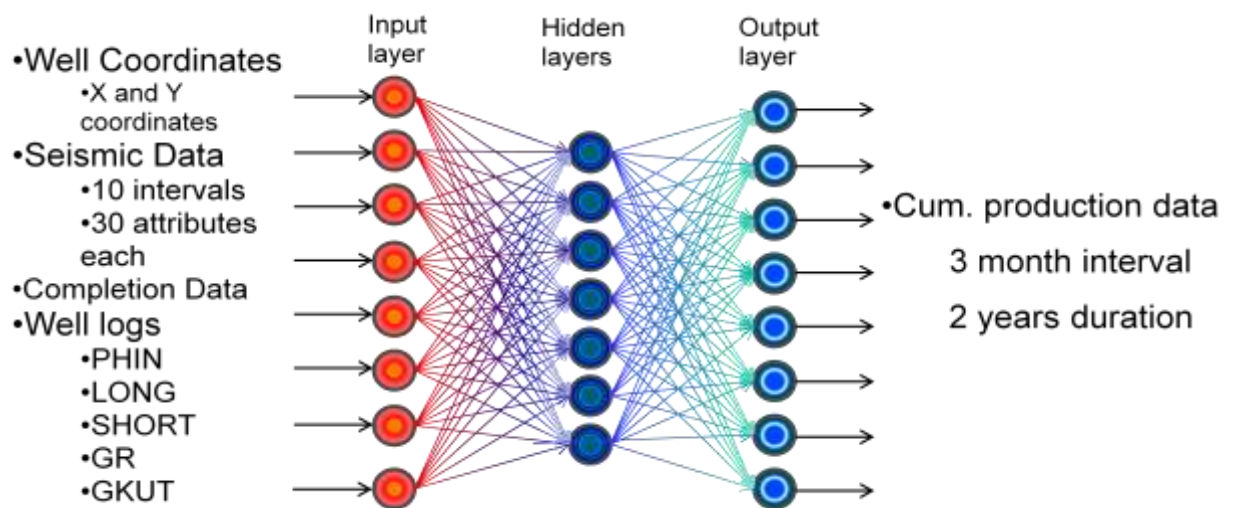
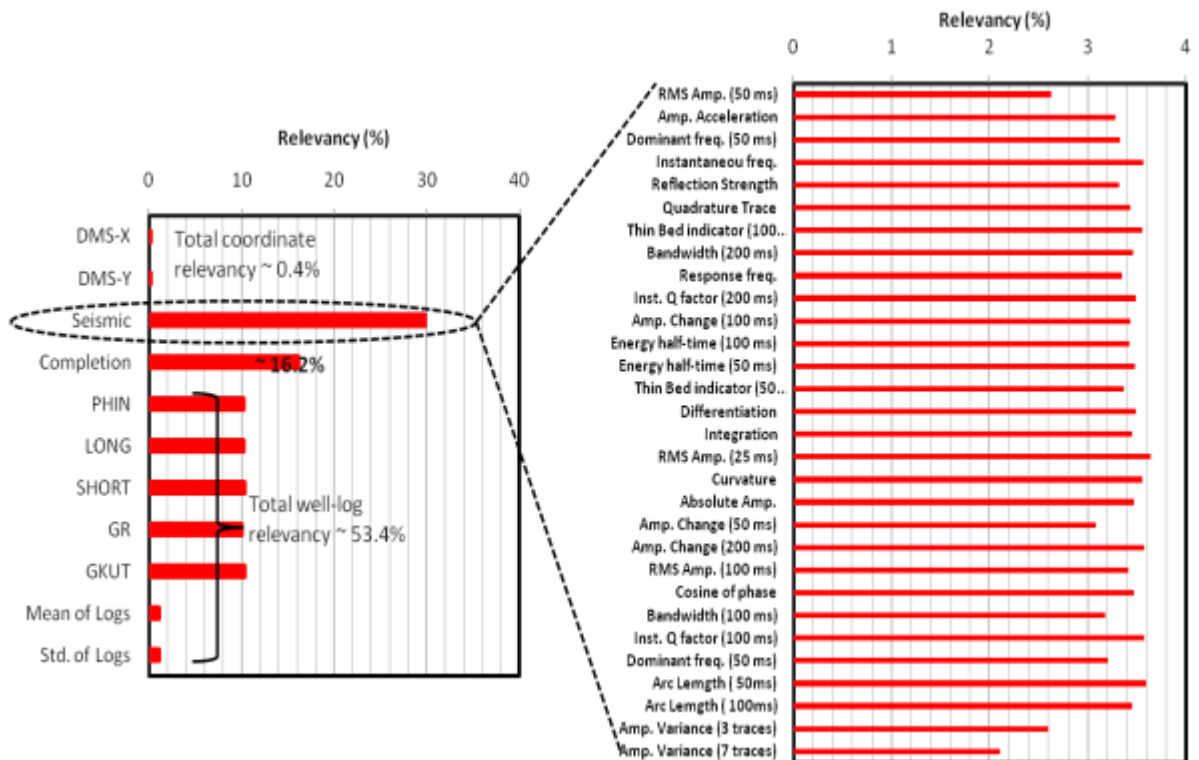**Fig. 5.10: Design of the Oil performance network**

The network training strategy was the same as followed in completion data network. In this approach 87 wells were used including: 77 training wells, 5 testing wells, and 5 validation wells. An accuracy of ~8% error in the testing cases and 2.5% in the training cases was observed. **Figure 5.11** shows the final architecture with 87 wells. In this architecture three hidden layers having 49, 42, and 29 neurons in each layer with 'logsig', 'tansig' and 'logsig' as transfer function, respectively were used. Training algorithm, learning algorithm and error minimization function are the same as were discussed in completion network.
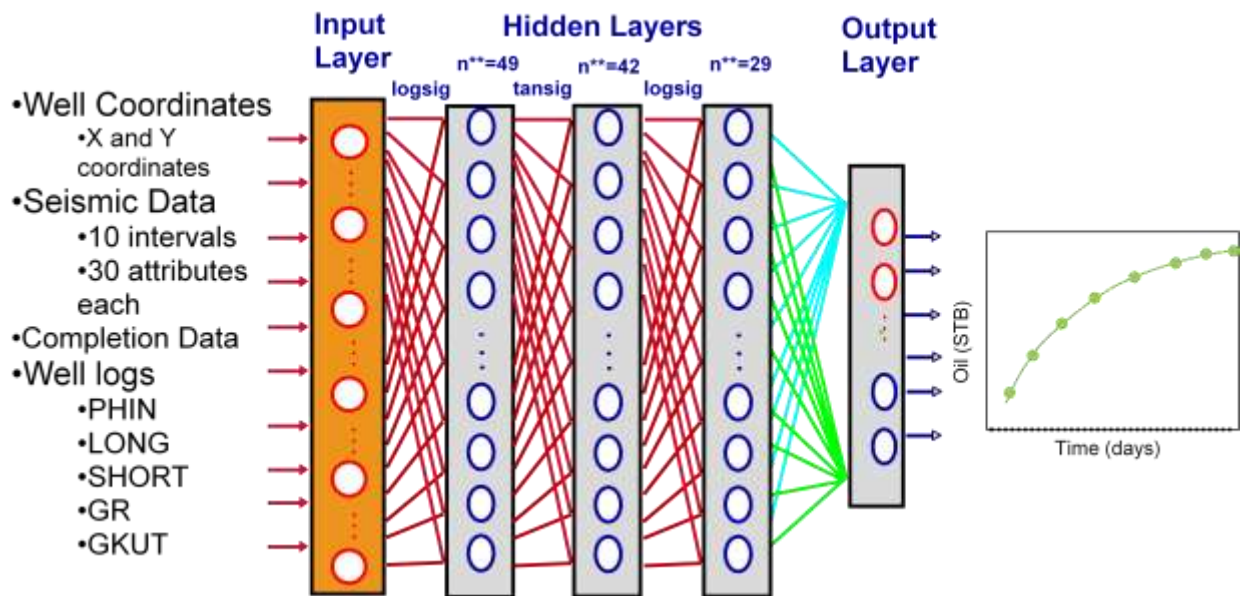
Fig. 5.11: Architecture of the Oil performance network

Figure 5.12 shows the relevancy of the inputs used in the oil performance network. This figure shows that seismic data is ~30% important in predicting two year oil

performance of a well at a given location. The relevancies of the completion parameter are observed to be at ~16% and well logs at ~53% in estimating the performance of the well.


Fig. 5.12: Relevancy of inputs used in oil performance network

Figure 5.13 shows the new wells were added with 2 years of production or more, this dataset was updated in Oct 2010. **Table 5.2** shows the production history of the wells in the ATM region. Upon further investigation it was found that 134 new wells were available in ATM region that had more than 2 years of production history. These new wells were incorporated in the analysis and were used to update the structure of the

network. The original design of the oil performance was preserved to predict 2 years of oil production at intervals of 3 months using well coordinates, seismic, completion and well log data.
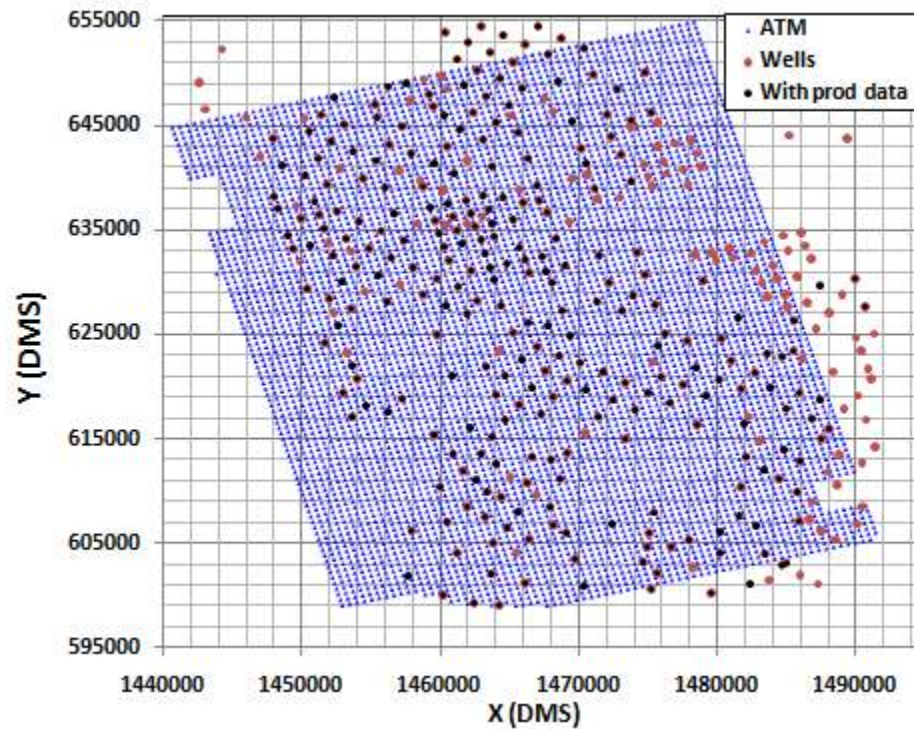

Fig. 5.13: Updated dataset for ATM region

Table 5.2: Production history of wells in ATM region

Years of production	# of wells
0.5	272
1	249
2	213
3	169
4	130
5	95

The updated network architecture is shown in **Figure 5.14**. The network was slightly modified in terms of number of neurons in the hidden layer and transfer function for each hidden layer. In this architecture three hidden layers having 50, 28, and 19 neurons in each layer with ' tansig', 'logsig' and 'tansig' as transfer were used. An accuracy of ~13% average error in the testing cases and ~ 5% in the training cases was observed for this network. This network topology was accepted as the final architecture for predicting oil production in the ATM region.
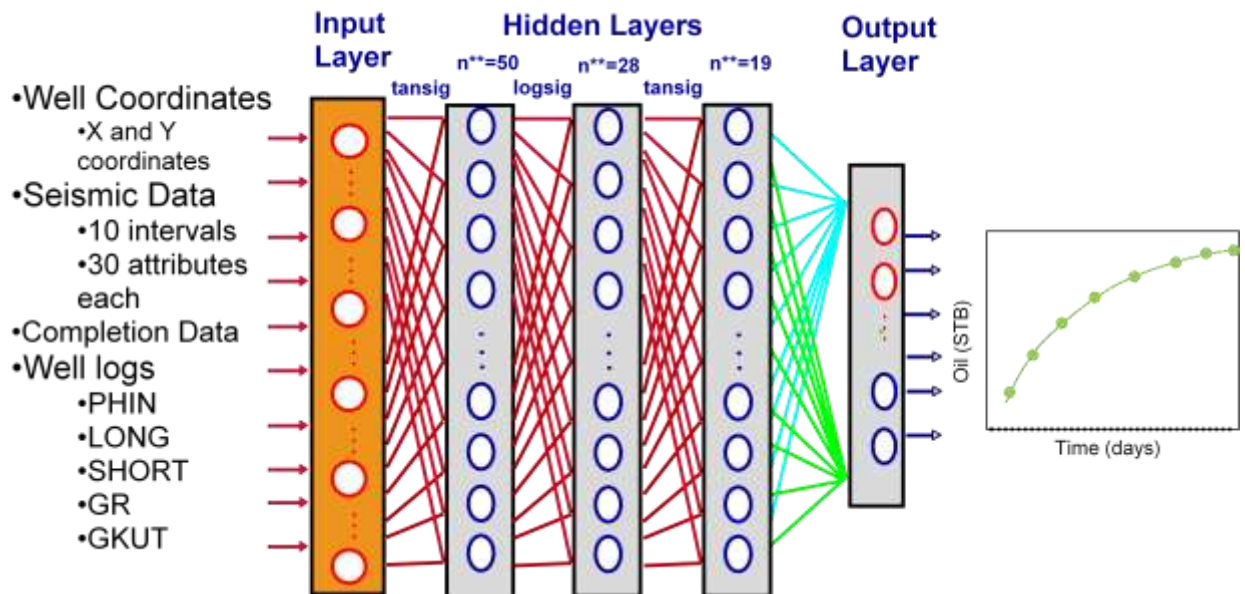

**Fig. 5.14: Updated final architecture of the Oil performance network**

5.4.2 Gas Production Prediction Network (GPPN)

The network design for gas network is same as was discussed in case of oil performance network as previously shown in Figure 5.10. Initially this network was also

built with 87 wells in ATM region and was updated as new data became available. In this new network 50 more wells (out of 136 new wells) were added randomly to the existing 87 wells. In terms of accuracy a ~13% error in the testing cases and ~6% error in the training cases were observed. **Figure 5.15** shows the final architecture with 87 wells. In this architecture three hidden layers having 62, 43, and 12 neurons in each layer with 'tansig', 'logsig' and 'tansig' as transfer function were used. **Figure 5.16** shows the relevancy of the inputs used in the oil performance network. This figure shows that seismic data is ~32% important in predicting two year oil performance of the well at a given location. The relevancies observed in this network are similar to the relevancies observed for the oil network. The completion parameter is observed to be at ~12% and well logs at ~55% in estimating the performance of a well.
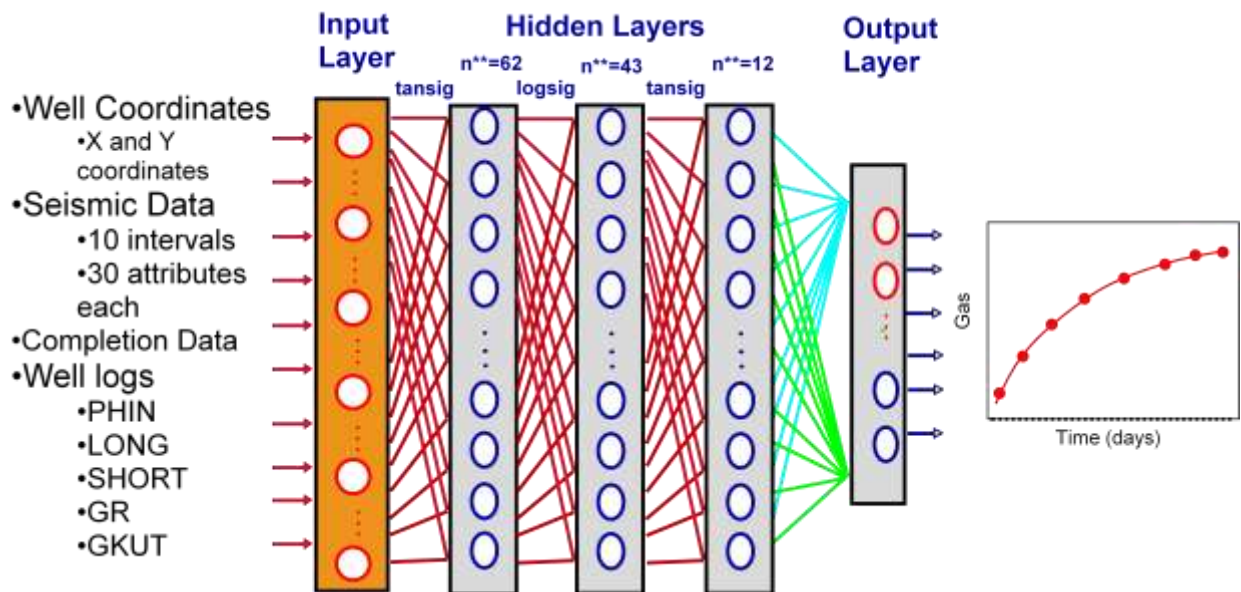
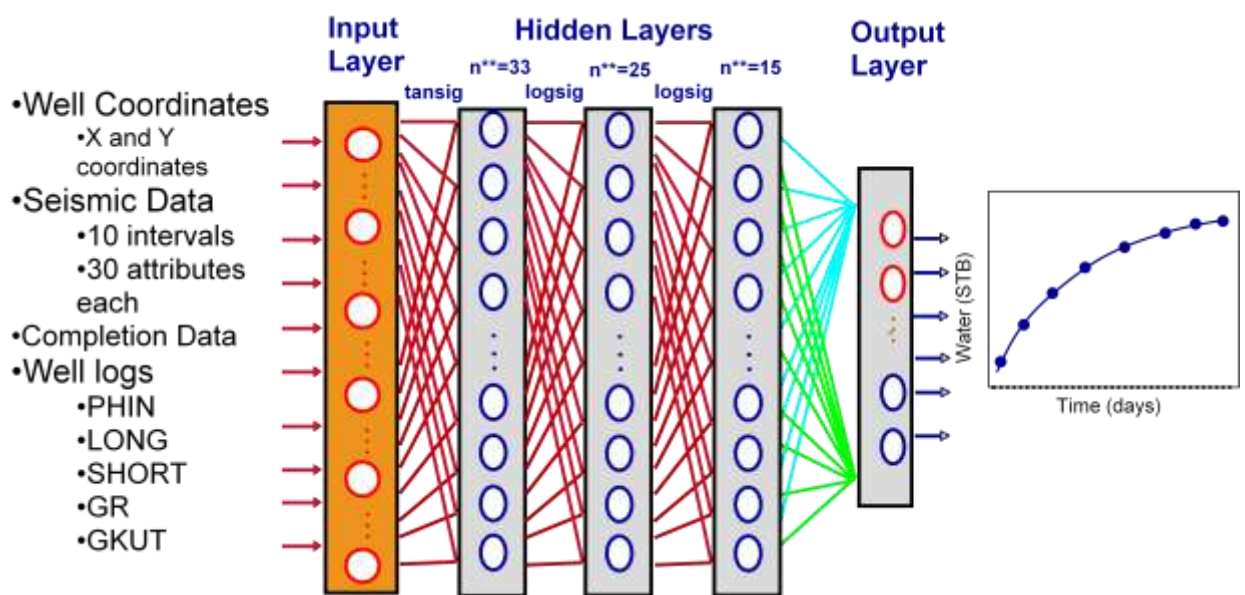**Fig. 5.15: Architecture of the gas performance network**
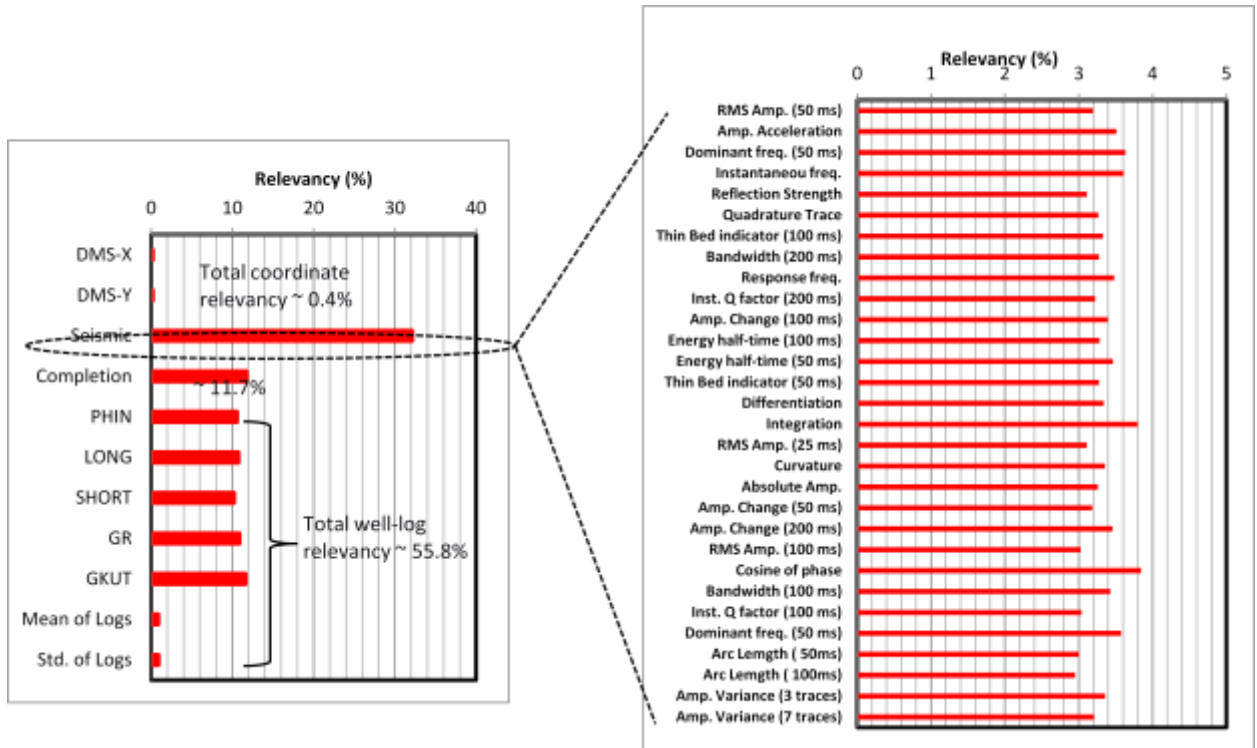
Fig. 5.16: Relevancy of inputs used in gas performance network

## 5.4.3 Water Production Prediction Network (WPPN)

The WPPN discussed in this section also uses the same design as for oil and gas networks. This network was also built with 87 wells in the ATM region with an accuracy of ~10% error in the testing cases and a ~2.5% error in the training cases were observed. **Figure 5.17** shows the final architecture with 87 wells. In this architecture three hidden layers having 33, 25, and 15 neurons in each layer with 'tansig', 'logsig' and 'logsig' as transfer functions respectively for each layer were used. **Figure 5.18** shows the relevancy of the inputs used in the oil performance network. This figure shows that seismic data is ~32% important in predicting two-year water performance of the well at a given location.

Although the network structure is different as compared with oil and gas network, the relevancies observed in this network are similar to the relevancies observed for the oil and gas network. This shows that the information available in terms of geophysical and completion data is somehow related to the fluid produced at a given location, and the networks developed in this study are able to comprehend that information.

Fig. 5.17: Architecture of the water performance network
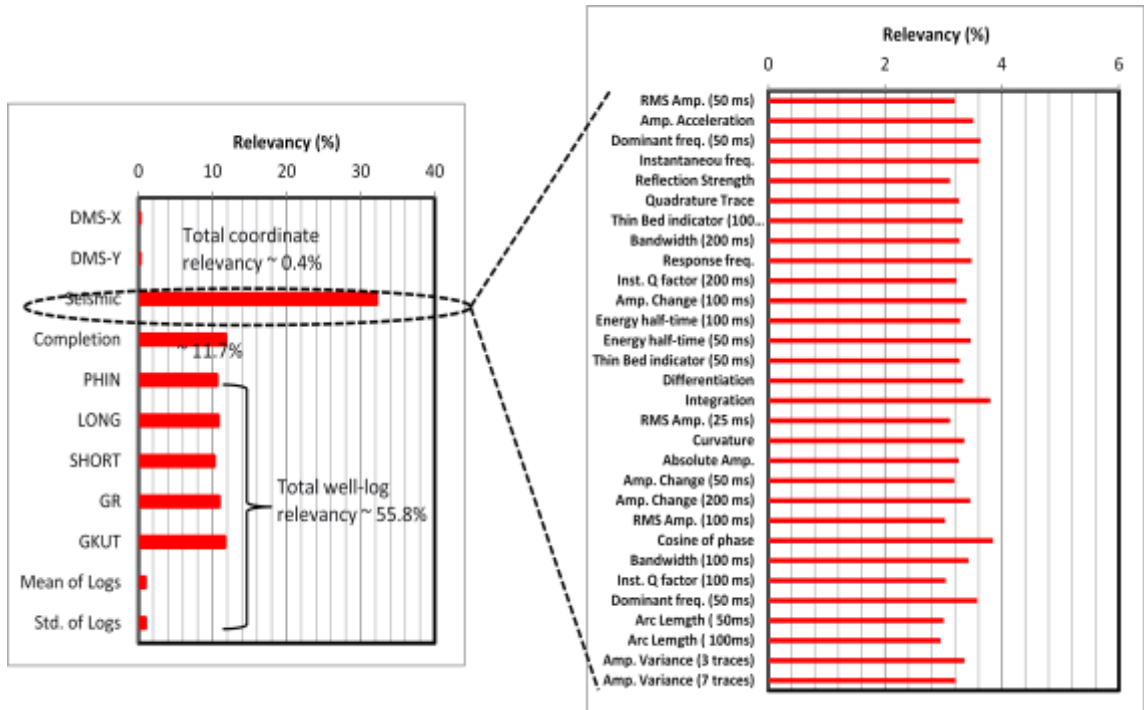
Fig. 5.18: Relevancy of inputs used in water performance networkl

5.5 Optimizing Completion Parameters

The hybrid ANN-EnOpt methodology described in **Section 4.2.3** is implemented to optimize the number of stages and amount of proppant used in stimulating a well. The approach is based on identifying a cost function that incorporates operating cost of well, cost of fracturing a well, royalty on production etc. have been considered. Two year oil production is used to calculate the net present value of the well. The cost data for individual parameters are taken from literature. It is assumed that the total cost of fracturing a well is mainly driven by the net amount of proppant used. The cost of proppant used in fracturing ranges ~20%-65% of the total cost of the proppant

[Huckabee, et al., 2005]. In this study, proppant cost is assumed to be 30% of the total cost of the fracturing; an average value expected by an operator in Huckabee's et al. (2005) study. The other important factor for optimization is the number of fracture stages. The cost of first stage is assumed to be \$5000 in addition to other completion costs and this cost is assumed to decrease for subsequent stages.

The dollar amounts for individual commodity are time sensitive, therefore; a general cost function is developed. This will allow changing the cost for individual parameter in future. The costs for individual parameter used in the function is described in the Table 5.3 and *'Net Present Value (NPV)'* function used in this work is defined as

$$Cost = CC + OC$$

$$CC = \frac{P * P_{cost}}{R_{pf}} + C_{TFS}$$

$$C_{TFS} = \sum_{i=1}^{N_{stages}} C_{fs} * (1 - R_{rf})^{i+1}$$

$$NPR = \sum_{k=1}^{8} \frac{production_i * (P_{oil} - OC)}{(1 + i)^{\frac{k}{4}}}$$

$$NPV = NPR - CC$$

where, '*Cost*' represents the total production cost, '*CC*' is the completion cost, '*OC*' represents the operating cost and royalty, '*P*' is total proppant used, '*P_{cost}*' is the cost of

proppant, 'R_{pf}' is the proppant's contribution in the total completion cost, 'C_{TFS}' is the total cost due to fracture stages, 'C_{fs}' is the cost of first fracture (owing to equipment cost etc.), 'Rrf' is the stage reduction factor, 'N_{stage}' is the total number of fracture stages, 'NPR' is net present revenue and 'NPV' is net present value, and 'i' is the annualized discounted factor. Here, 'P' and 'N_{stage}' are a part of the optimization function.

Chapter 6 Results and Discussion

The expert systems discussed in Chapter 5 are utilized to make the respective predictions for the entire field. In this chapter the results obtained from individual expert systems are discussed. The order of the discussion is same as the expert systems introduced in Chapter 5.

6.1 Completion Data Network

The completion network was developed using 3 hidden layers with 49, 38 and 22 neurons and the transfer functions '*logsig*', '*tansig*' and '*tansig*', respectively. An average error of ~8% during the testing cases was observed with this architecture. During the analysis of the data, the highest errors are observed in tubing string data prediction and pump data predictions as shown in **Figure 6.1**. This may be attributed to the ranges of these parameters exposed to the expert system during the training of the system. **Figure 6.2** shows the histogram of the "minimum cum length (ft)" in the pump data group where maximum errors are observed while testing the expert system. It can be seen that out of 87 wells 84 wells have values below 80 ft for this parameter and 2 values are above 150 which is twice the normal range of the parameter. The expert system is able to predict the values within an error range of 12% for this parameter also.
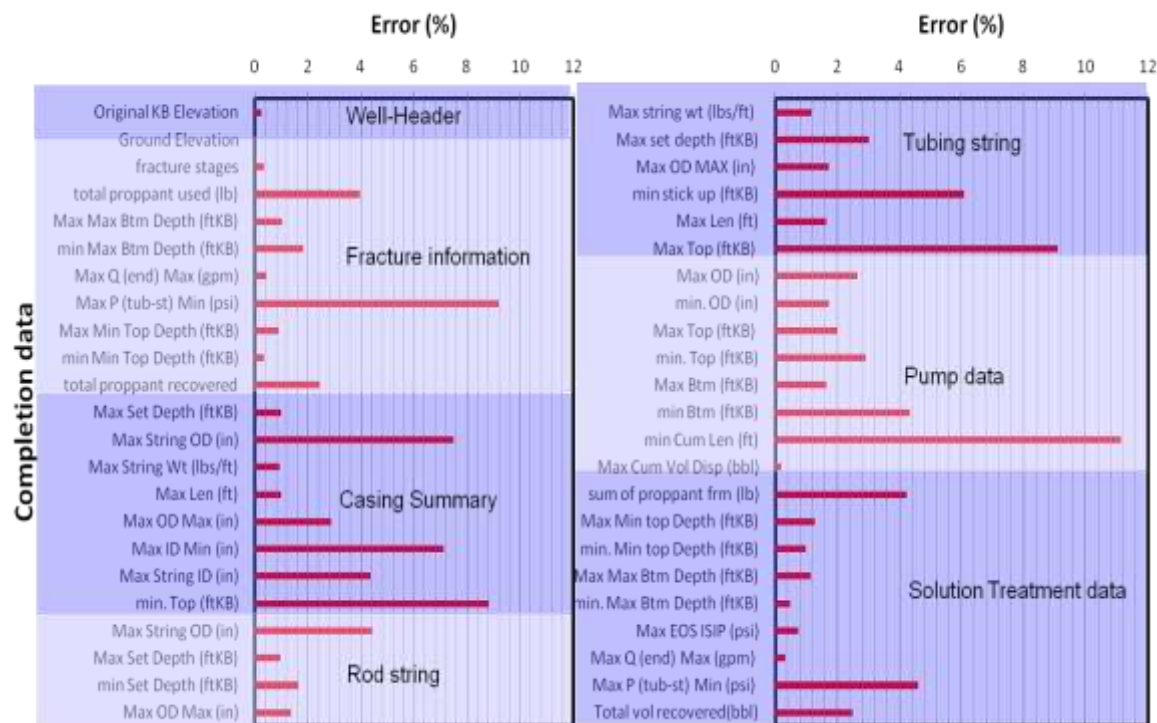
**Fig. 6.1: Average error for individual completion parameters predicted by expert system**
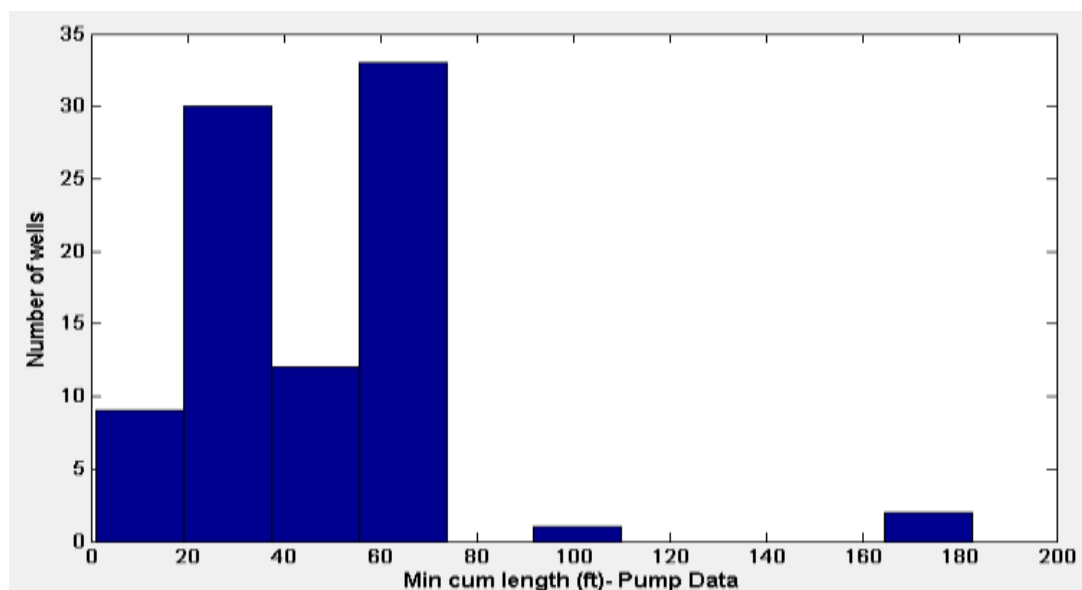
Fig. 6.2: Minimum cum length (Pump data) values used in training the expert system

Figure 6.3 shows an example of the comparison between the actual completion parameters observed in the field with the completion parameters predicted by the expert system. All the parameters predicted by the expert system show a good quality match. It was previously shown in Table 5.1 that these parameters had different ranges. The parameters represented here vary from each other by several orders of magnitude, therefore; logarithmic scale is chosen to represent all the parameters on a same figure. The parameter values represented in Figure 6.3 are in the same order as shown in Table 5.1.

The expert system developed in this section provides an overall trend for the ATM region at an undrilled location. These parameters are based on the geological properties of the formation and the location of a well. Results presented here show a good accuracy in predicting these parameters for unused wells, thus, increases the confidence in this network. This expert system is used to predict the completion parameter for the entire ATM region as shown in **Figures 6.4-6.6** as examples. These completion parameters are then used along with synthetic well logs [Mohammadnejad, 2011] to predict well performances using 'production performances network'. This network will help in a quick assessment of the completion parameters at proposed wells in the field.
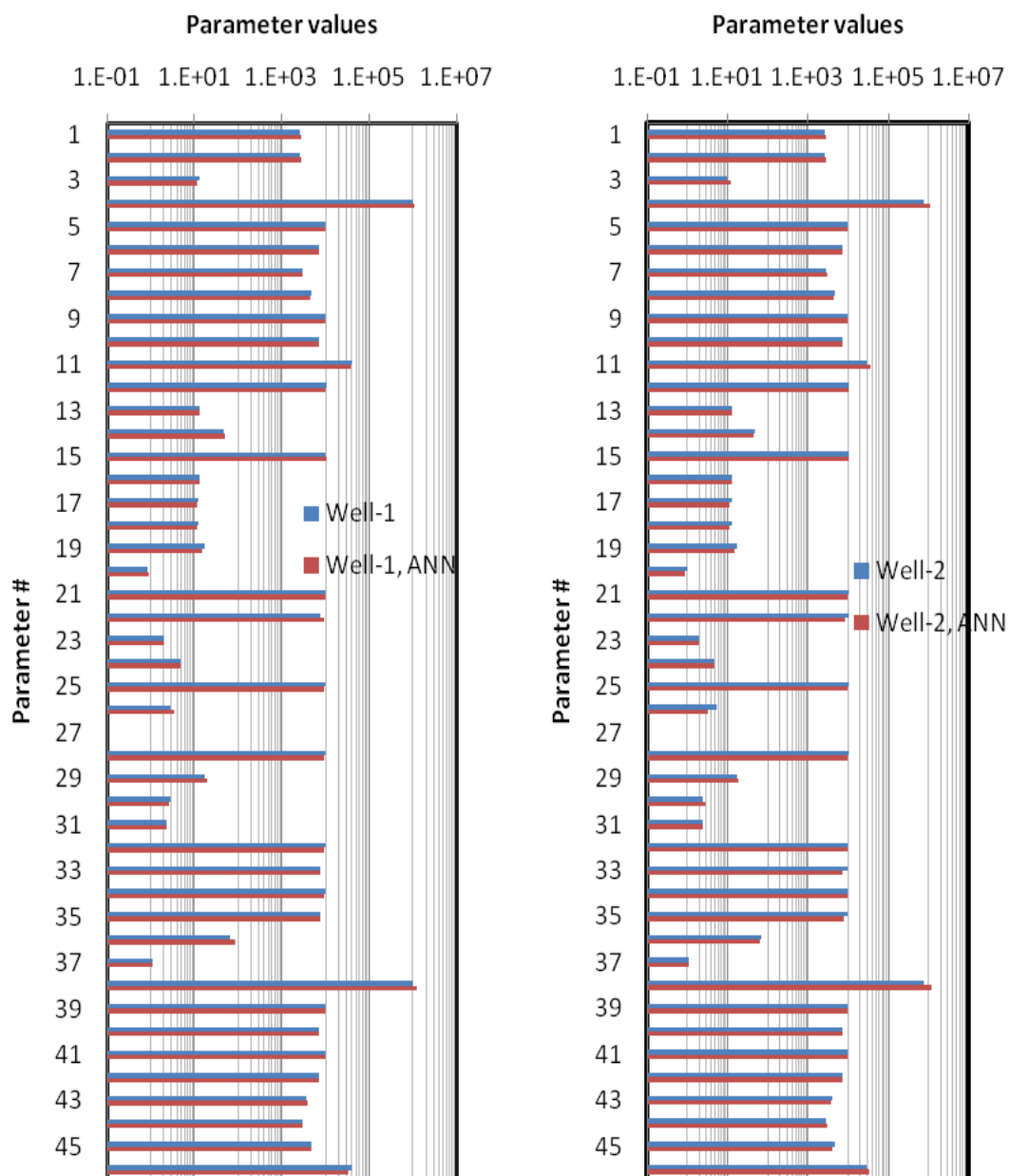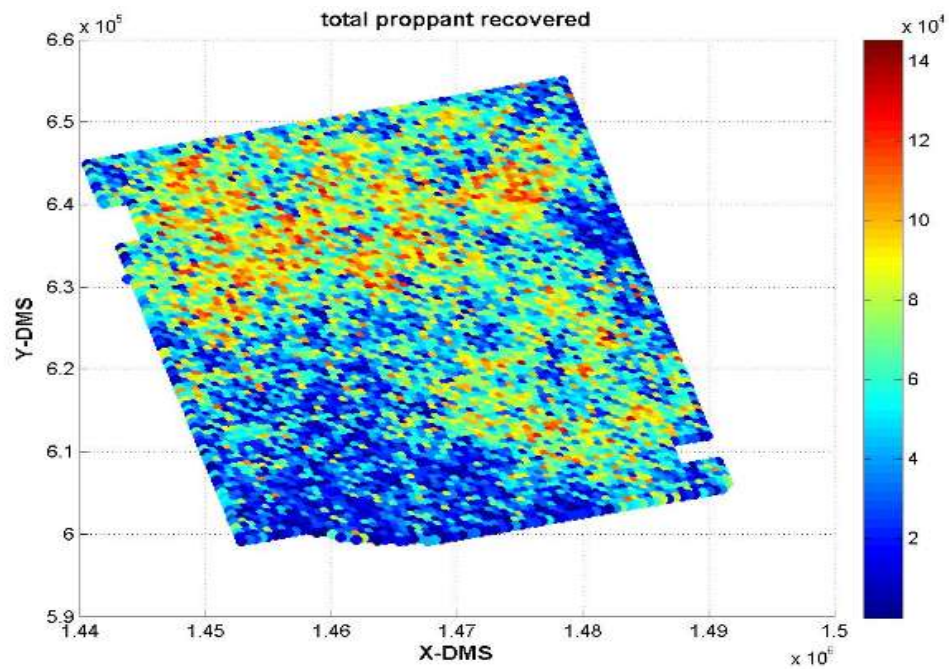
Fig. 6.3: Comparison of results predicted by expert system
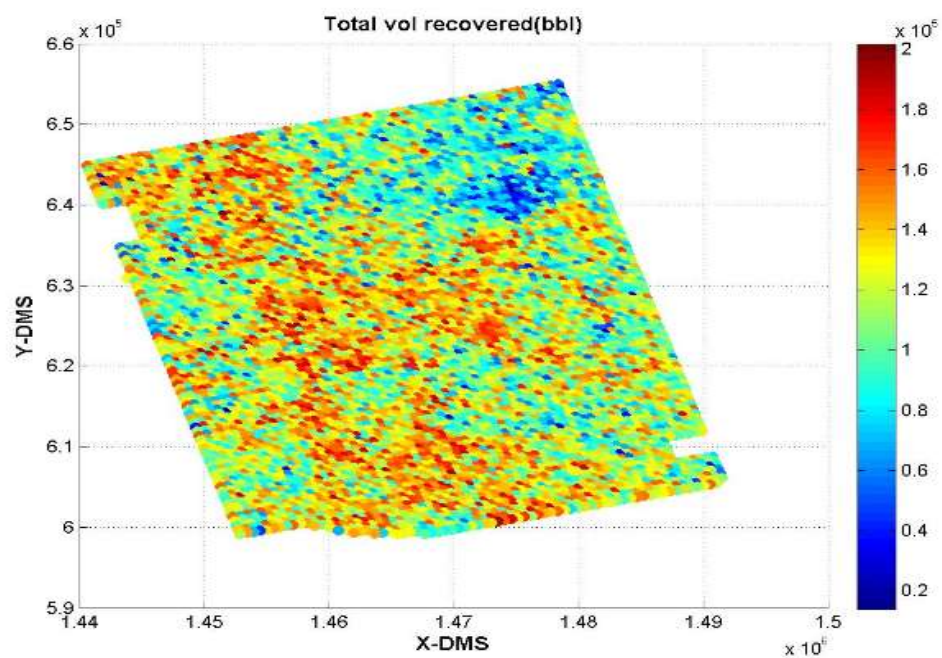
Fig. 6.4: Total volume recovered (Solution treatment) as predicted by expert system
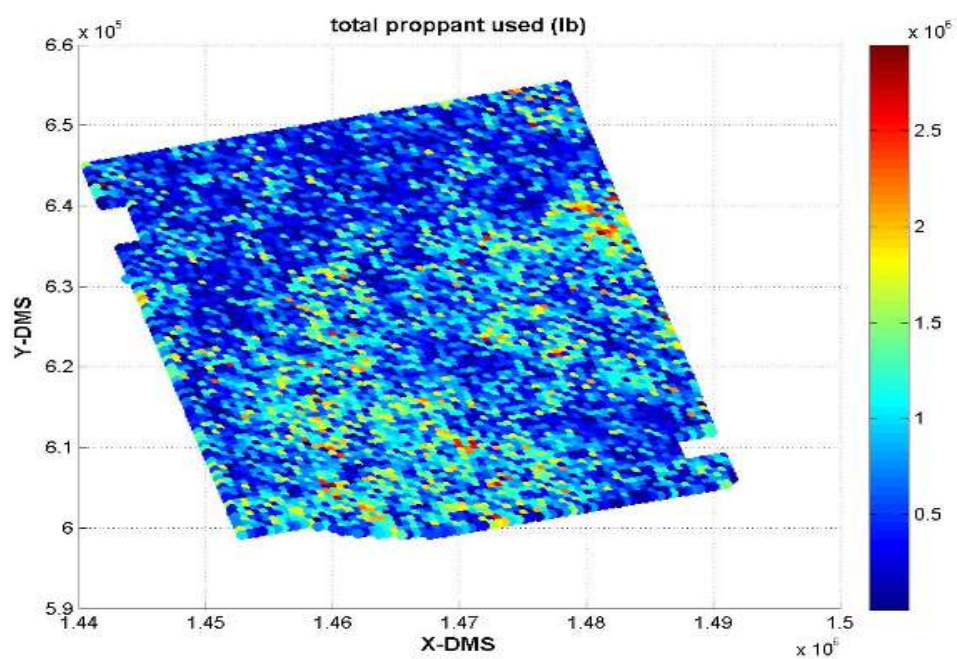
**Fig. 6.5: Total proppant used (Fracture summary) as predicted by expert system**

Fig. 6.6: Total proppant recovered (Fracture summary) as predicted by expert system

6.2 Well Performance Prediction Networks

In this section oil, gas and water production performance networks are discussed in detail. The first part of the discussion is based on the network developed with 87 wells initially used and the second part of the discussion is based on testing the network with additional wells and results obtained after improving the architecture of the oil and gas production performance networks.

6.2.1 Oil Production Prediction Network (OPPN)

The oil network discussed in Chapter 5 predicts the cumulative oil production with an average error of ~8% with the testing cases is observed with this architecture. **Figure 6.7** shows that highest errors are observed for the first 3 months production period. The highest errors are possible in the initial life of the well because of the presence of extensive noise in the data due to human intervention (for e.g. unexpected shut down, cleaning etc). As the production in the field was observed to stabilize with time, error is also observed to reduce with time as can be seen in the cross plots in **Figures 6.7-6.10**. The initial error is observed as ~21% for the first 3 month prediction, and reduces to ~3% for predictions at 21 and 24 months.
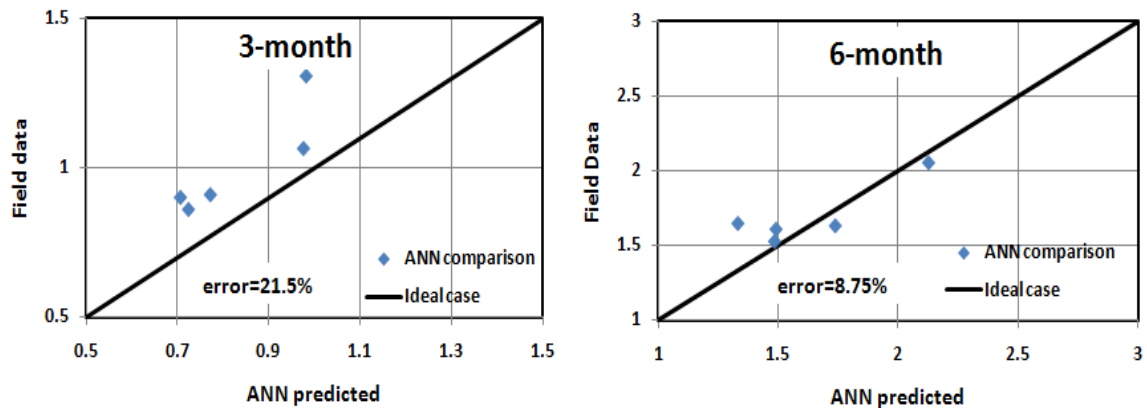
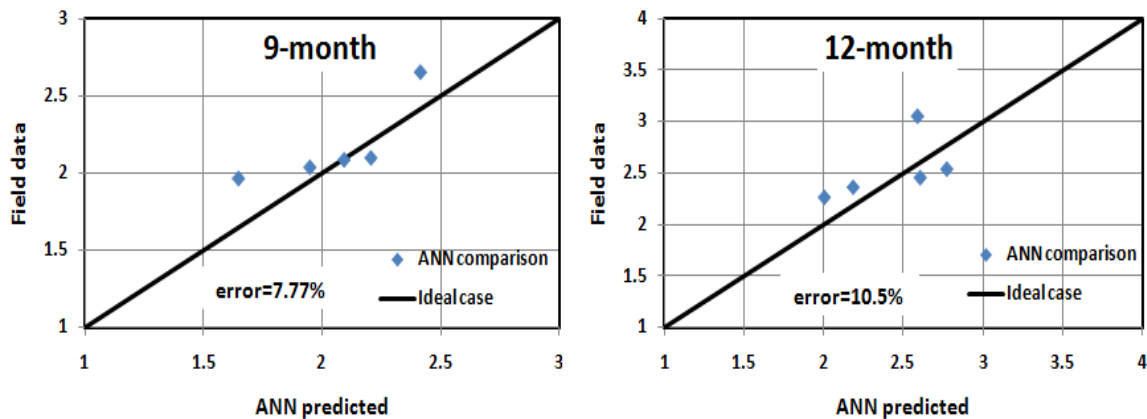**6.7: Cross plot comparing 3 and 6 month of oil production**

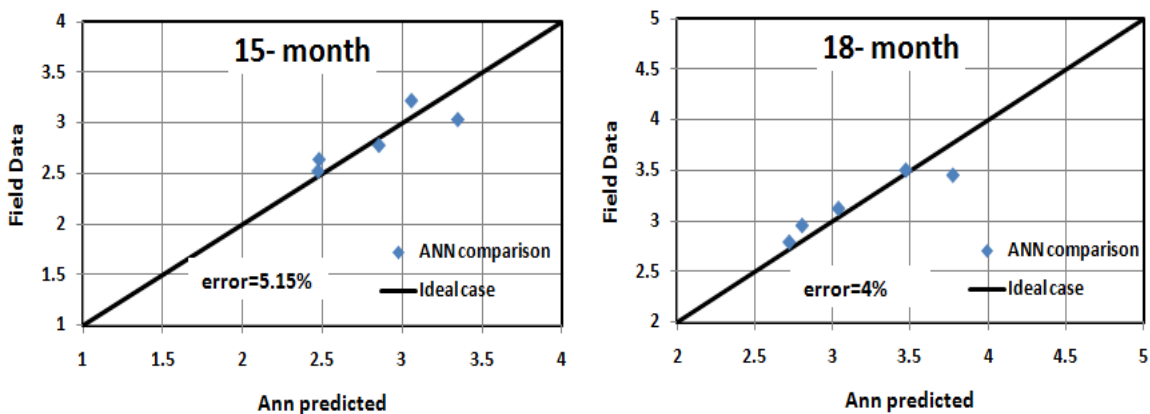**Fig. 6.8: Cross plot comparing 9 and 12 month of oil production**

Fig. 6.9: Cross plot comparing 15 and 18 month of oil production
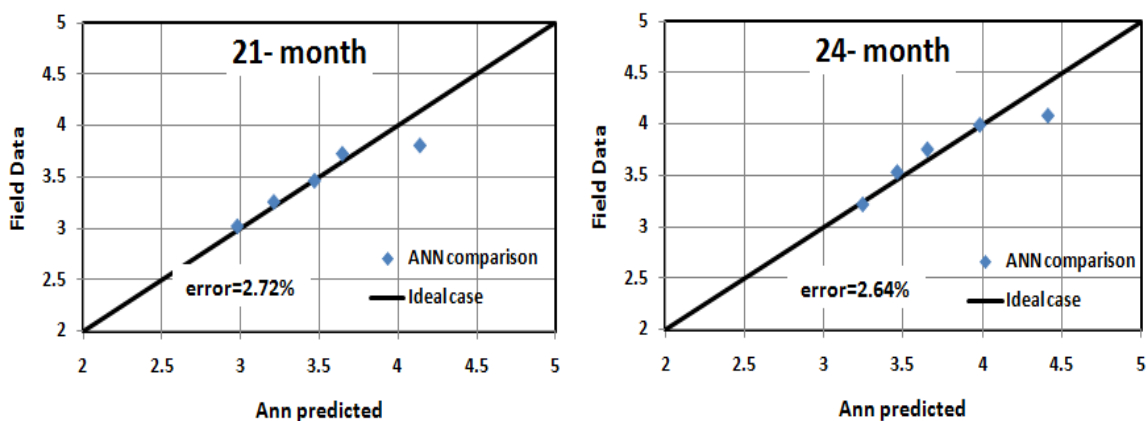

Fig. 6.10: Cross plot comparing 21 and 24 month of oil production

The cross plots show a consistency in forecasting oil production with reduced error for the second year of production. OPPN predicts cumulative production from a well, thus, the production predicted by the network will help in economical evaluation of a well prior to the drilling. Therefore, this network is expected to help in improving the economical production from the tight oil reservoir. The prediction values can also be compared on a bar plot where one-to-one correspondence can be seen better as shown in **Figures 6.11 and 6.12**. The results show a good quality match with the field production data.
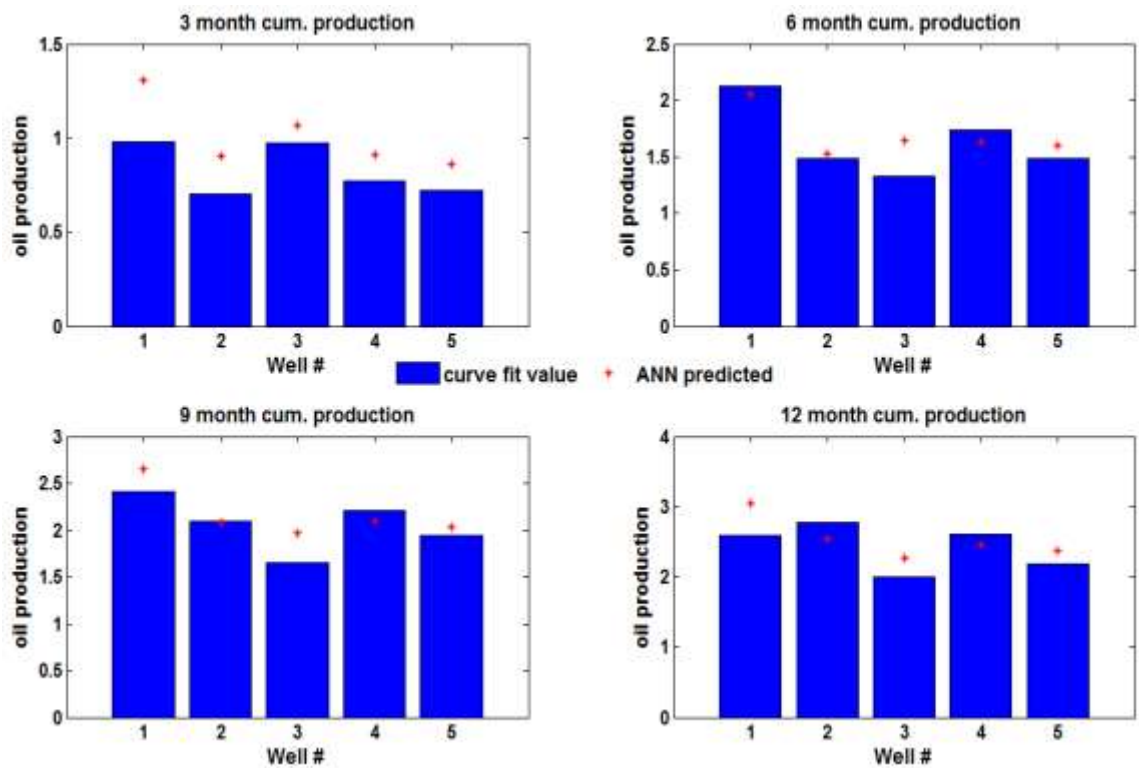

**Fig. 6.11: Comparison of oil production for the first year**
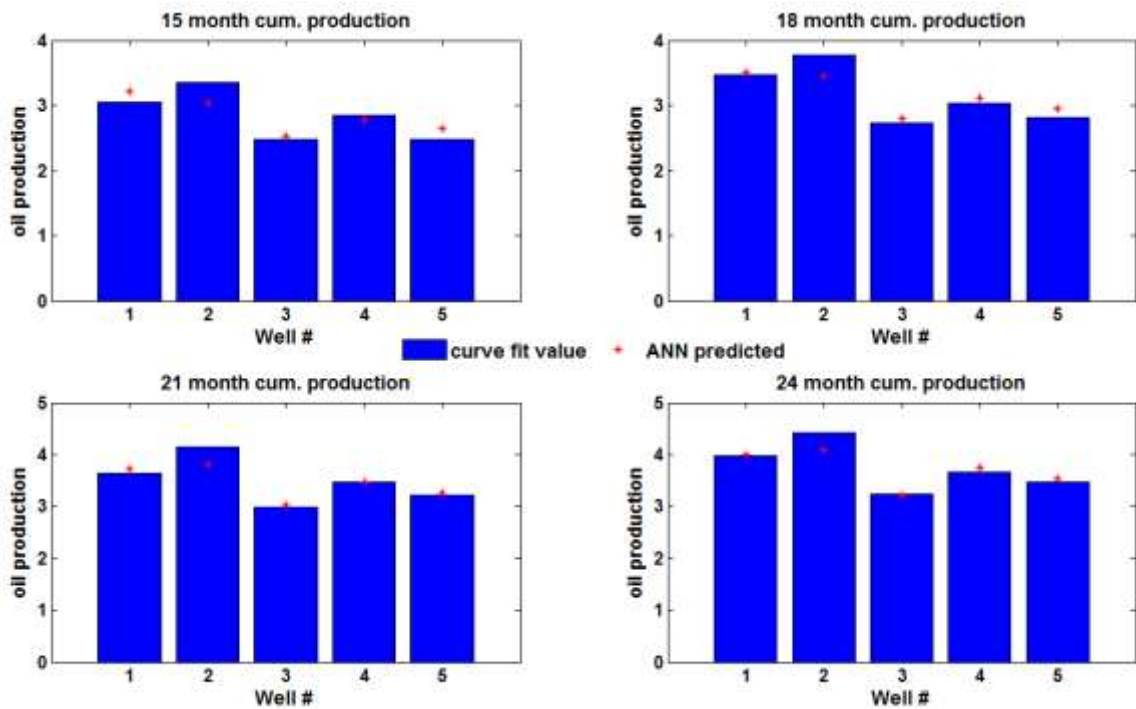
Fig. 6.12: Comparison of oil production for the second year

One year cumulative oil production was compared with the field values (note that 1 year field data was interpolated in Midland using the well information). **Figure 6.13** shows the one year cumulative oil prediction made by expert system and **Figure 6.14** shows the cumulative production observed in the field. It can be seen that the expert system developed in this study is able to predict the overall trend in the oil production for the ATM region. The expert system is able to identify and distinguish the prolific regions in the ATM region. As it can be seen in Figure 6.13, the North-East and South-East region of ATM is prolific while the area is still unexplored as shown in the original production map (Figure 6.14).
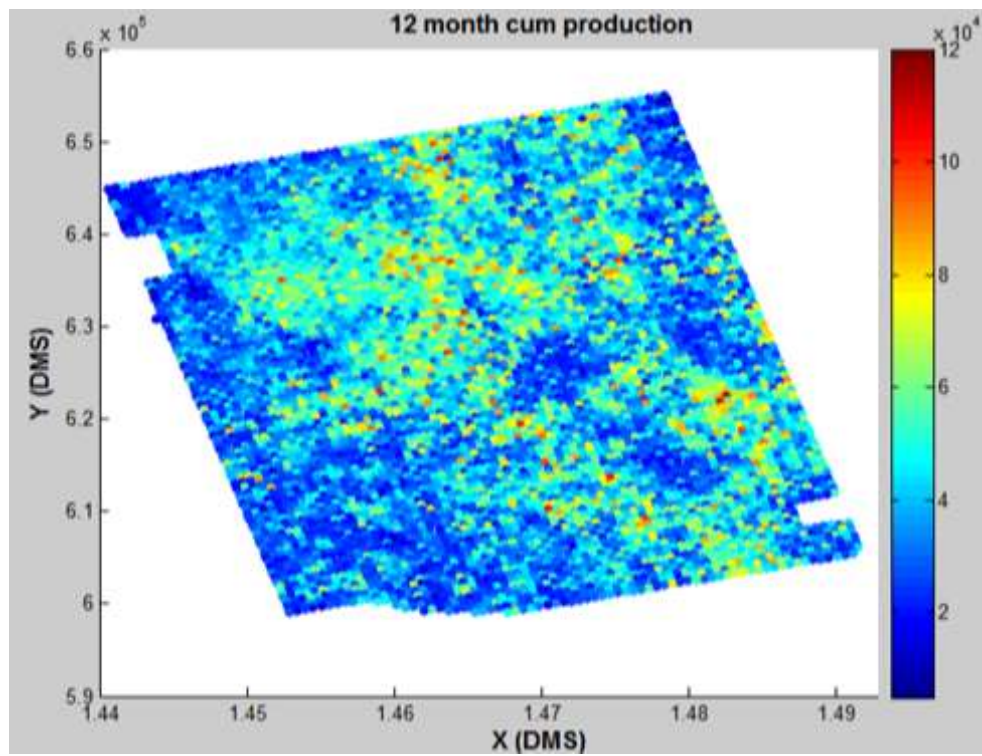
**Fig. 6.13: 1 year cumulative oil production (STB) predicted by the expert system**
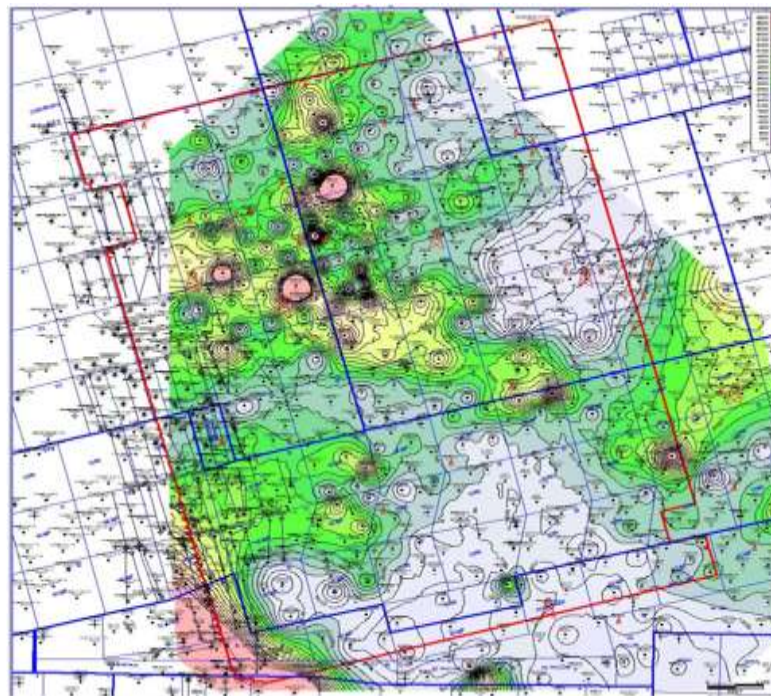
Fig. 6.14: 1 year cumulative oil production (STB) observed in the field

In addition, this expert system was tested with the data provided later in the course of study (October 2010) with updated production history for wells in the ATM region. The average error in predicting the oil production was observed to be ~65% which is much higher than the error obtained in testing wells originally provided. Upon analysis of the production data it was found that the new wells are low producing wells and they fall outside the bounds of previously used production data as it can be seen in **Figure 6.15 and 6.16**. Figure 6.15 shows the histogram of the 2-year cumulative production data used in the training (87 wells), (which shows a range of ~2-14 units of oil in the training and testing wells); whereas the new wells have a cumulative production ranging between ~1.8-2.8 units of oil as shown in Figure 6.16.

The previous network was not trained with low producing wells and thus the reason for a high error in predicting this production range. In order to make the OPPN more robust, and to reduce the prediction error for low producing wells, 50 wells were randomly selected and introduced during re-training of the network. The original network architecture was used as the base network. The current architecture is shown in Figure 5.14 which is a slightly modified version of the previous OPPN (Figure 5.11). This network is able to predict the cumulative oil production with an average error of ~13%. In this network, a total of 137 wells (87 old wells + 50 new wells) were used, where 111 wells were used in training, 13 wells were used each for testing and validations.

The new wells added to the OPPN increased the range of cumulative oil production, while the geological properties at these locations lies in the similar ranges as

for old wells used in OPPN. As can be compared in Figure 5.12 and Figure 5.14, the modified OPPN is a similar architecture; suggesting OPPN (Figure 5.12 and Figure 5.14) to be stable networks. **Figures 6.17-6.24** show the comparison of actual and predicted cumulative production predicted by modified OPPN. These results show a major improvement as the average error is reduced from ~65% to ~13%. Thus, it can be inferred, adding more information to the network improved the neural relationship in predicting the oil production. Therefore, it is also possible to improve the OPPN even further by adding more information of the wells and may also help in improving the expertise of the network outside ATM region.
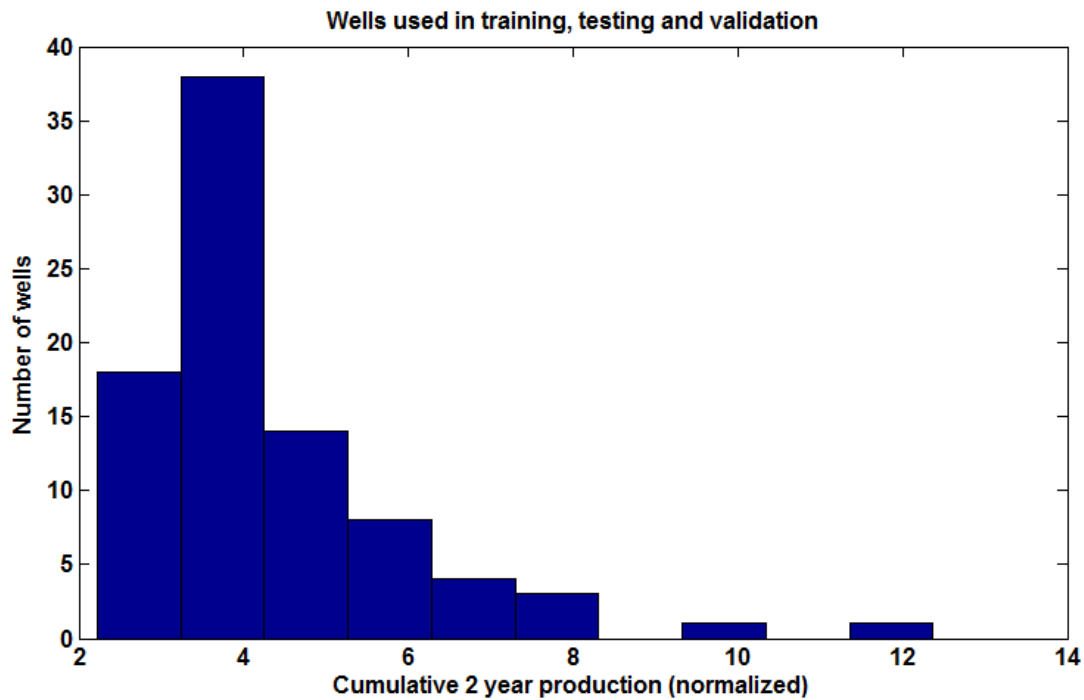
Fig. 6.15: Histogram showing the production ranges of well in September 2009 dataset
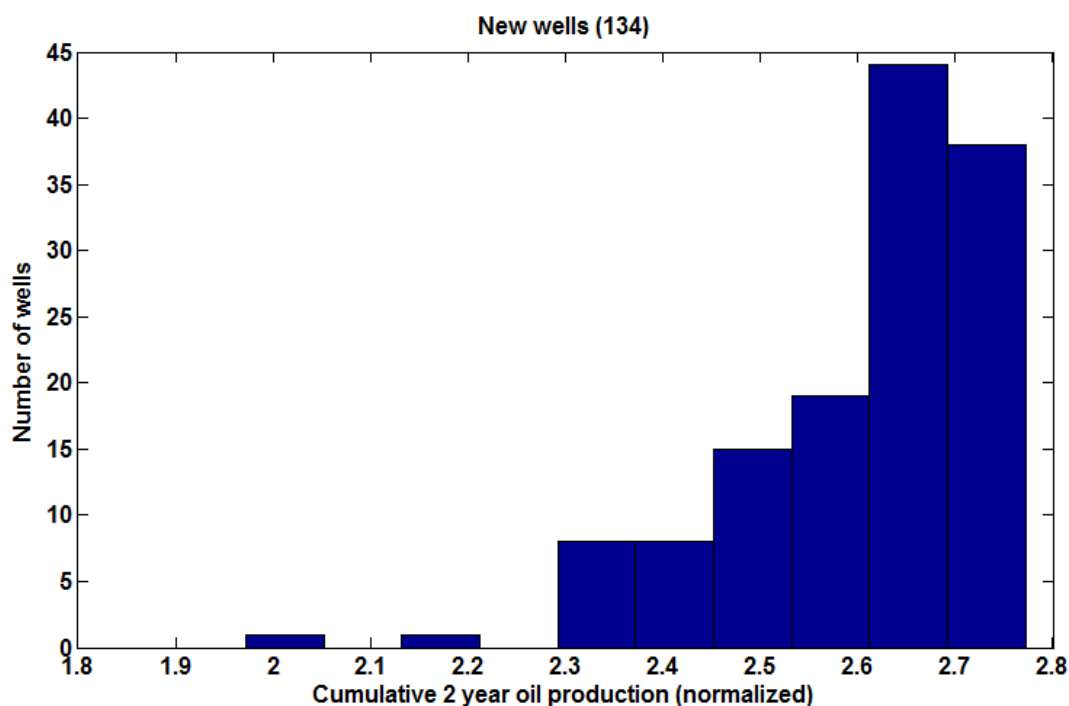
Fig. 6.16: Histogram showing the production ranges of well in October 2010 dataset
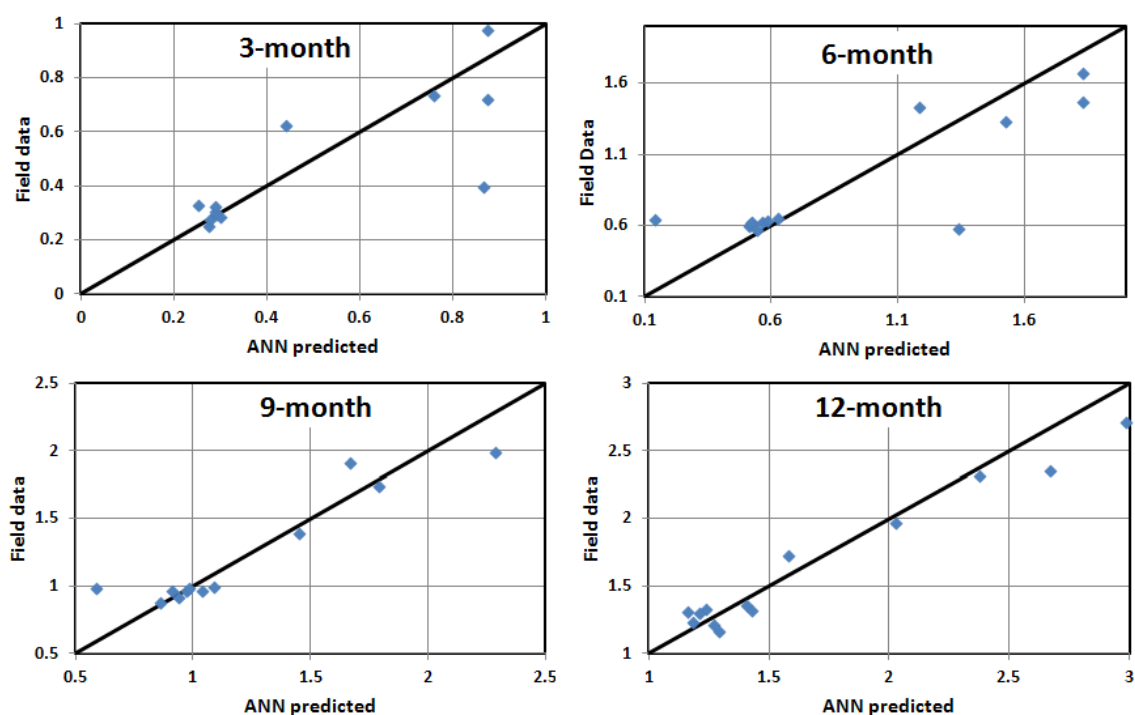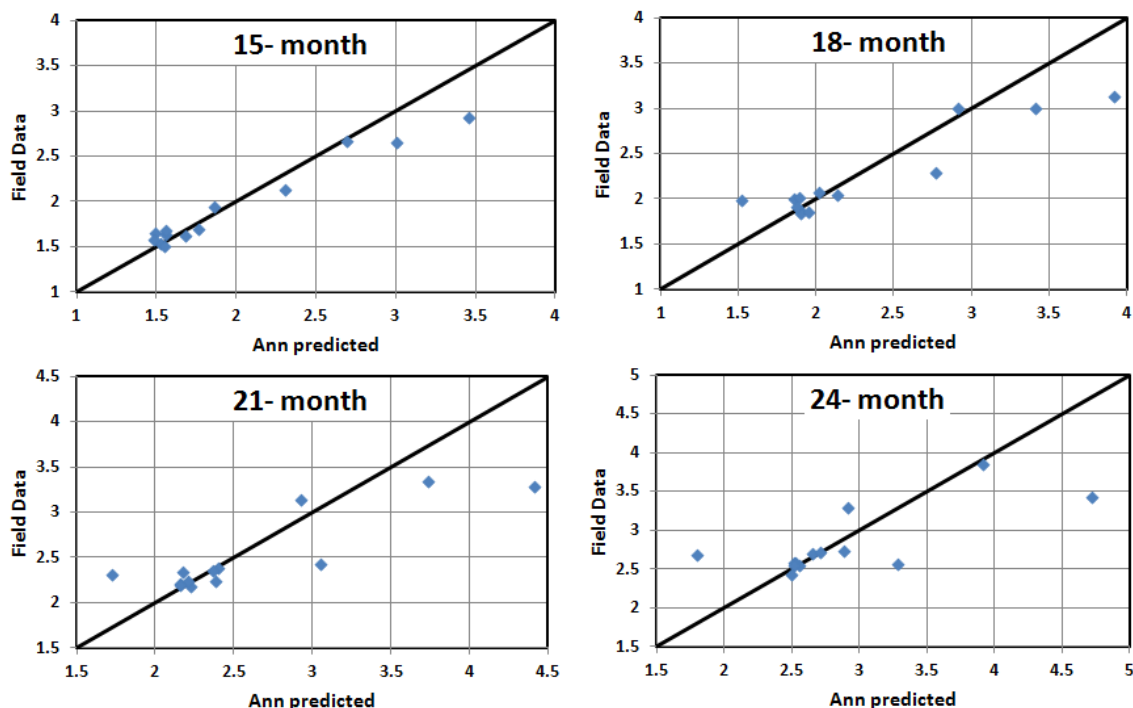

Fig. 6.17: Cross plot comparing quarterly oil production for the first year with the updated network
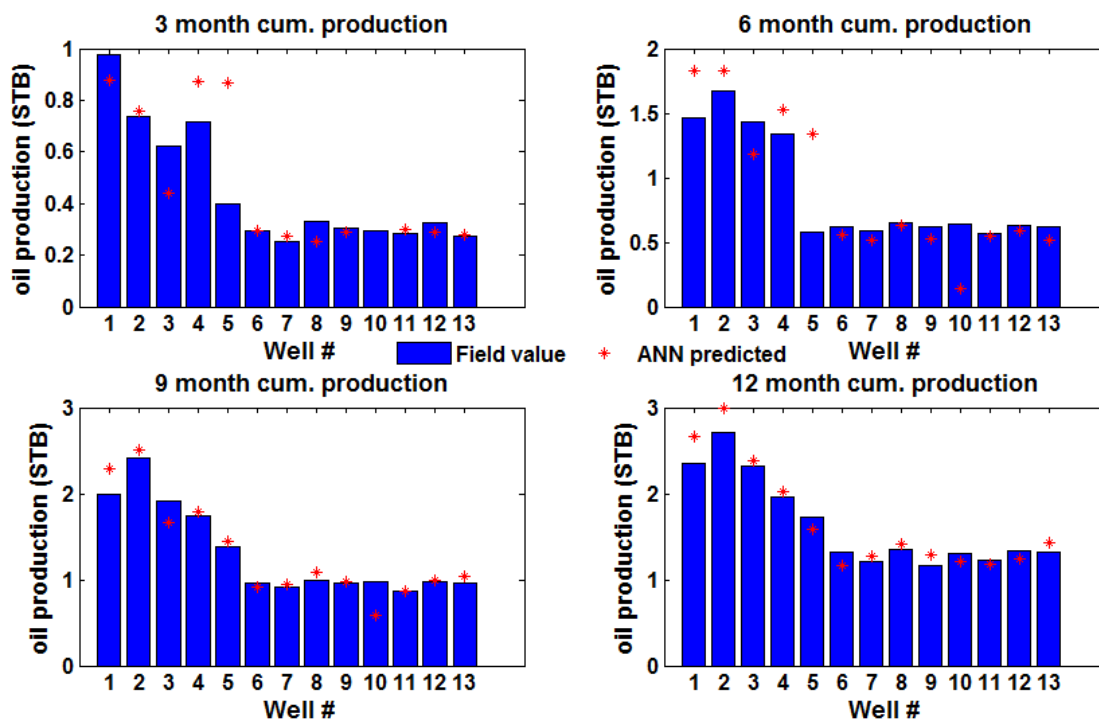
Fig. 6.18: Cross plot comparing quarterly oil production for the second year with the updated network

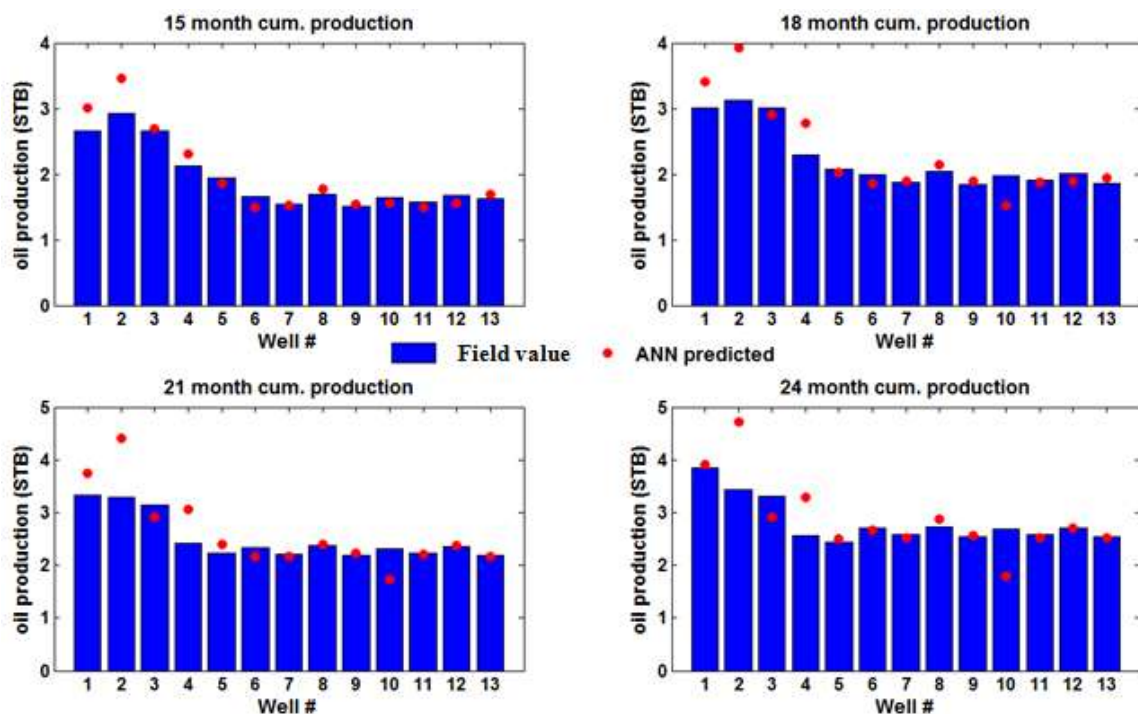**Fig. 6.19: Comparison of quarterly production (oil) during the first year**

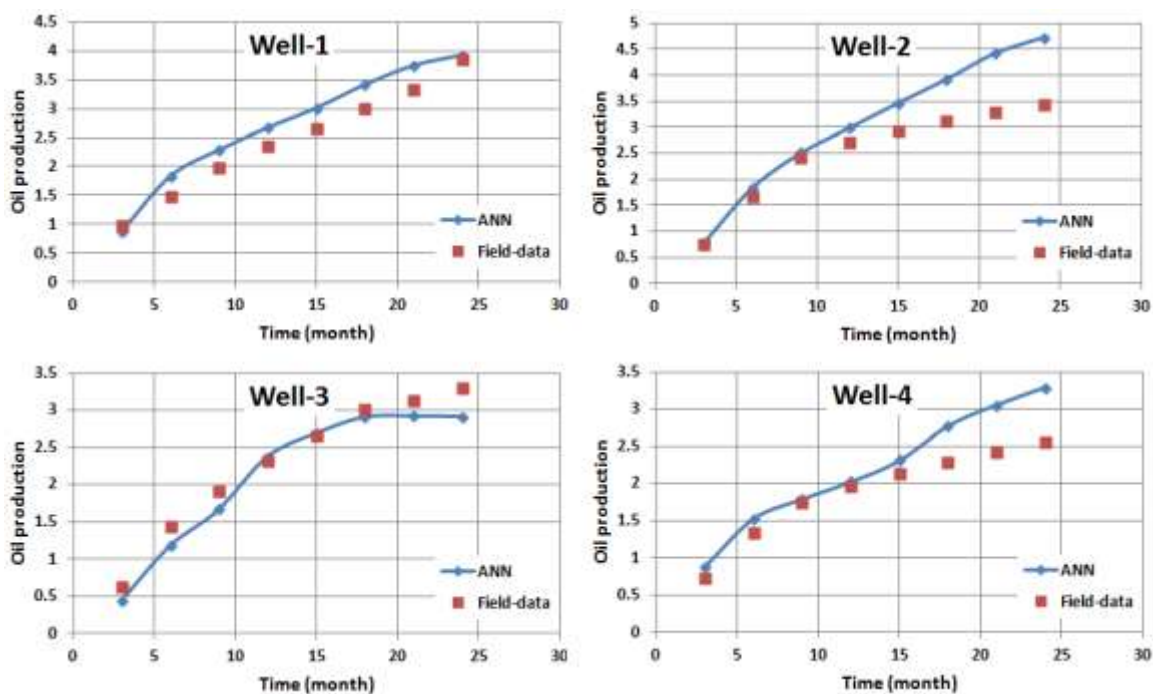**Fig. 6.20: Comparison of quarterly production (oil) during the second year**

Fig. 6.21: Comparison of predicted vs actual production for each testing well (1-4)
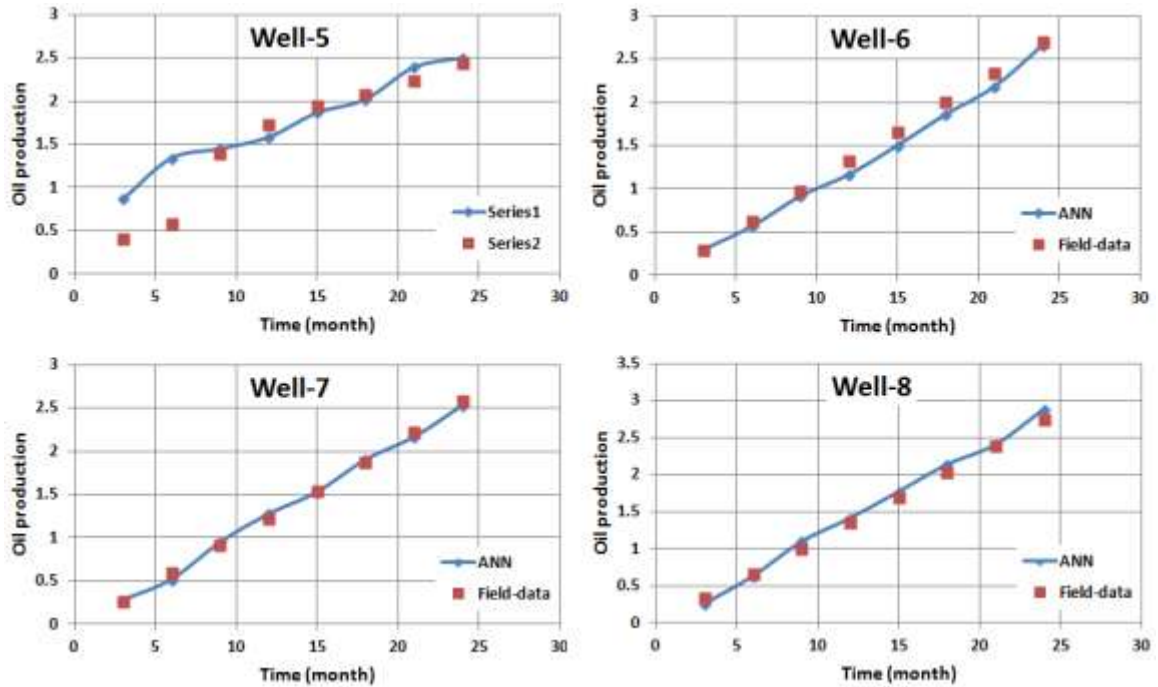
Fig. 6.22: Comparison of predicted vs actual production for each testing well (5-8)
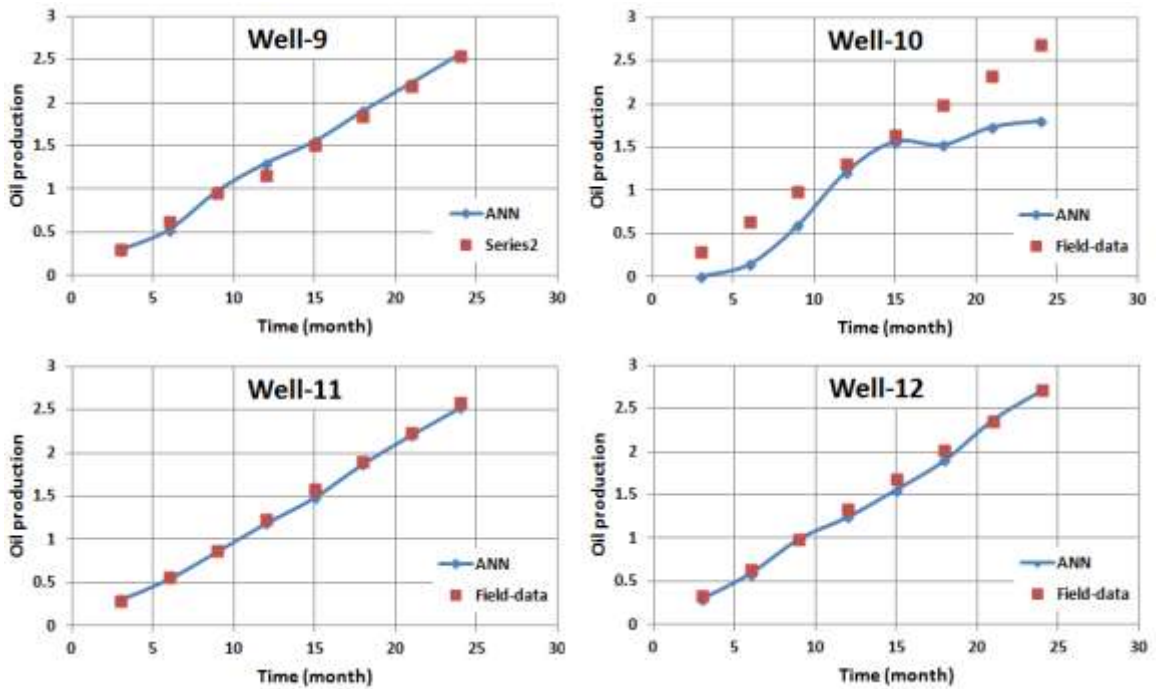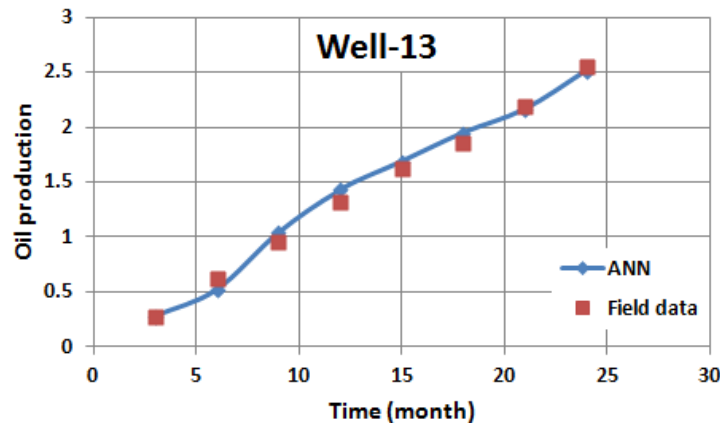

Fig. 6.23: Comparison of predicted vs. actual production for each testing well (9-12)

Fig. 6.24: Comparison of predicted vs. actual production for each testing (well 13)

The expert system (Shown in Figure 5.14) is used to predict the performance of the network at every location in the ATM region. At an undrilled location only geological coordinates and seismic data are available and in order to generate two year cumulative oil production curves, well logs and completion parameters are also required. Well logs and completion parameters are generated by the expert system discussed earlier. Once the complete information is available at a given location, the oil production expert system is used to generate completion surfaces. **Figures 6.25** through **6.28** show the oil production at each location within the ATM region predicted by the expert system. As can be observed in Figure 6.28, North-East and South-East regions show potential locations for further drilling. This observation is consistent with the results generated by expert system shown in Figure 5.12.

The oil expert system is also tested with new wells in the ATM region. Eighty four wells were reserved by the sponsoring company to test the working of the expert

systems. The predictions from the expert systems are very good as 70% of the wells predict close results with less than 10% error compared with the actual field results as shown in **Figure 6.29**. As can be seen more than 90% of the wells predict oil prediction with less than 20% error. These results show the robustness of the expert system developed for a tight oil reservoir. The methodology developed in this work show promising results for developing tight oil reservoir.

Error histogram presented in Figure 6.29, shows the robustness of the OPPN. This network can be used for finding infill drilling locations in the ATM region. The results predicted by the expert system are used to identify the best 100 locations in the ATM region as shown in **Figure 6.30**. These locations have been selected by sorting the cumulative oil production at the end of second year forecasted for each location in the reservoir. This network helps in identifying the sweet spots in the reservoir and less prolific regions in the reservoir. The AES based methodology developed in this work will enable in finding the locations that could have been missed by pattern drilling mostly used in complex reservoirs, viz., tight oil reservoirs. Thus, this methodology is expected to help in efficient development of tight oil reservoir by selecting prolific locations of proposed wells.
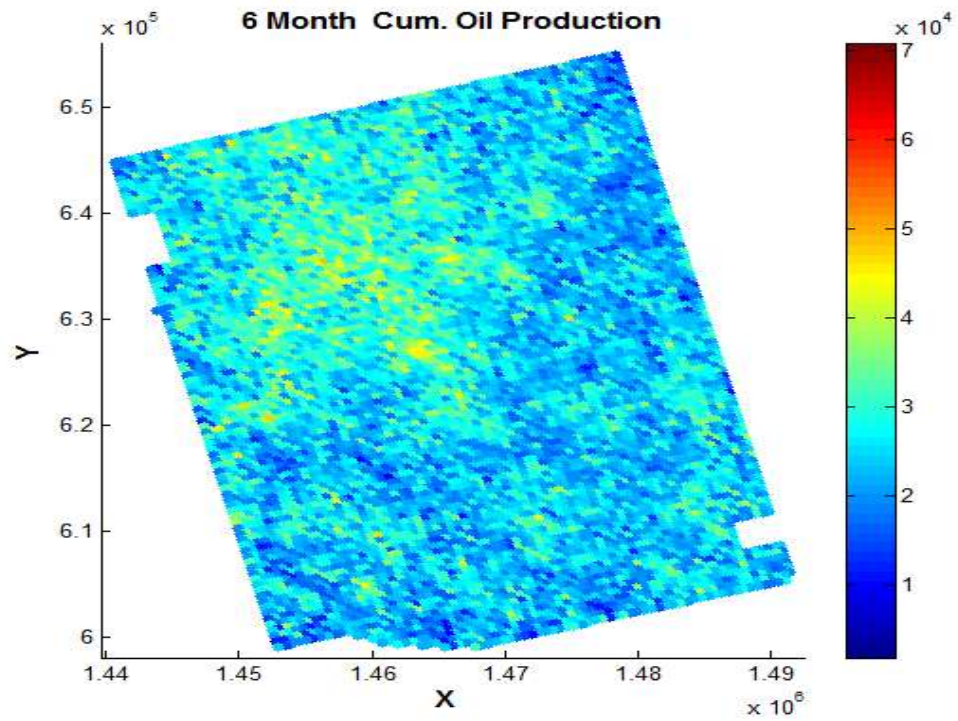
Fig. 6.25: 6 month cumulative oil production predicted by expert system
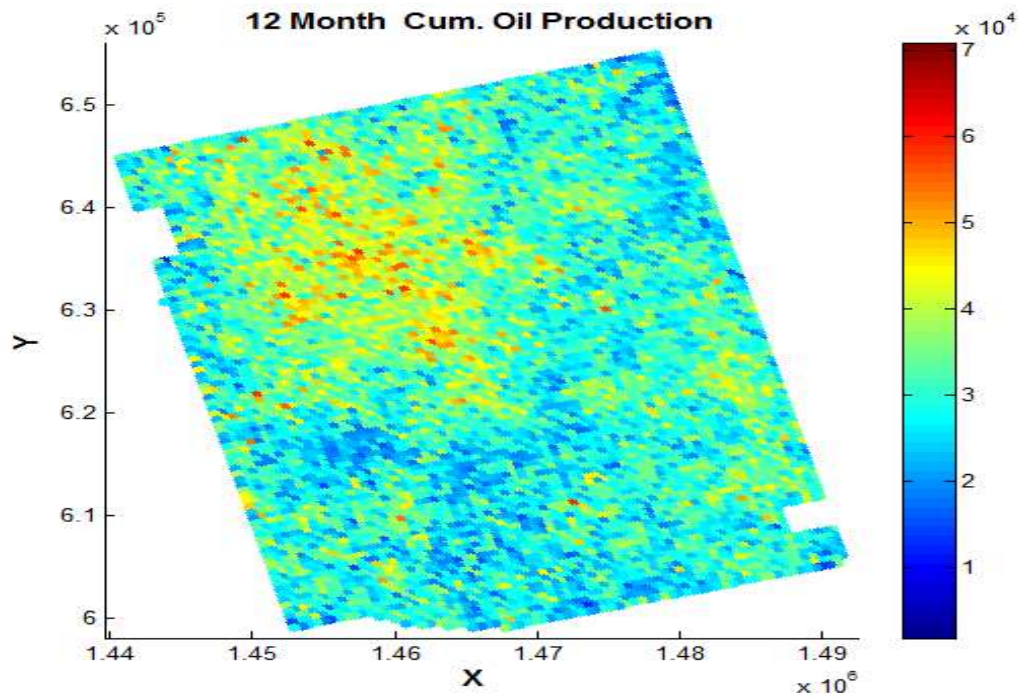
Fig. 6.26: 12 month cumulative oil production predicted by expert system
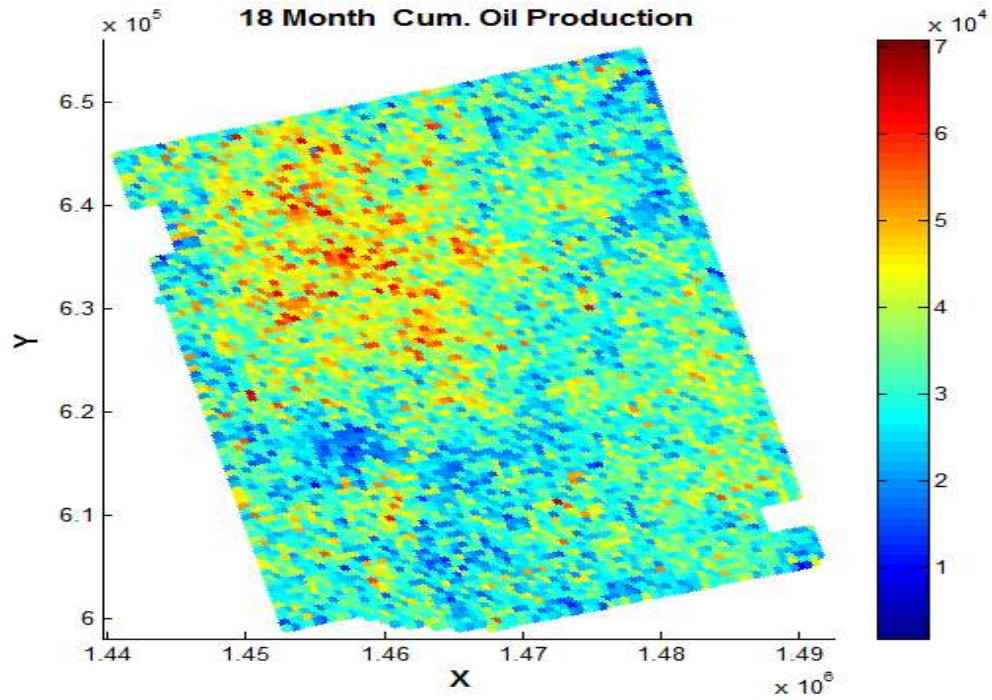
Fig. 6.27: 18 month cumulative oil production predicted by expert system
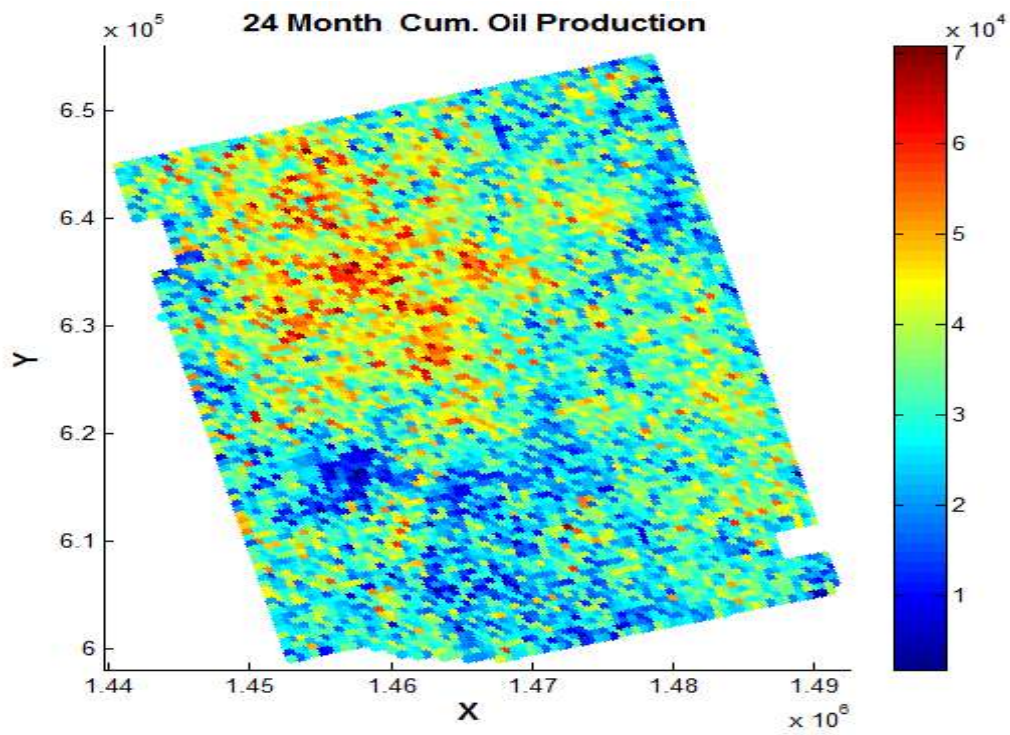
Fig. 6.28: 24 month cumulative oil production predicted by expert system
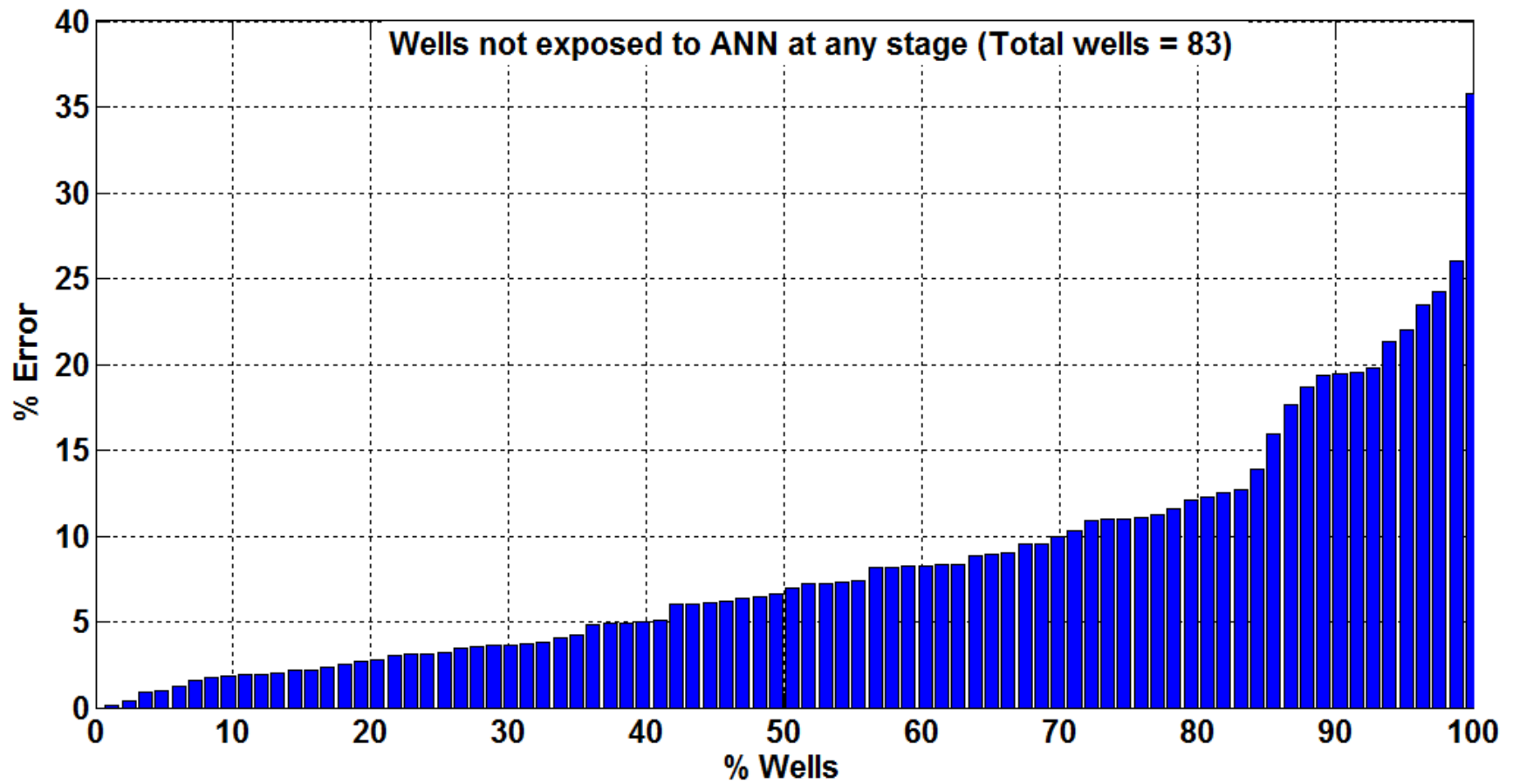
Fig. 6.29: Error histogram in predicting oil production with new wells in ATM
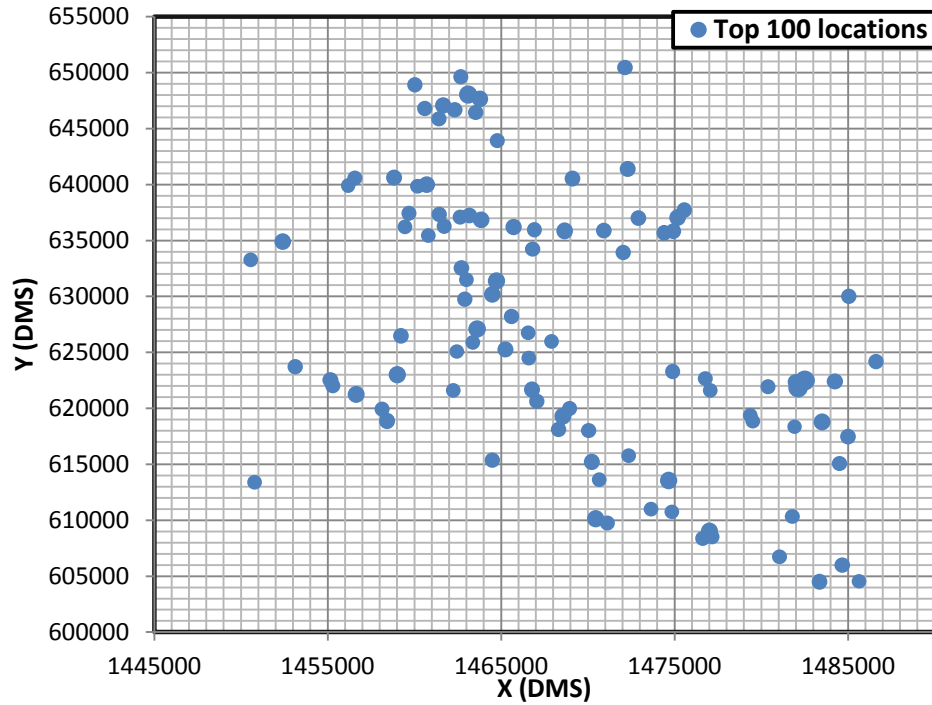
Fig. 6.30: Top 100 oil producing locations in ATM region

6.2.2 Gas Performance Prediction Network (GPPN)

The GPPN discussed in Chapter 5 predicts the cumulative gas production with an average error of ~13% using the testing cases observed with this architecture. **Figure 6.31** shows that highest errors are observed again for the first 3-months production prediction. The reason may be attributed to human interventions as previously stated. **Figure 6.32** shows that average error in predicting cumulative gas prediction stabilizes at 10% for the second year production, unlike oil production network where errors in prediction were observed to decrease with time.
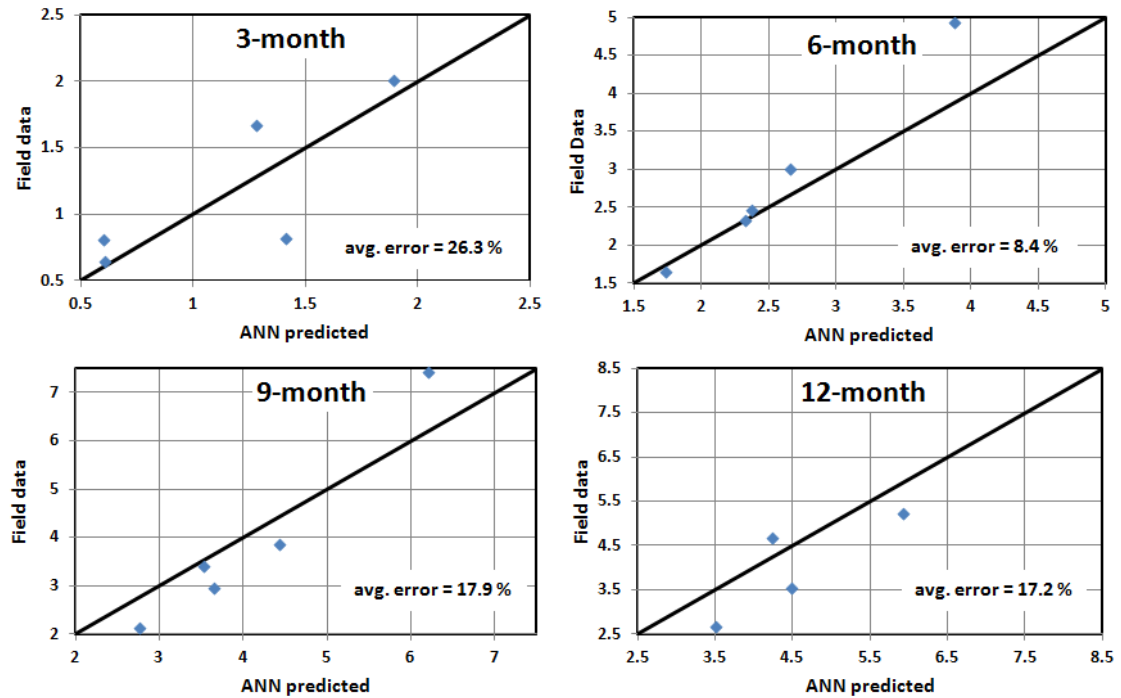
Fig. 6.31: Cross plot comparing 3 and 12 month of gas production with updated network
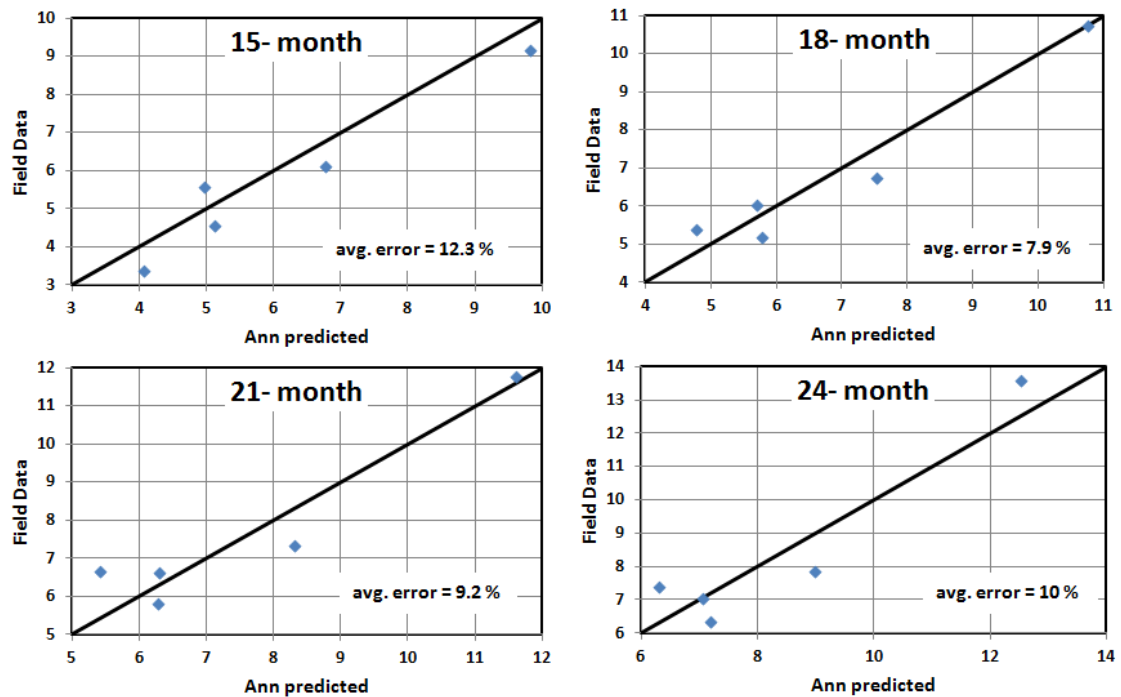
Fig. 6.32: Cross plot comparing 15 and 24 month of gas production with updated network

Figures **6.33** and **6.34** compare the quarterly productions predicted by the network for the testing wells. It can be seen that the expert system is able to predict the gas production closely for the testing case. Finally, production for each testing well is also compared in **Figures 6.35** and **6.36**.
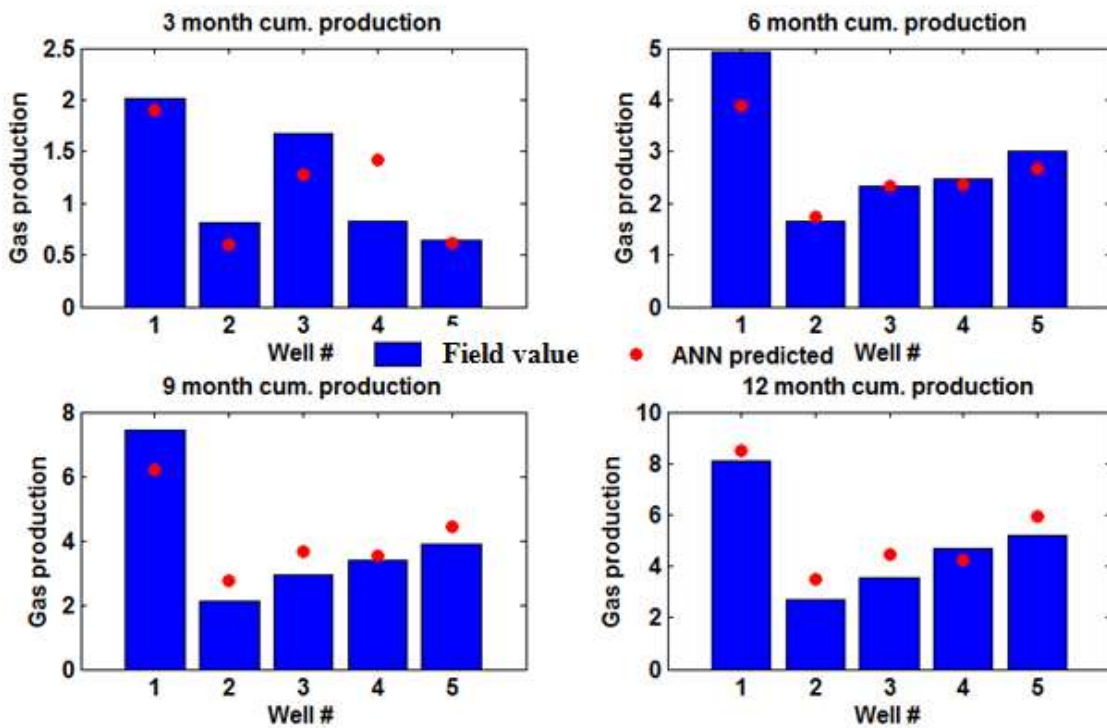
Fig. 6.33: Comparison of quarterly gas production (first year)
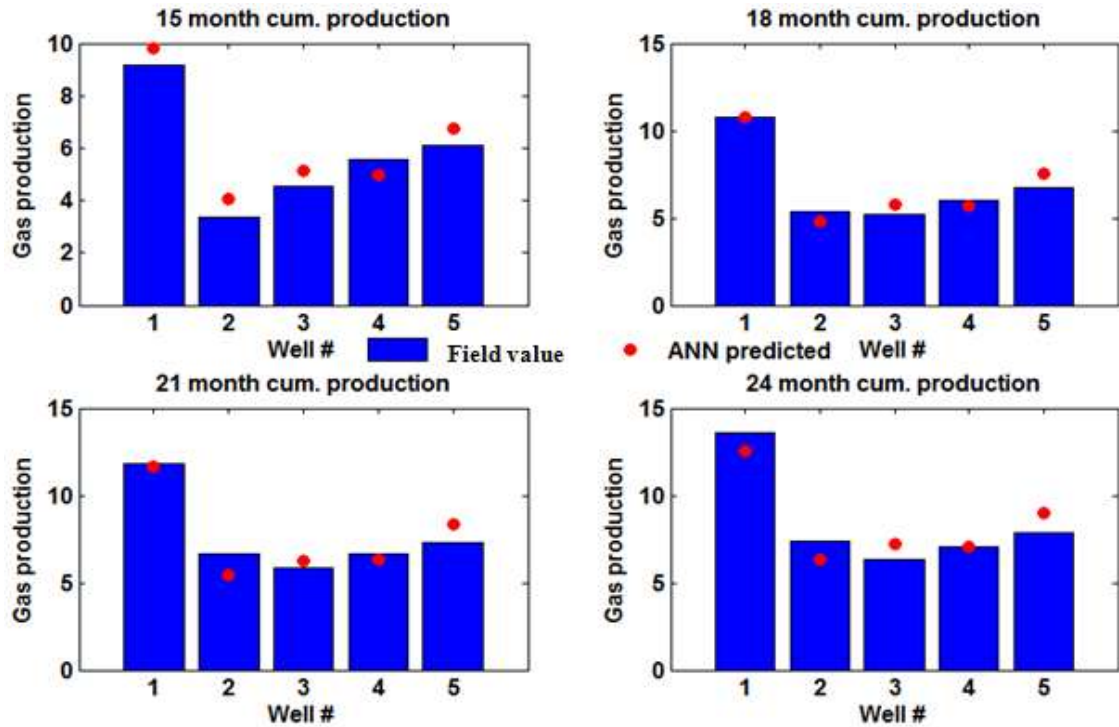
Fig. 6.34: Comparison of quarterly gas production (second year)
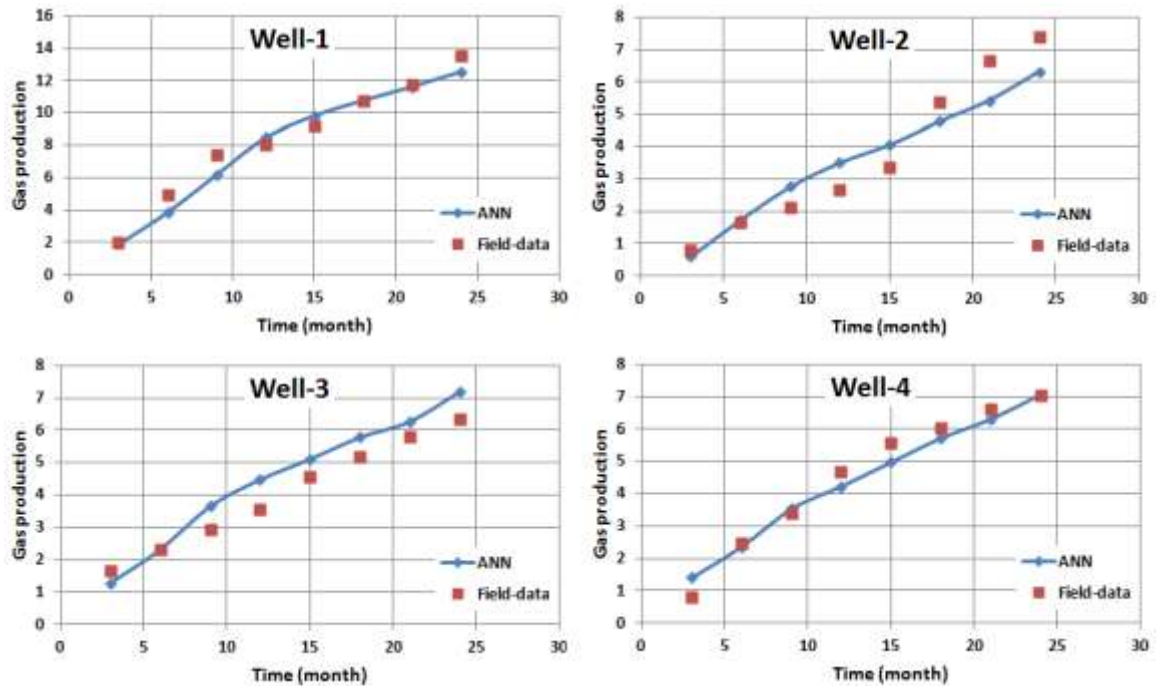
Fig. 6.35: Comparison of cumulative gas production (MCF) for individual wells
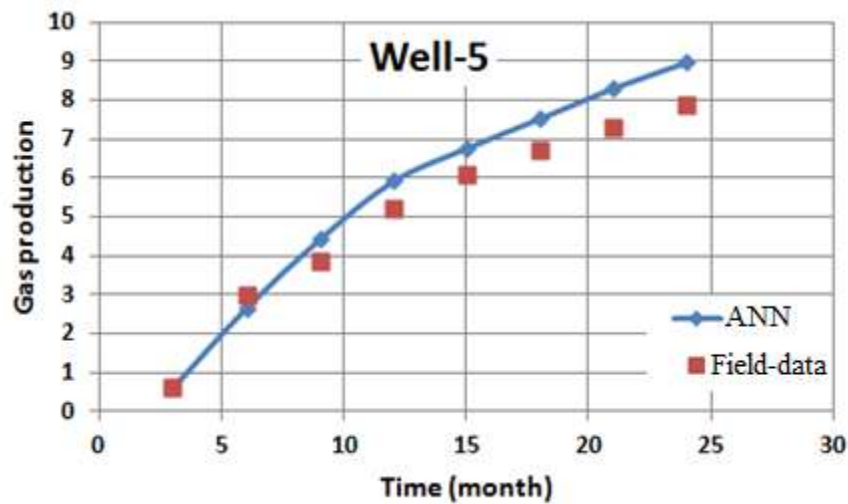
Fig. 6.36: Comparison of cumulative gas production (MCF) for individual wells

The gas production expert system was also tested with the additional production data provided in October 2010 using the updated production history for wells in the ATM region. The errors observed in predictions made by the gas production expert system were of the range of ~80-100%. **Figure 6.36 and 6.37** shows that the new wells are higher gas producing wells as they again fall outside the range of production values shown to the network during the training phase of the original expert system. It can be seen that gas network was exposed to a cumulative production range of ~ 0-35 units of gas whereas the new wells have cumulative gas production ranging between ~30-600 units of gas as shown in Figure 6.37. The difference in range of cumulative production is one order of magnitude larger than the initial training range. The previous network had not been trained with such wells with high gas production and thus the reason for a high error in predicting this production range.

This analysis suggested in retraining the network with these new wells to make the expert system more robust. The training strategy followed in gas network is the same as oil production network, where 50 wells were randomly selected and introduced during re-training of the network. The current architecture is shown in Figure 5.15. This network is able to predict the cumulative gas production with an average error of ~15% for the testing cases. In this network 6 wells were used each for testing and validations and 124 wells were used for training the network. **Figures 6.38 and 6.39** show the cross plot of the predictions made by expert system. **Figures 6.40 and 6.41** compare the quarterly production predicted by the network for the testing wells. It can be seen that the expert system is able to predict the gas production closely for the testing case. Finally, production for each testing well is also compared in **Figure 6.42**.
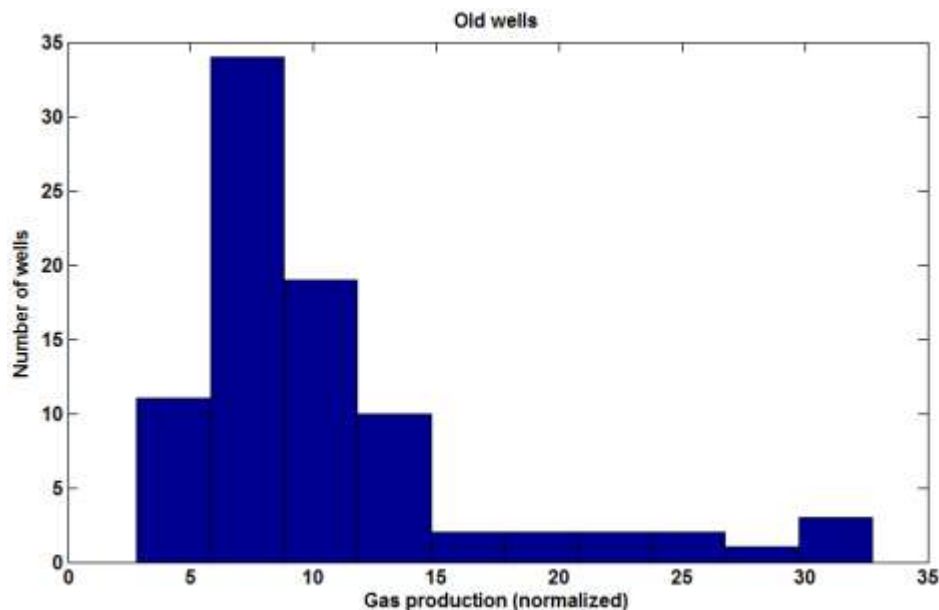
Fig. 6.37: Histogram showing the gas production ranges of well in September 2009 dataset
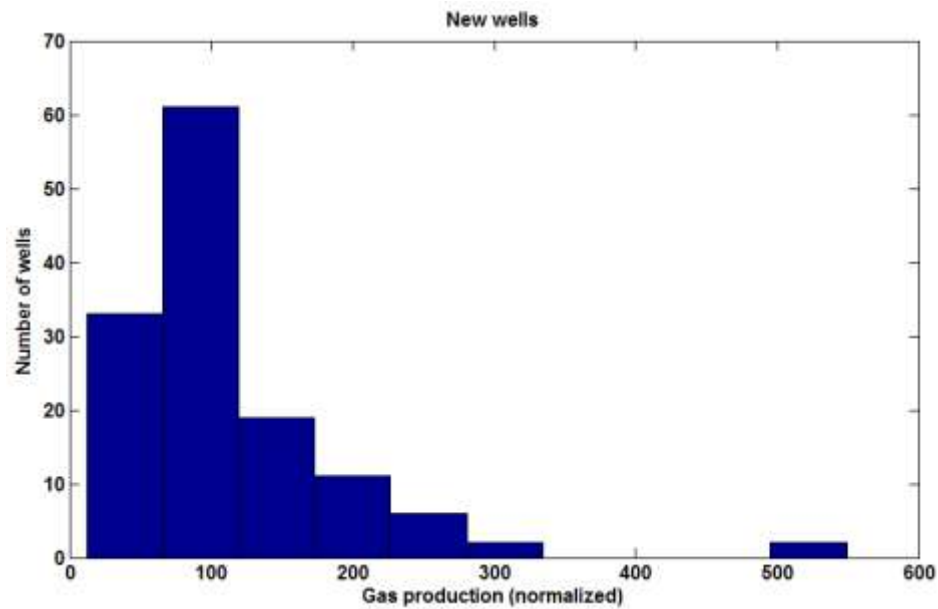
Fig. 6.38: Histogram showing the gas production ranges of well in October 2010 dataset
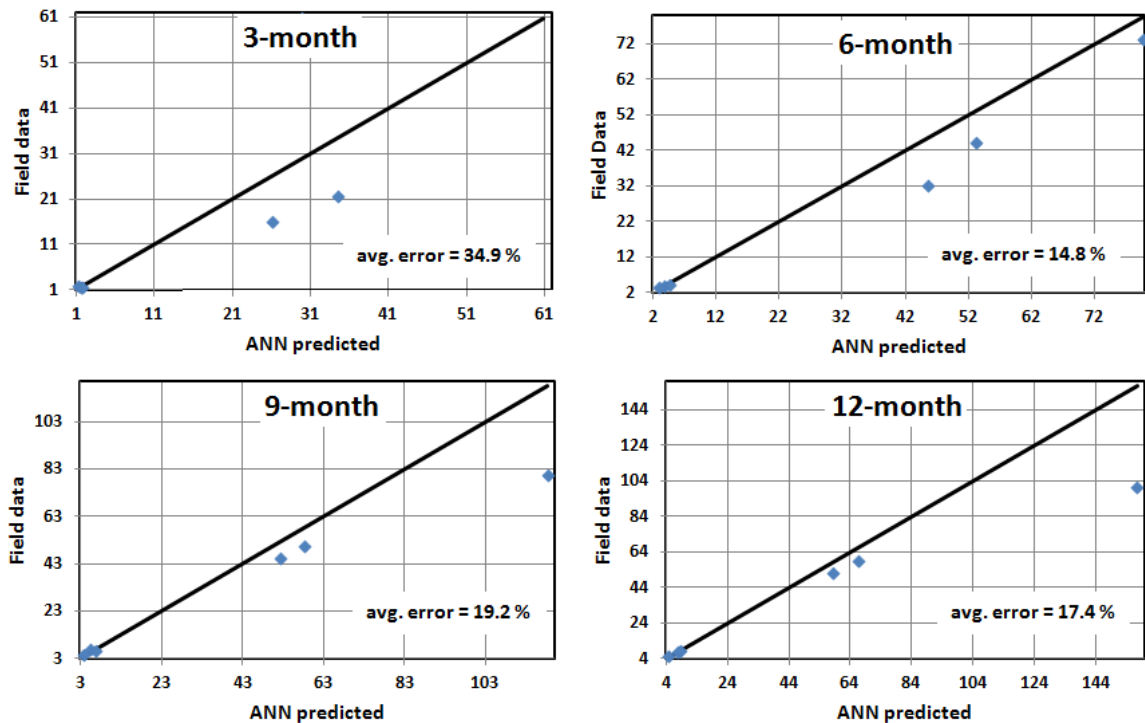
Fig. 6.39: Cross plot of quarterly production (gas- MCF) with updated network
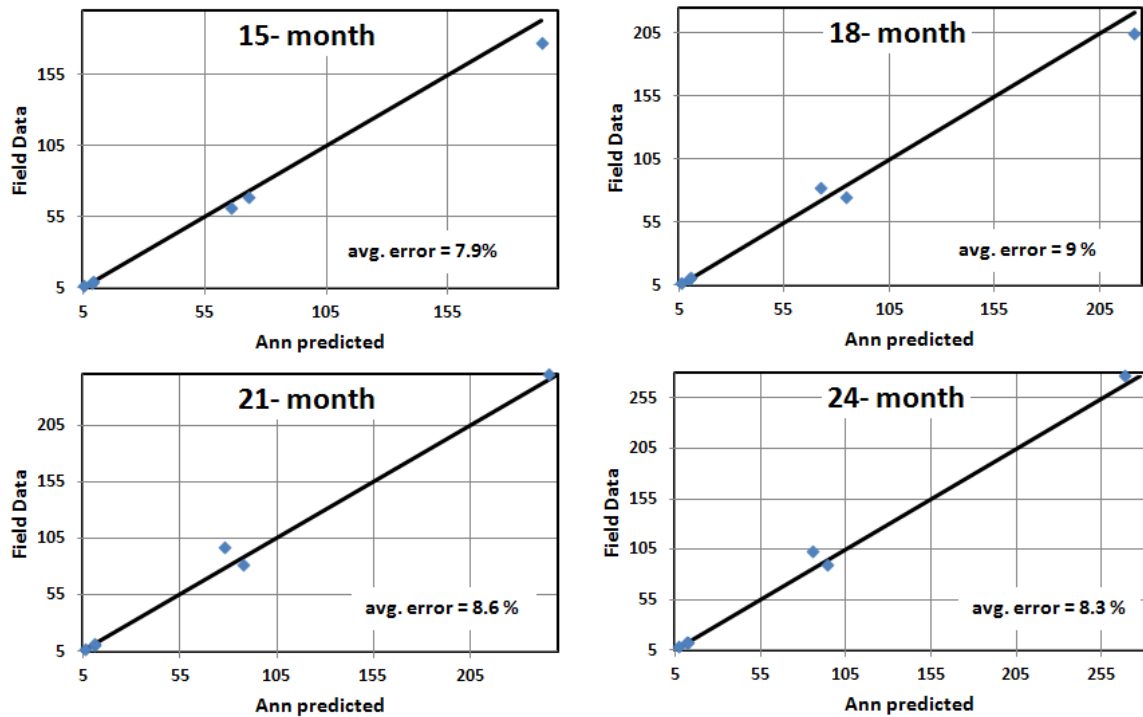
Fig. 6.40: Cross plot of quarterly production (gas- MCF) with updated network
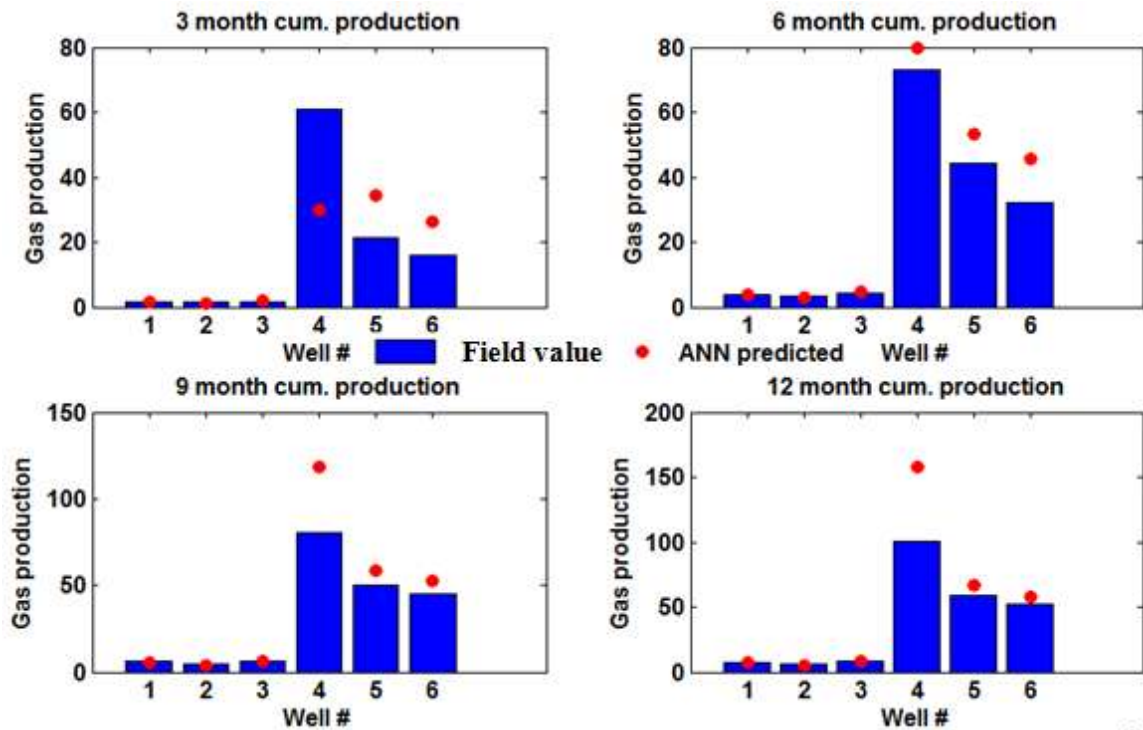
Fig. 6.41: Comparison of quarterly production with updated network (first year)
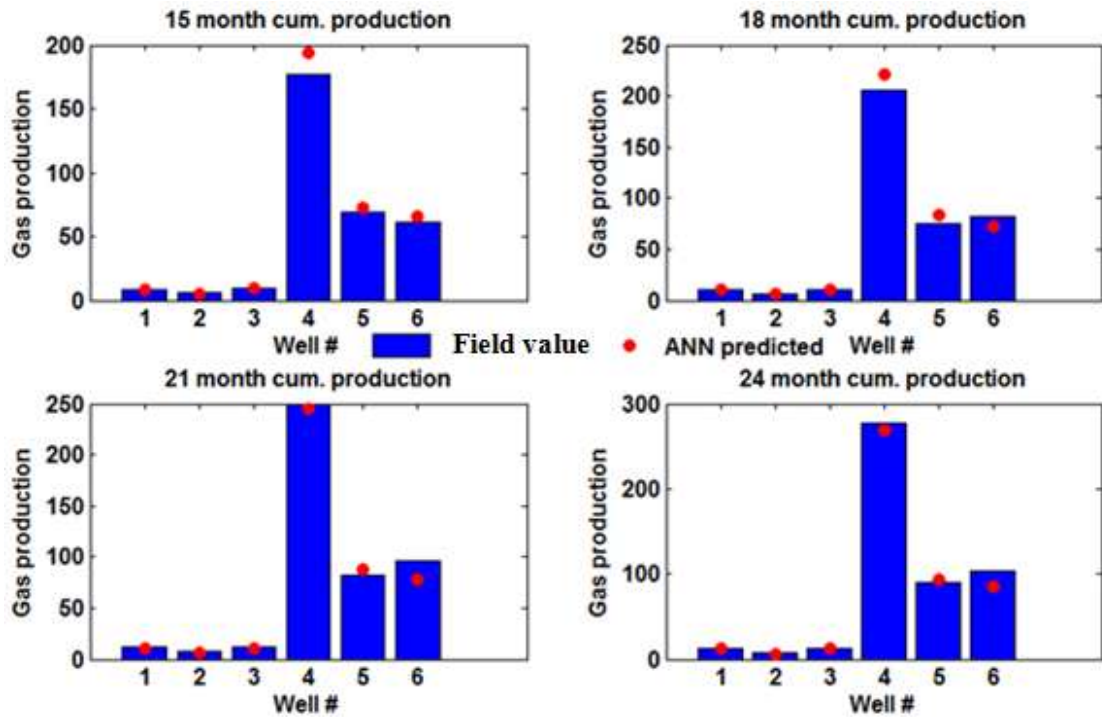
Fig. 6.42: Comparison of quarterly production with updated network (second year)
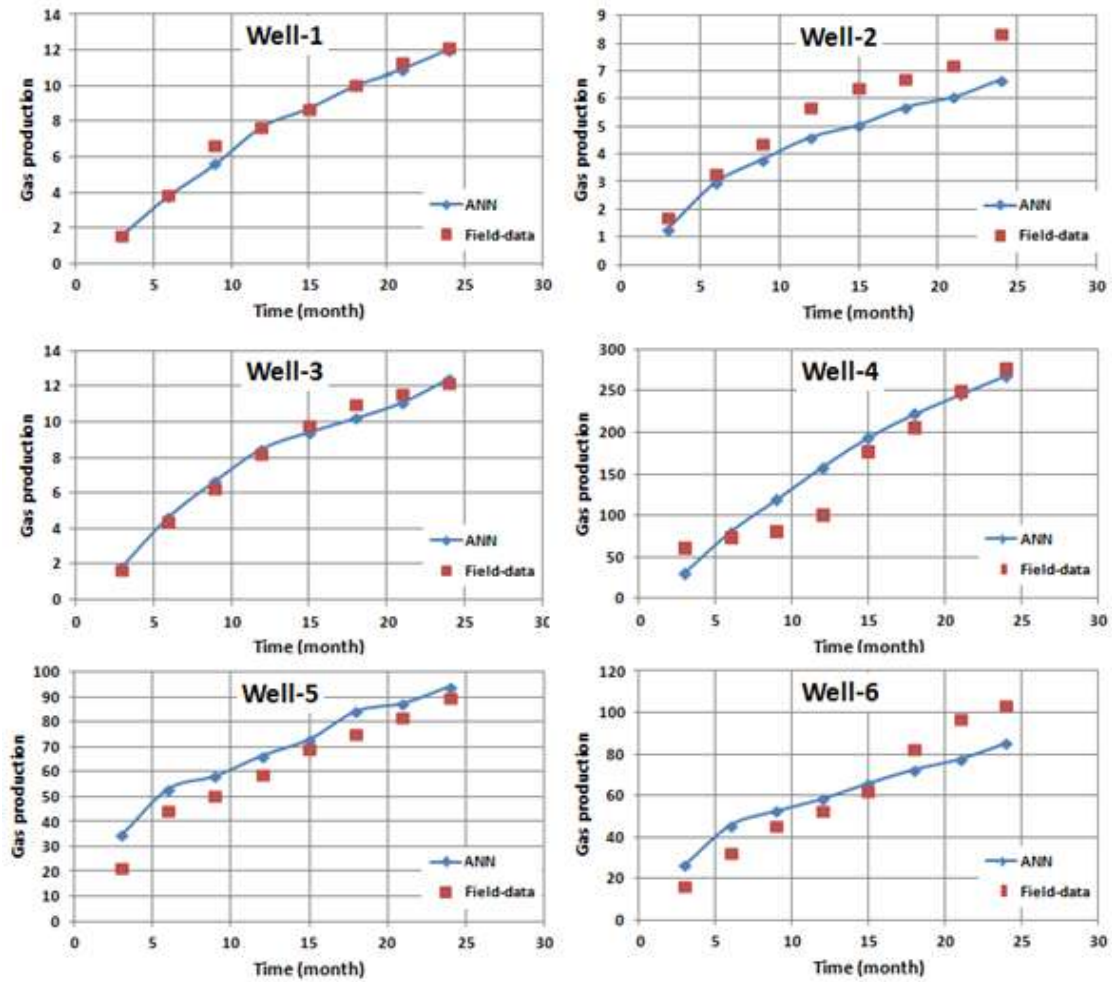
Fig. 6.43: Comparison of cum. gas production for individual wells with updated network

6.2.3 Water Performance Prediction Network (WPPN)

The WPPN discussed in Chapter 5 predicts the cumulative oil production with an average error of ~10% with the testing cases as generated by the architecture shown in Figure 5.17. **Figure 6.43** shows that highest errors are observed again for the first 3-

months production period. **Figure 6.44** shows that average error in predicting cumulative

gas prediction stabilizes at ~10% for the second year production.
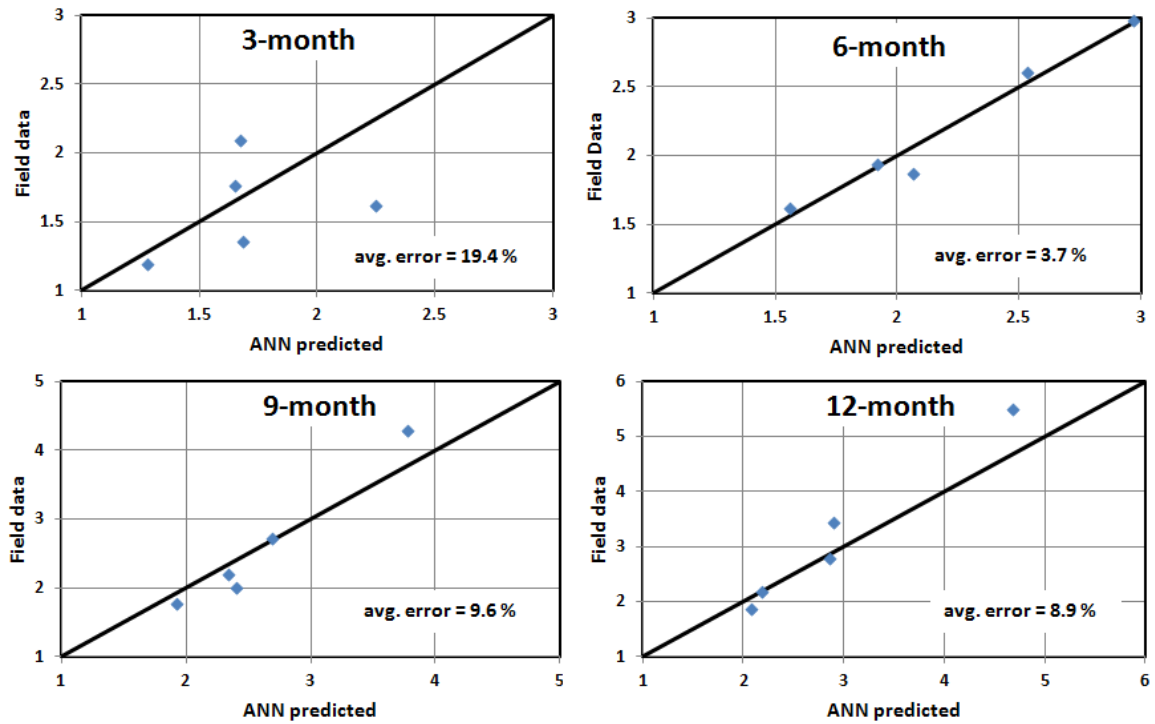
Fig. 6.44: Cross plot comparing cumulative water production (first year)
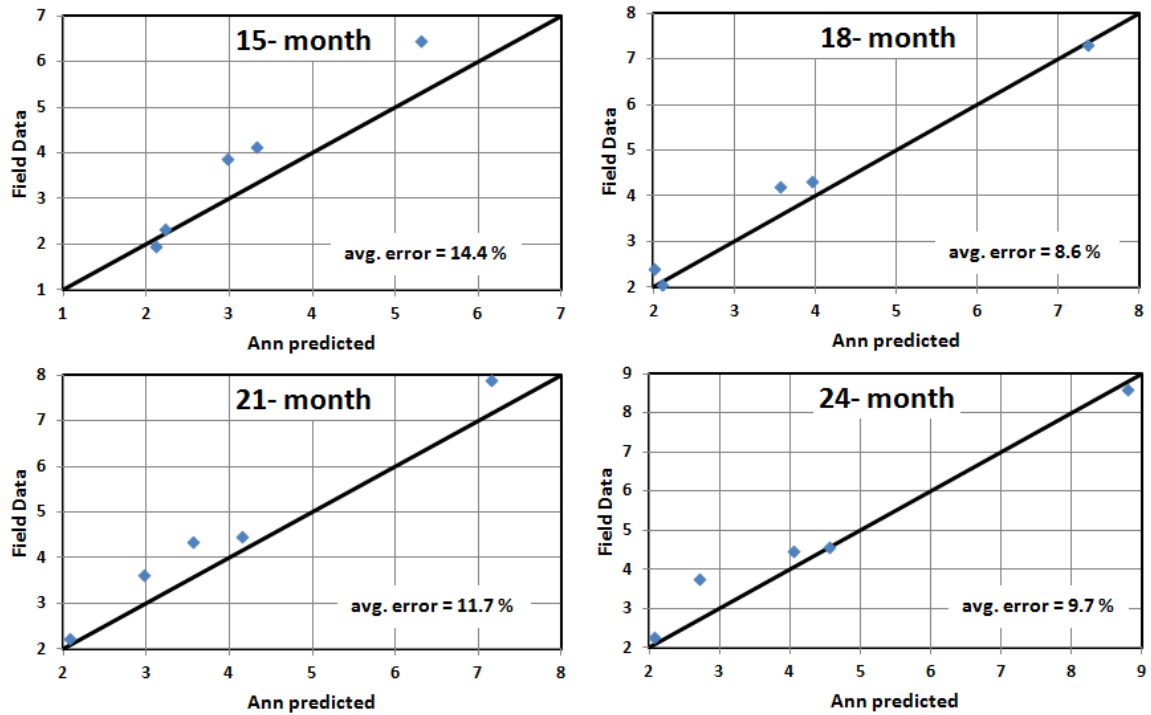
Fig. 6.45: Cross plot comparing cumulative water production (second year)

Figures 6.45 and 6.46 compare the quarterly cumulative water production predicted by the network for the testing wells. It can be seen that the expert system is able to predict the water production closely for the testing case. Finally, production for each testing well is also compared in **Figures 6.47 and 6.48**.
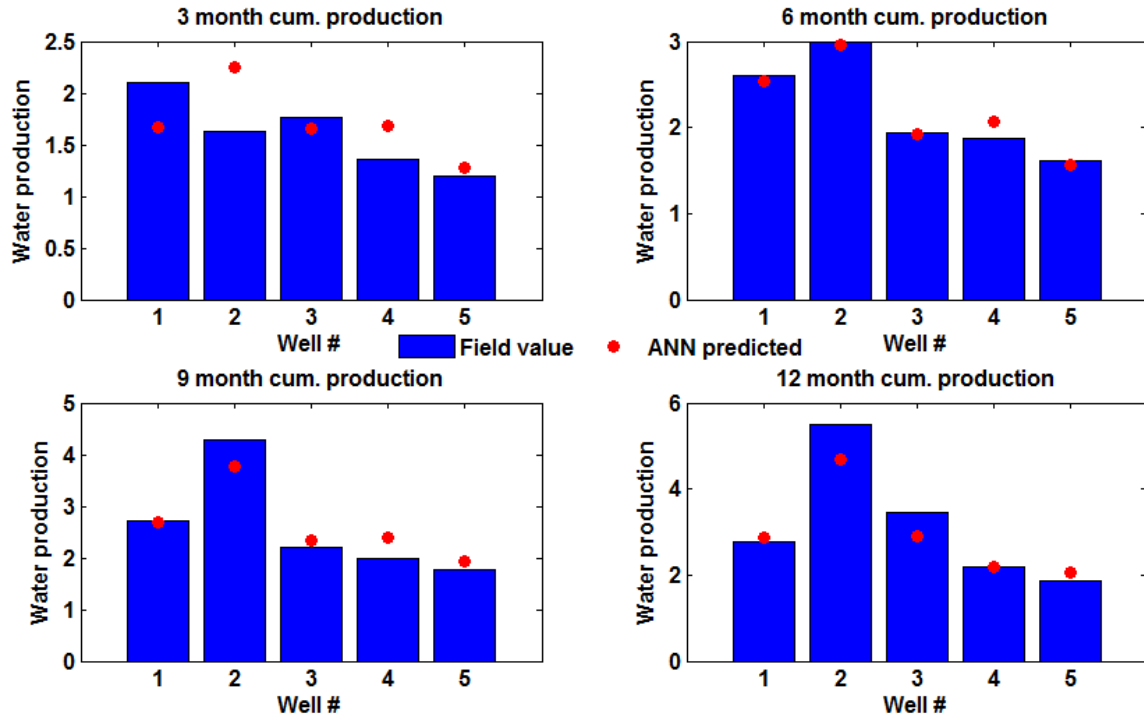
Fig. 6.46: Comparison of quarterly water production (first year)
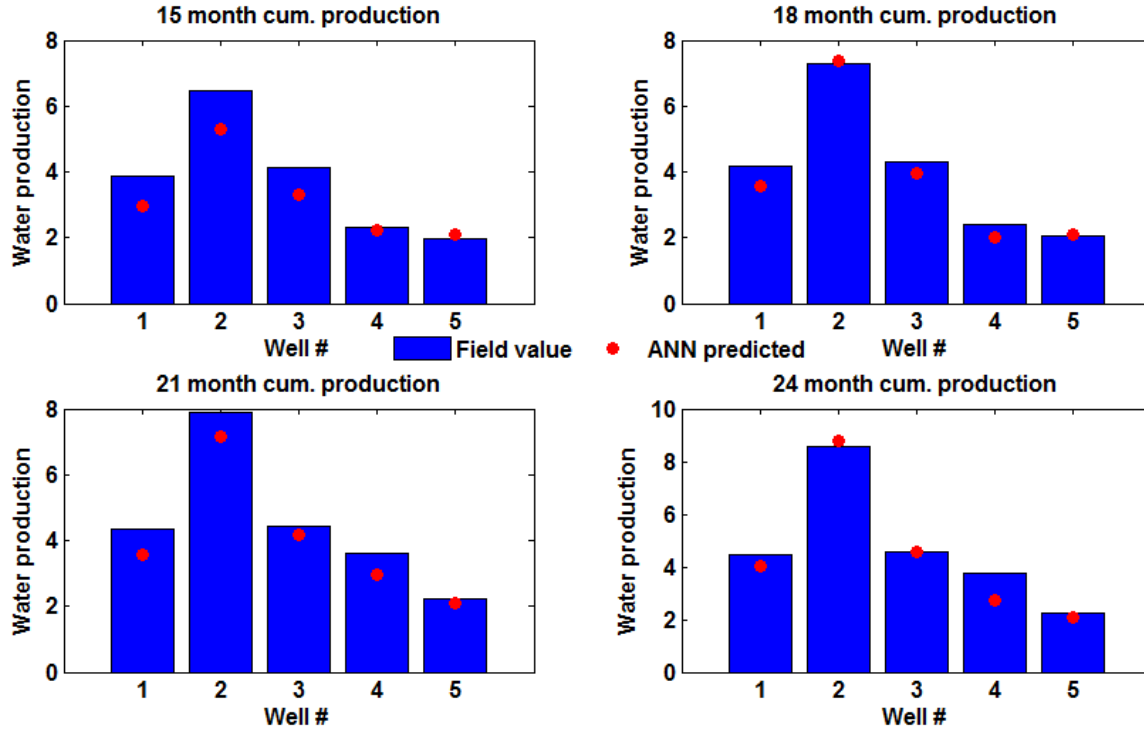
Fig. 6.47: Comparison of quarterly water production (second year)
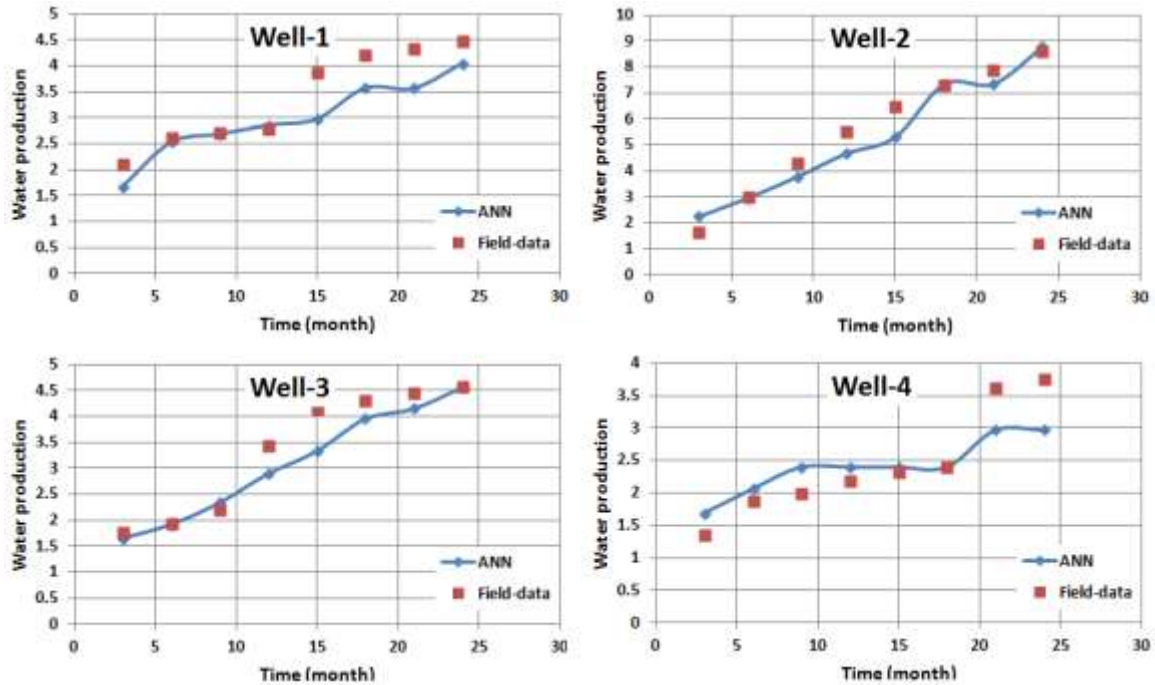
Fig. 6.48: Comparison of cumulative water production for testing wells
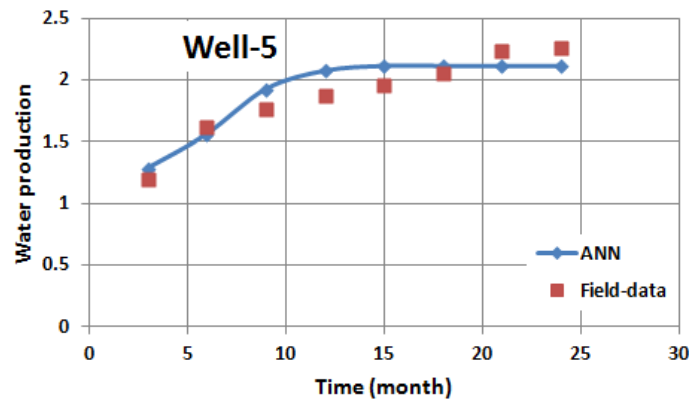
Fig. 6.49: Comparison of cumulative water production for testing well

6.3 Optimizing the Completion Design

Methodology explained in **Section 5.5** is used to optimize the completion parameters.

The cost of parameters used to calculate *NPV* are listed in the **Table 6.1**. Major

parameters affecting the objective function were identified as the total number of stages and amount of proppant used. However, the objective function is subject to changes in future and plays a critical role in optimizing the completion parameters. It is observed that lowering the total amount of proppant used in fracturing the well, reduces the overall cost of completing the well, whereas the loss in production is not observed. The process simultaneously increases the NPV of the well for duration of two years. The method is tested for an expert system, with an expertise to predict two year production for a given well. The results of the analysis will change when the production decline in the third year is significant, and stimulating the well could not be ignored.

Table 6.1: Costs for NPV calculations

Parameter	Cost	Units
P_{cost}	0.25	$/lb
OC	25	$/bbl
R_{pf}	0.5	fraction
C_{fs}	5000	$/stage
R_{rf}	15	%
P_{oil}	90	$/bbl
Royalty	15	% of production

As an example, one well is used to optimize the completion parameter. With this methodology, it took a total of 281 neuro-simulations to identify a best case scenario. **Figure 6.50** shows the results iteration-by-iteration in improving NPV of the well. In this figure, 'iteration-0' represents the value of NPV calculated by the algorithm with the

mean values of the completion parameters. The mean values are calculated by arithmetical average of the upper and lower bounds of a given completion parameter.
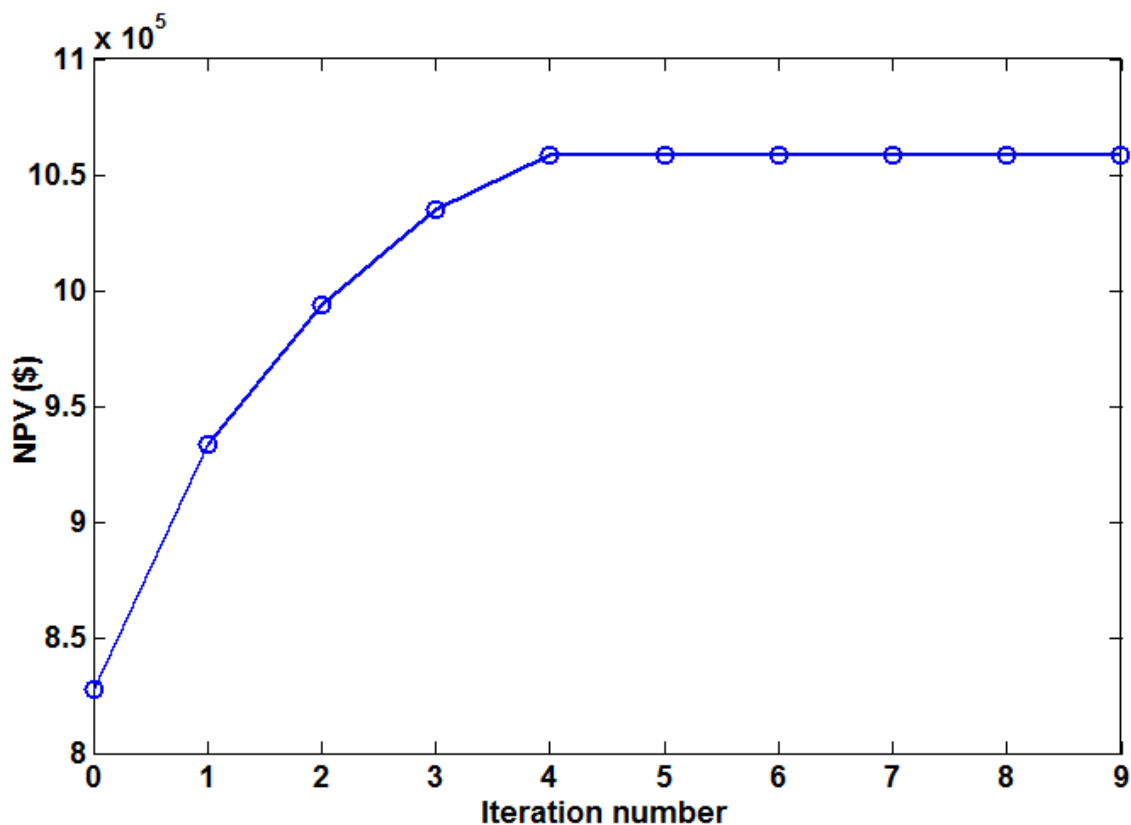
Fig. 6.50: Improvement in NPV with ANN-EnOpt algorithm

The completions are compared for a well in **Table 6.2**. It can be seen from the table that ANN-EnOpt efficiently improves the value of the well by adjusting completion parameters. In this example, a production is increased by 1.5% where as the NPV is increased by 37%. The reason of high increase in the NPV value is attributed to the decrease in the amount of proppant used while increasing number of stages. This method

is implemented for all the 87 wells initially used for ANN-study in the ATM region.
Figure 6.51-6.52 shows the increase in the NPV and two-year cumulative production of
each well respectively.

Table 6.2: Example in optimizing completion (Well-1)

Completion parameter	Completion value		
	Field	Average	Optimized
'fracture stages'	13	13	18
'total proppant used (lb)'	817983	1466751	332041.2
'Max Max Btm Depth (ftKB)'	9884	9980	10360
'Max Q (end) Max (gpm)'	2940	4120.2	5166
'Max P (tub-st) Min (psi)'	4300	2423	4800
'Max Min Top Depth (ftKB)'	9864	10015	10340
'Max Set Depth (ftKB)'	10077	10277.5	10630
'Max String ID (in)'	4.892	8.8035	12.715
'Max set depth (ftKB)'	9947.4	8785.45	10569.8
'Max OD MAX (in) '	2.875	3.9375	5.5
'Max OD (in)'	2.875	2.625	2.875
'Max Top (ftKB) '	9910.9	8734.35	10533.2
'Max Btm (ftKB)'	9911.9	8735.45	10534.3
'Max Cum Vol Disp (bbl)'	1	1.425	1.65
'Max EOS ISIP (psi)'	3412	3640	4750
NPV ($)	697670.3	376554.8	956486.8
% improvement in NPV over field		-46.0268	37.09724
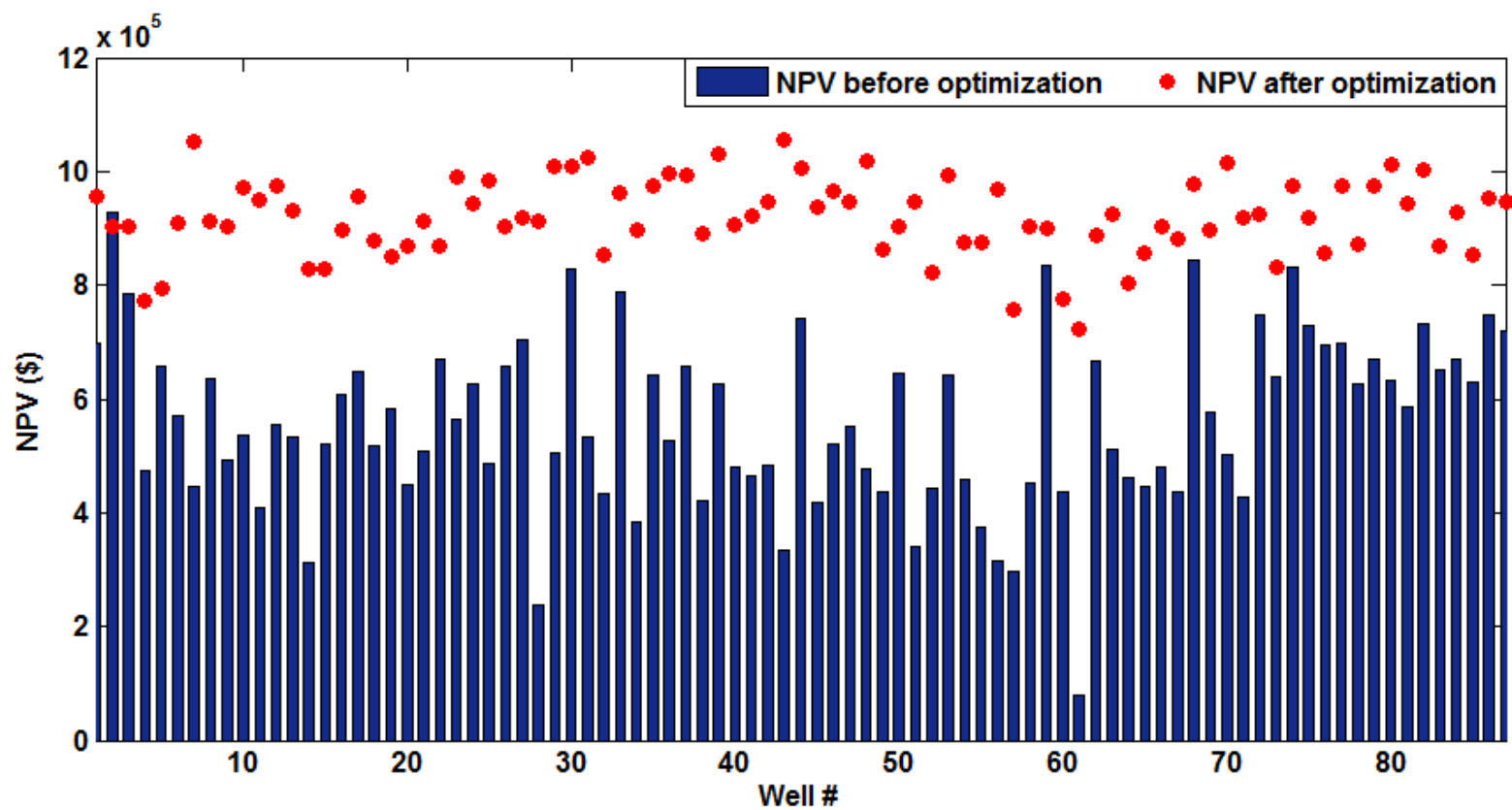
Fig. 6.51: Optimized NPV for 87 wells in ATM
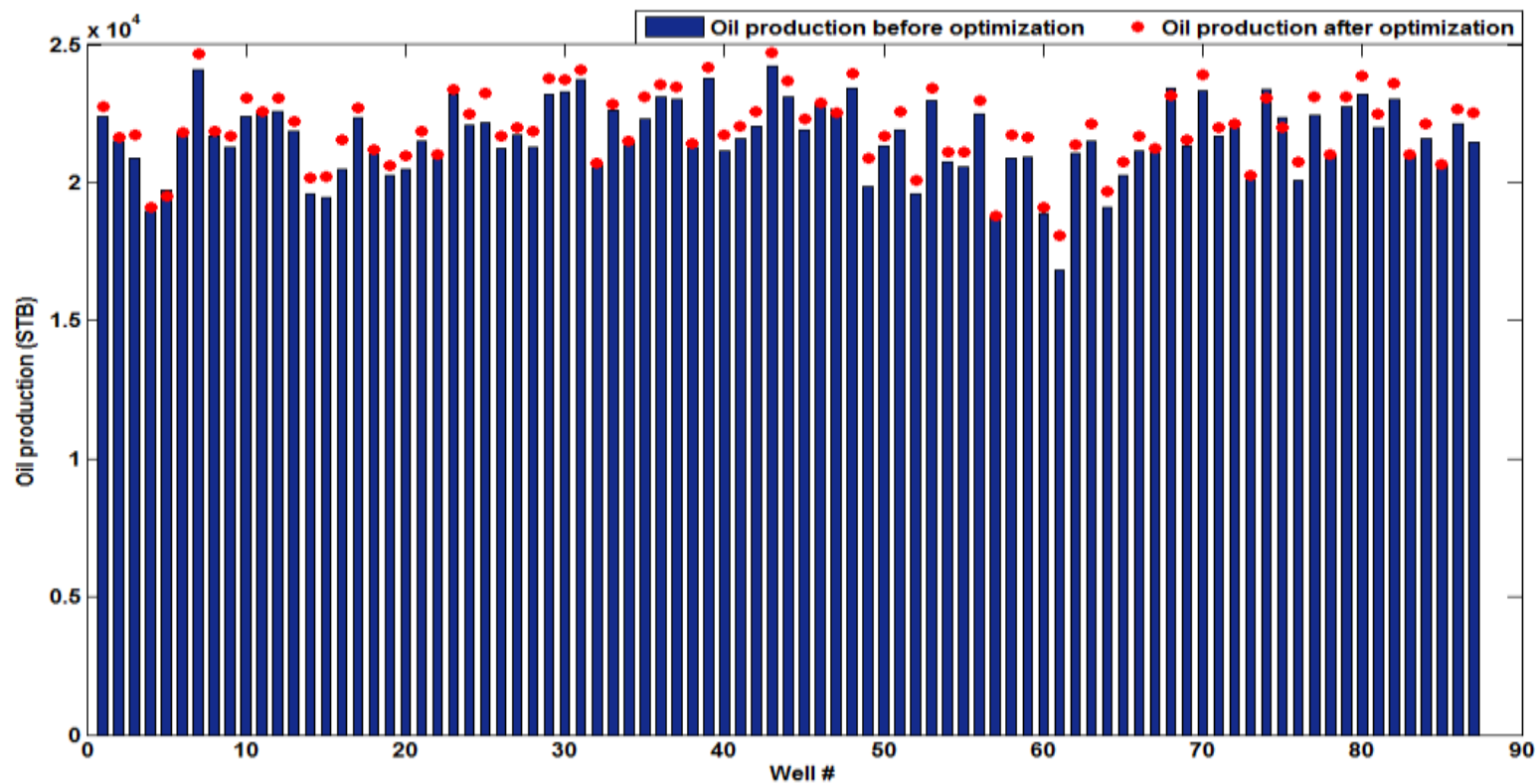
Fig. 6.52: Optimized production for 87 wells in ATM

Chapter 7 Summary of Findings

This research represents a general methodology to characterize tight oil plays with the use of expert systems. In this work, a field example is discussed where the developed methodology is applied and tested with the field results. The expert systems developed in Chapter 5 are field specific expert systems. Precautions must be taken while extending the expert system over to another field and/or extrapolating. It is observed that these networks work as effective interpolation tools, but a slightly larger error is observed for regions that fall outside the training range of these expert systems. However, the developed methodology can be applied for different tight oil reservoirs around the world. It was also observed that by improving the range of dataset, expertise of the networks can be improved. Following conclusions are drawn from the study:

- A quick assessment of completion design can be correlated using geological properties and the current completion design practices on the existing wells in a tight oil reservoir. This network is expected to reduce time and resources for designing completion parameters in a tight oil reservoir.

- New potential locations for further drilling are identified in the field application.

- The methodology developed in this work is expected to assist in developing complex tight oil reservoir economically by identifying the more promising infill drilling locations.

- Hybridization of ANN-EnOpt has shown some promising results. The method can be useful in developing fast-optimization protocols. By coupling of these two methods, a complex problem can be analyzed much more rapidly. For example, it takes ~1 minute to optimize the completion parameters by this method, which represents only a fraction of the time that will be required for full scale models.

The methodology developed in this work is not limited to tight oil reservoirs. The work has the potential to establish a framework in developing models for shale gas reservoirs. Development of shale gas reservoirs is a challenging task and artificial expert systems can play an important role in unlocking the extensive resources that exist in these formations. This work is based on vertical wells a given reservoir and, it can be extended to horizontal well application such as developments in Bakken play. The field application developed in this work is restricted to a two-year production period with cumulative production as the output of the network. Production decline characteristics can be incorporated into the existing methodology that forecasts cumulative production over an elongated period of time. While developing field application for ATM region, it was

observed that the expert systems work well for the field specific problems. Possibility of generalizing expert systems can also be studied to develop a universal expert system. In such expert systems utilization of raw measurements for seismic data instead of processed seismic data will be necessary to avoid operator specific biases. In this way, it will be possible to expand the applications of the expert system to nearby fields.

References

Al-Fattah, S. M., & Startzman, R. A. (2001). Predicting Natural Gas Production Using Artificial Neural Network. *SPE Hydrocarbon Economics and Evaluation Symposium.* Dallas, TX: SPE.

Aminian, K., & Ameri, S. (2005). Application of artificial neural networks for reservoir characterization with limited data. *Journal of Petroleum Science and Engineering* , 212-222.

Arevalo-Villagram, J., Gutierrza-Acosta, T., & Martinez-Romero, N. (2005). Analysis of long term behaviour in tight gas reservoirs: case histories. *SPE Latin American and CaribbeanPetroleum Engineering Conference.* Rio De Janeiro: SPE.

Artun, E. F. (2008). *Optimized Design of Cyclic Pressure Pulsing in Naturally Fractured Reservoirs Using Neural-Network Based Proxy Models.* University Park, PA: The Pennsylvania State University.

Artun, E., Mohaghegh, S., Toro, J., Wilson, T., & Sanchez, A. (2005). Reservoir characterization using intelligent seismic inversion. *Eastern Regional Meeting.* Morgantown, W.V.: SPE.

Babadagli, T., & Al-Salm, S. (2002). Improvement of permeability prediction for carbonate reservoirs using well log data. *Asia Pacific Oil and Gas Conference and Exhibition.* Melbourne, Australia: SPE.

Barnes, A. E. (2001). *Seismic Attributes in Your Facies.* Colorado, USA: CSEG Recorder.

Biglarbigi, K., Dammer, A., Mohan, H., & Carolus, M. (2008). Economics of oil shale development in the United States. *Annual Technical Conference and Exhibition.* Denver, Colorado: SPE.

Chakhmakhchev, A., & Fryklund, B. (2008). Critical Success Factors of CBM Development ¬Implications of Two Strategies to Global Development. *19th World Petroleum Congress.* Madrid, Spain: World Petroleum Congress.

Chaudhri, M. M., Phale, H. A., & Liu, N. (2009). An improved approach for ensemble-based production optimization: Application to a field case. *EUROPEC.* Amsterdam, The Netherlands: SPE.

Chaudhri, M. M., Phale, H. A., Liu, N., & Oliver, D. S. (2009). An improved approach for ensemble-based production optimization. *SPE Western Regional Meeting.* San Jose, CA: SPE.

Chelini, V., Muttoni, A., Mele, M., Rossi, E., Galimberti, R., & Ortenzi, A. (2010). Gas shale reservoir characterization: A North Africa case. *Annual Technical Conference and Exhibition.* Florence, Italy: SPE.

Chen, Y., Oliver, D. S., & Zhang, D. (2008). Efficient ensemble-based closed loop production optimization. *SPE/DOE Improved Oil Recovery Symposium.* Tulsa, Oklahoma: SPE.

Chevron USA. (2006). *Oil Shale Research, Development & Demonstration Project- Plan of Operations.* Retrieved August 12, 2011, from http://www.blm.gov/pgdata/etc/medialib/blm/co/field_offices/white_river_field/oil_shale .Par.37256.File.dat/OILSHALEPLANOFOPERATIONS.pdf

Clarkson, C. R., & Bustin, R. M. (2010). Coalbed Methane: Current Evaluation Methods, Future Technical Challenges. *Unconventional Gas Conference.* Pittsburgh, PA: SPE.

Collett, T. S. (2002). Energy resource potential of natural gas hydrates. *The American Association of Petroleum Geologists , 86* (11), 1971-1992.

Cramer, D. D. (2008). Stimulating unconventional reservoirs: lessons learned, successful practices, area for improvement. *Unconventional Reservoirs Conference.* Keyston, Colorado: SPE.

Dakshindas, S. S., Ertekin, T., & Grader, A. S. (1999). Virtual well testing. *Eastern Regional Conference and Exhibition.* Charleston, West Virginia: SPE.

Decker, C. (2004). *Better Characterization of Unconventional Gas Reservoirs.* Retrieved August 25, 2011, from GasTIPS: http://media.godashboard.com/gti/4ReportsPubs/4_7GasTips/Fall04/BetterCharacOfUnc onventionalGasReservoirs.pdf

Demirbas, A. (2010). Methane hydrates as potential energy resource: Part 1 - Importance, resource and recovery facilities. *Energy Conversion and Management , 47*, 1547-1561.

Dyni, J. R. (2006). *Geology and Resources of some World Oil-Shale Deposits.* Reston, Virginia: U.S. Department of Interior, U.S. Geological Survey.

EIA. (2011). *Annual Energy Outlook 2011 with Projections to 2035.* Washington, DC: EIA.

EIA. (2011, May). *North American Shale Plays*. Retrieved 9 2011, from EIA: http://www.eia.gov/oil_gas/rpd/northamer_gas.pdf

Elkamel, A. (1998). An artificial neural network for predicting and optimizing immiscible flood performance in heterogeneous reservoirs. *Computers & Chemical Engineering , 22* (11), 1699-1709.

Ertekin, T., & Silpngarmlers, N. (2005). Optimization of formation analysis and evaluation protocols using neuro-simulation. *Journal of Petroleum Science and Engineering , 49*, 97-109.

Erturk, M. (2011). Economic analysis of unconventional liquid fuel sources. *Renewable and sustainable energy reviews , 15* (6), 2766-2771.

Evensen, G. (1994). Sequential data assimilation with a non-linear quasi-geostrophic model using monte carlo methods to forecast error statistics. *Journal of Geophysical Research , 99* (C5), 143-162.

Evensen, G., Hove, J., Meisingset, H. C., Reiso, E., Seim, K. S., & Espelid, O. (2007). Using the EnKF for Assisted History Matching of a North Sea Reservoir Model. *Reservoir Simulation Symposium.* Houston, TX: SPE.

Fausett, L. (1994). *Fundamentals of Neural Networks: Architechtures, Algorithms and Applications* (1 ed.). Prentice-Hall.

Flores, R. M. (1998). Coalbed methane: From hazard to resource. *International Journal of Coal Geology , 35* (1-4), 3–26.

Gharbi, R. B., & Mansoori, A. G. (2005). An introduction to artificial intelligence applications in petroleum exploration and production. *Journal of Petroleum Science and Engineering , 49* (3-4), 93-96.

Goldberg, D. E., & Kuo, C. H. (1985). Genetic Algorithm in pipeline optimization. *Journal of Computing in Civil Engineering , 1* (2), 128-141.

Graupe, D. (2007). *Principles of Artificial Neural Networks* (2 ed., Vol. 6). Hackensack, NJ: World Scientific.

Harding, T. J., Radcliffe, N. J., & King, P. R. (1998). Hydrocarbon Production Scheduling With Genetic Algorithms. *SPEJ , 3* (2), 99-107.

Haykin, S. S. (1994). *Neural networks: a comprehensive foundation* (2 ed.). Michigan: Macmillan.

Hecht-Nielsen, R. (1987). Counterpropagation networks. *Applied Optics , 26* (23), 4979-4983.

Holditch, S. A., Ayers, W. B., Lee, J. W., Bickley, J. A., McVay, D. A., Blasingame, T. A., et al. (2007). *Unconventional Gas Reservoirs—Tight Gas, Coal.* NPC Global Oil and Gas Study.

Hopfield, J. J. (1982). Neural networks and physical systems with emergent collective computational abilities. *Proceedings of the National Academy of Sciences , 79* (8), 2554-2558.

Huckabee, P., Vincent, M. C., Foreman, J., & Spivey, J. P. (2005). Field results: Effects of proppant strength and seive distribution upon well productivity. *Annual Technical Conference and Exhibition.* Dallas, TX: SPE.

Humphries, M. (2008, January 17). *Federation of American Scientists.* Retrieved September 1, 2011, from: http://www.fas.org/sgp/crs/misc/RL34258.pdf

Ikegawa, Y., Miyakawa, K., Suzuki, K., Masuda, M., Narita, H., & Ebinuma, T. (2010). SS: Hydrates: Experimental results for long term CO2 injection near methane hydrate formations. *Offshore Technology Conference.* Houston, TX: OTC.

Jafroodia, N., & Zhang, D. (2011). New method for reservoir characterization and optimization using CRM–EnOpt approach. *Journal of Petroleum Science and Engineering , 77* (2), 155-171.

Jenkins, C. D., & Boyer, C. M. (2008). Coalbed and shale reservoirs. *JPT , 60* (2), 92-99.

Johnson, H. R., Crawford, P. M., & Bunger, J. W. (2004). *Strategic Significance of America's Oil Shale Resources.* Washington, D.C.: U.S. Department of Energy.

Kabir, C., Rasdi, F., & Igboalisi, B. (2010). Analyzing production data from tight oil wells. *Canadian Unconventional Resources and International Petroleum Conference* (pp. 48-58). Calgary: JCPT.

Kalyoncuoglu, F. S., & Tigdemir, M. (2004). An alternative approach for modelling and simulation of traffic data: artificial neural networks. *Simulation Modeling Practise and Theory , 12* (5), 351-362.

Karambeigi, M. S., Zabihi, R., & Hekmat, Z. (2011). Neuro-simulation modeling of chemical flooding. *Journal of Petroleum Science and Engineering , 78* (2), 208-219.

Kawata, Y., & Fujita, K. (2001). Some predictions of possible unconventional hydrocarbons availability untill 2100. *SPE Asia PAcific Oil and Gas Conference and Exhibition.* Jakarta, Indonesia: SPE.

Khalifat, A., Qutob, H., & Barakat, N. (2011). Tight gas sands development is criticalto future world energy resources. *SPE Middle East Unconventional Gas Conference.* Muscat, Oman: SPE.

Khalifat, A., Qutob, H., Barakat, N., & Hamdine, S. (November 2010). Increasing the world's gas reserves by the exploitation of unconventional tight gas reservoirs. *SPE/PAPG Annual Technical Conference.* Islamabad, Pakistan: SPE.

Khlaifat, A., Qutob, H., & Barakat, N. (2010). Increasing the world's gas reserves by the exploitation of unconventional tight gas reservoirs. *SPE/PAPGAnnual Technical Conference.* Islamabad, Pakistan: SPE.

Klienberg, R. L., Allison, E. C., Holditch, S. A., Collett, T. S., Howard, J. J., Hardage, R. A., et al. (July 2007). *Oil Shales and Hydrates.* NPC Global Oil and Gas.

Kohonen, T. (1982). Self-Organized formation of topologically correct feature maps. *Biological Cybernetics , 43* (1), 59-69.

Lakatos, I., & Lakatos, J. S. (2009). Role of conventional and unconventional hydrocarbons in the 21st century: Comparison of resources, reserves, recovery factor and technologies. *EUROPEC/EAGE Annual Conference and Exhibition.* Amsterdam, The Netherlands: SPE.

Lee, W. J., & Hopkins, C. W. (1994). Characterization of tight reservoirs. *SPEJ , 46* (11), 956-964.

Legrand, N., Kok, J. D., Neff, P., & Clemens, T. (2010). Recovery mechanism and oil recovery from a tight, fractured basement reservoir, Yemen. *SPE Annual Technical Conference and Exhibition.* Florence, Italy: SPE.

Lim, J.-S., Kang, J. M., & Kim, J. (1999). Interwell log correlation using artificial intelligence approach and multivariate statistical analysis. *SPE Asia Pacific Oil and Gas Conference and Exhibition.* Jakarta, Indonesia: SPE.

Majorowicz, J. A., & Osadetz, K. G. (2001). Gas hydrate distribution and volume in Canada. *The American Association of Petroleum Geologists , 85* (7), 1211-1230.

Mazzotti, M., Pini, R., & Storti, G. (2009). Enhanced coalbed methane recovery. *The Journal of Supercritical Fluids , 47* (3), 619-627.

Mcculloch, W. S., & Pitts, W. (1943). A logical calculus of the ideas immanent in nervous activity. *Bulletin of Mathemetical Biophysics , 5*, 115-133.

Meyer, R. F., & Attanasi, E. D. (2003, August). *Heavy Oil and Natural Bitumen-Strategic Petroleum Resources.* Retrieved September 1, 2011, from USGS Fact sheet: http://pubs.usgs.gov/fs/fs070-03/fs070-03.html

Miller, B., Paneitz, J., Yakely, S., & Evans, K. (2008). Unlocking tight oil: selective multi-stage fracturing in the Bakken shale. *SPE Annual Technical Conference and Exhibition.* Denver, Colorado: SPE.

Mohaghegh, S., Arefi, R., Ameri, S., Aminiand, K., & Nutter, R. (1996). Petroleum reservoir characterization with aid of artificial neural networks. *Journal of Petroleum Science and Engineering , 16* (4), 263-274.

Mohammadnejad, A. (2011). *Development of Novel Unconventional Reservoir Characterization Tools With the Applications on Wolfcamp Oilfield.* University Park: The Pennsylvania State University.

Mohr, A., & Evans, G. (2009). Long term prediction of unconventional oil production. *Energy Policy , 38* (1), 265-276.

Molnar, D., Aminian, K., & Ameri, S. (1994). The use of well log data for permeability estimation in a heterogeneous reservoir. *SPE Eastern Regional Conference.* Charleston, West Virginia: SPE.

Mongomery, S. L. (1996). Permian "Wolfcamp" limestone reservoirs: Powell Ranch field, Eastern Midland basin. *AAPG Bulletin , 81* (10), 1349-1365.

Moritis, G. (2008). Oil shale promise. *Oil and Gas Journal , 106* (41), 16.

Morooka, C. K., Guilherme, I. R., & Mende, J. R. (2001). Development of intelligent systems for well drilling and petroleum production. *Journal of Petroleum Science and Engineering , 32* (2-4), 191-199.

Nejad, A. M. (Ongoing Work). *Predicting Payzones and Well Logs using Artificial Expert System.* University Park: The Pennsylvania State University.

Nikravesh, M. (1998). Neural network knowledge-based modeling of rock properties based on well log databases. *SPE Western Regional Meeting.* Bakersfield, CA: SPE.

Nikravesh, M., & Aminzadeh, F. (2001). Past, present, and future intelligent reservoir characterization trends. *Journal of Petroleum Science and Engineering , 31* (2-4), 67-79.

Nilsen, C., McCosh, K., & Kapila, M. (2008). Tar-Sands Drilling-Waste Management: A Clean Solution. *IADC/SPE Drilling Conference.* Orlando, Florida: World Petroleum Congress.

Palmer, I. (2010). Coalbed methane completions: A world view. *International Journal of Coal Geology , 82* (3-4), 184-195.

Priddy, K. L., & Keller, P. E. (2005). *Artificial Neural Networks-An Introduction* (Vol. TT68). Bellingham, Washington: The International Society for Optical Engineering.

Ramaiaha, G. B., Chennaia, R. Y., & Satyanarayanaraob, G. K. (2010). Investigation and modeling on protective textiles using artificial neural networks for defense applications. *Material Science and Engineering B , 168* (1-3), 100-105.

Ramgulam, A., Ertekin, T., & Flemings, P. B. (2007). Utilization of artificial neural networks in the optimization of history matching. *Latin American & Caribbean Petroleum Engineering Conference.* Buenos Aires, Argentina: SPE.

Richard, N. (2010). Annual Energy Outlook 2011Reference Case. Washington, DC.

Rosenblatt, F. (1962). *Principles of Neurodynamics: Perceptrons and the Theory of Brain Mechanisms.* Michigan: Spartan Books.

Russum, D. A. (2010). Evaluating unconventional reservoirs: The questions we need to answer. *Canadian Unconventional Resources & International Conference.* Calgary, Alberta: CSUG/SPE.

Saeki, T., Fujii, T., Inamori, T., Kobayashi, T., Hayashi, M., Nagakubo, M., et al. (2008). Extraction of Methane Hydrate Concentrated Zone for Resource Assessment in the Eastern Nankai Trough, Japan. *Offshore Technology Conference.* Houston, TX: OTC.

Samuel, R. G., & Miska, S. (2000). Formation Characterization of A Horizontal Well While Drilling: An On-Site Tool. *IADC/SPE Drilling Conference.* New Orleans, Louisiana: SPE.

Schalkoff, R. J. (1997). *Artificial Neural Networks.* The MIT Press and The McGraw-Hill Companies, Inc.

Schalkoff, Robert J. (2009). *Intelligent Systems: Principles, Paradigms and Pragmatics.* Sudbury, MA: Jones & Bartlett Publisher.

Shell oil. (2006). *Oil Shale Test Project.* Retrieved August 11, 2011, from Bureau of Land Management: http://www.blm.gov/pgdata/etc/medialib/blm/co/field_offices/white_river_field/oil_shale .Par.79837.File.dat/OSTPlanofOperations.pdf

Shepherd, G. M. (2004). *The synaptic organization of the brain.* (5, Ed.) Oxford University Press.

Sheppard, M. C. (2005). *Athabasca Oil Sands- From Laboratory to Production: the Letters of Karl A. Clark.* Alberta: Geoscience Publishing.

Silpngarmlers, N., & Ertekin, T. (2002). Artificial Neural Network Architectures for Predicting Two-Phase and Three-Phase Relative Permeability Characteristics. *SPE Annual Technical Conference and Exhibition.* San Antonio, Texas: SPE.

Slatt, R. M., Singh, P., Philip, P. R., Marfurt, K. J., Abousleiman, Y., & O'Brien, N. (November 2008). Workflow for stratigraphic characterization of unconventional gas shales. *SPE Shale Gas Production Conference.* Fort Worth, TX: SPE.

Stark, P. H., Chew, K., & Fryklund, B. (Dec, 2007). The role of unconventional hydrocarbon resources in shaping energy future. *International Petroleum Technology Conference.* Dubai, U.A.E.: IPTC.

Stark, P., & Fryklund, B. (2007). The role of unconventional hydrocarbon resources in shaping the energy future. *International Petroleum Technology Conference.* Dubai, UAE: IPTC.

Stark, P., Chew, K., & Jackson, P. (December 2008). Importance of unconventional oil resources in shaping the far East energy future. *International Petroleum Conference.* Kuala Lumpur, Malaysia.

Surguchev, L. (2000). IOR evaluation and applicability screening using artificial neural networks. *SPE/DOE Improved Oil Recovery Symposium.* Tulsa, Oklahoma: SPE.

Tang, Y. (2009). Plunger lift dynamic characteristics in single well and network system for tight gas well deliquification. *APE Annual Technical Conference and Exhibition.* New Orleans, Louisiana: SPE.

Thararoop, P., Karpyn, Z., Gitman, A., & Ertekin, T. (2008). Integration of seismic attributes and production data for infill drilling strategies- A virtual intelligence approach. *Journal of Petroleum Science and Engineering , 63* (1-4), 43-52.

Torrecilla, J. S., Otero, L., & Sanz, P. D. (2007). Optimization of an artificial neural network for thermal/pressure food processing: Evaluation of training algorithms. *Computers and Electronics in Agriculture , 56* (2), 101-110.

USGS. (2000, October). *Coal bed methane: Potential and Concerns.* Retrieved September 1, 2011, from U.S. Department of Interior, USGS: http://pubs.usgs.gov/fs/fs123-00/fs123-00.pdf

USGS. (2008). *Unconventional resources.* Retrieved September 2009, from http://www.pttc.org/tech_centers/unconventional/unconventional_wp.pdf

Vanstone, B., & Finnie, G. (2009). An empirical methodology for developing stockmarket trading systems using artificial neural networks. *Expert Systems with Applications , 36* (3), 6668-6680.

Vassilellis, G. D. (2009). Roadmap to moetization of unconventional resources. *SPE EUROPEC/EAGE Annual Converence and Exhibition.* Amsterdam, The Netherlands: SPE.

Vefring, E. H., Nygaard, G., Fjelde, K. K., Lorentzen, R. J., Nævdal, G., & Merlo, A. (2002). Reservoir characterization during underbalanced drilling: Methodology, accuracy, and necessary data. *SPE Annual Technical Conference and Exhibition.* San Antonio, Texas: SPE.

Wardsystems. (1998). *Neurshell 2 Manual*. Retrieved Jauary 20, 2010, from http://www.wardsystems.com/manuals/neuroshell2/

Wattenbarger, R. A. (2002). Trends in tight gas sand production. *Journal of Canadian Petroleum Technology , 41* (7), 17-20.

Xu, S., & Chen, L. (2008). A Novel Approach for Determining the Optimal Number of Hidden Layer Neurons for FNN's and Its Application in Data Mining. *International Conference on Information Technology and Applications* (pp. 683-686). Sydney, Australia: ICITA.

Yegnanarayana, B. (1999). *Artificial Neural Networks.* India: Prentice-Hall of India Pvt. Ltd.

Yuko, K., & Kazuo, F. (April, 2001). Some predictions of possible unconventional hydrocarbon availability untill 2100. *SPE Asia Pacific Oil and Gas Conference.* Jakarta, Indonesia: SPE.

Appendix A

Completion Parameters

Out of 46 parameters discussed in Chapter 5, 15 parameters were identified as important by field completion engineers in Chevron ETC. Parameters that are considered to be important are described in details and their respective value from the completion file. An example is also shown describing the value extracted for a given well.

Fracture stages

These are the total number of stages that are planned/carried at a given location.

For e.g. well "ABBY #4509" has 8 different stages for fracture carried at different times. Therefore the input value for this well will be used as 8

Total proppant used (lb)

This is the total amount of proppant used in all the fracture stages at a given location.

For e.g. well "ABBY #4509" has 8 different stages for fracture carried at different times. Where total amount of proppant used is 704844 lb

Max Btm depth (ftKB)

In case of a multiple stage fracture, this value represents the lowest depth where fracture was carried.

For e.g. well "ABBY #4509" has 8 different stages for fracture carried at different depths. Where the maximum depth observed was 10365 ft (stage 1)

Max Q (end) Max (gpm)   This value represents the max flow rate achieved during any fracturing job.

For e.g. well "ABBY #4509" has 8 different stages for fracture, where different flow rates were observed in each of the fracture stage. In this the maximum flow rate observed was 2801 gpm which was observed in 'stage 5'

Max P (tub-st) Min (psi)   It is the maximum pumping pressure that was reached during fracturing. This value varies with every stage of fracturing. In our analysis we used the maximum value observed in all the stages.

For e.g. well "ABBY #4509" has 8 different stages for fracture. In this the maximum pressure observed was 4760 psi which was observed in 'stage 1' and 'stage 4'

Total proppant recovered (bbl)   This parameter indicates the formation quality and flow back

effects on the pump. In our analysis we use the total amount of fluids recovered in all the stages i.e. clean volume recovered and slurry recovered.

For e.g. in well " ABBY #4509" a total of 24472.02 bbl of fluid is recovered

Max Set Depth (ftKB)   This parameter determines which all formations; the well has been drilled through (and completed). In this case it represents the lowest depth of the formation the well has been drilled to.

Max String ID (in) (Casing)   This is the string ID value in inches. For e.g. in well " ABBY #4509" it is 8.921 inches

Max set depth (ftKB) (Tubing String)   This parameter indicates from which formation the fluids are produced.

For e.g. in well " ABBY #4509" it is 7477 feet

Max OD MAX (in) (Tubing String)   If different strings are used then this value will represent the maximum of the two values. For e.g. in well " ABBY #4509" it is 2.375 inches

Max OD (in) **(Pump data)**	OD of the pump is used. For e.g. in well " ABBY #4509" it is 2.375 inches
Max Top (ftKB) **(Pump data)**	The MD to the top of the installed SRP pump for a given location. For e.g. in well " ABBY #4509" it is 7407 feet
Max Btm (ftKB) **(Pump data)**	The MD to the bottom of the installed SRP pump for a given location. For e.g. in well " ABBY #4509" it is 7408 feet
Max Cum Vol Disp (bbl) **(Pump data)**	This value represents the cumulative value dispersed by the pump. For e.g. in well " ABBY #4509" it is 0.4 bbl
Max EOS ISIP (psi) **(Solution Treatment)**	End of Stage Initial Shut In Pressure value. This value will be different for different stages. In our analysis we used the maximum ISIP value observed in all the stages. For e.g. in well " ABBY #4509" it is ~3820 psi

Vita

Yogesh Bansal

Yogesh Bansal was born in Delhi, India, on May 19, 1984. He graduated with B.Tech. in Chemical Engineering from University School of Chemical Technology, Guru Gobind Singh Indraprastha University, Delhi, India, in June, 2007. After graduation, he came to United States of America for graduate studies. He received a master's degree in Petroleum and Natural Gas Engineering from The Pennsylvania State University, University Park, PA. After successful completion of his master's degree he stayed to join the doctoral program of the university in January, 2009.

Mr. Bansal received third place in the student paper contest in the SPE Eastern Regional Meeting in 2009. He received graduate scholarships in the department. He also had the opportunity to do summer internships at Chevron in 2009 and 2010 and with BP in 2011. He successfully defended his Ph.D. on Nov 28, 2011, and he has accepted a position with BP Inc. as a Reservoir Engineer Specialist in Houston, Texas.